THE INTERACTION OF SPHERICAL COLLOIDAL PARTICLES WITH A PLANAR SURFACE

A thesis presented for the degree of Doctor of Philosophy in the University of London.

by

Michael Hull

Imperial College of Science and Technology, London, S.W.7.

December, 1969.

ABSTRACT

The rate of deposition of polystyrene latex particles on to smooth plastic films has been determined with the rotating disc technique.

When the particles were negatively charged and the film positively charged, the deposition rate was in close agreement with the Levich theory of diffusion-controlled transport to a rotating disc. The results also constitute a confirmation of the Stokes-Einstein equation for diffusion of spherical particles.

With negative particles and a negative film, high electrolyte concentrations were required to produce measurable deposition and the kinetics could not be accounted for by the appropriate modification of the Derjaguin-Landau-Verwey-Overbeek theory of colloid stability for the case of sphere-plate interactions (including a treatment for the diffusion of particles in a linear potential field). A theoretical analysis of the effect of surface roughness on the magnitude of the potential energy barrier to deposition has been made, from which it was found that a surface roughness comprising spherical projections of the order of 50 Å high and 300 Å in radius reduces the total interaction energy by a factor of two. However, even allowing for these surface roughness effects, deposition was not in accord with theory. Furthermore, the anomalous deposition in this system was not proportional to time or sol concentration,

although the sol itself was substantially unaffected by electrolyte under the conditions of the experiment.

The evidence strongly suggests that - even with this seemingly ideal model for studying sphere-plate interaction - anomalous deposition occurred preferentially on to areas of locally favourable potential or geometry (or both). This phenomenon may prove to be of importance in practical deposition systems.

ACKNOWLEDGEMENTS

I would like to thank Dr. J. A. Kitchener for suggesting the topic for the research described in this thesis, and for his constructive criticism, encouragement and help during the course of this work.

I am grateful to Dr. P. R. Swann and Mr. W. A. Bishop of the Department of Metallurgy for their help in electron microscopy, and to Mr. P. Marlow of the Department of Chemical Engineering for taking the electron-micrographs of Fig. (8.4).

I would like to thank my colleagues in the Department of Mineral Technology and in the Unilever Research Laboratory, Port Sunlight, for many stimulating and helpful discussions.

Finally, I would like to thank Unilever Research Limited for financial assistance during the course of this work.

TABLE OF CONTENTS

1.0 INTRODUCTION

The deposition of particles from colloidal suspensions on effectively "infinite" plane surfaces is of considerable technological importance. A few examples will indicate the wide range of problems in which an understanding of this deposition process would be advantageous. (1) In the filtration process for water purification the colloidal material present in untreated water can be effectively removed by deposition on the very much larger particles making up the filter bed. (2) In the mining industry the "slime" coating of mineral particles in the froth flotation process can so alter the surface chemical properties of these particles that greatly reduced yields of mineral concentrate are obtained. (3) It has been found in the detergency of textiles that liberated dirt may re-deposit on the cleaned fabric and can subsequently be very difficult to remove even in the presence of surface-active agents. (4) In any process involving the flow of fluids containing particles of colloidal size through pipes, deposition of the particles on the walls of the pipes can present quite an important industrial problem. One particular example of this type of problem is that of heat exchange columns. If thermally insulating particles present in the fluid in the heat exchanger deposit on the walls, then it is evident that a gradually reduced efficiency of the heat exchange unit will result.

Though this problem of deposition is of technological importance, little fundamental work on the deposition process has yet been performed. Hunter and Alexander[1] examined the deposition

of kaolinite in a column of coarse silica particles, and attempted to correlate the deposition to the stability of the kaolinite sols. A number of technical studies on the re-deposition of liberated soil on fabrics has been summarized by Durham[2]. Also preliminary work on the quite distinct problem of the removal of deposited particles has received some attention[3]. Thiessen[4] showed by electron micrographs of deposited gold particles on kaolin platelets that there is a different surface chemical nature on the edges of the platelets, where deposition occurred, from the faces, where deposition did not occur. Also he showed that in the presence of anionic surface-active agents deposition only occured on the platelet edges, whereas with both cationic surface-active agents and barium chloride solutions the deposition occurred on both the faces and edges. These facts indicated that the surface potential of the kaolin surface was responsible for the deposition and varied, in either magnitude or sign, from the faces to the edges of the platelets.

Unfortunately, owing to both the heterogeneity of surfaces (as exemplified by the work of Thiessen) and hydrodynamic considerations, measurement of deposition on textile fibres or in granular filters can only be used to give a qualitative picture of the deposition process. Ideally, the deposition of colloidal particles on plane surfaces could provide a test of the Derjaguin-Landau-Verwey-Overbeek (D.L.V.O.)[5] theory of the stability of lyophobic colloids; however, for this to be obtained one requires a deposition system in which the diffusion of particles to the deposition surface is known and controllable.

Durham[6] and von Lange[7], in their studies of soil re-deposition on textile fibres, have indicated that the D.L.V.O. theory of colloid stability should provide a sound basis for the representation of the deposition process.

Marshall[8] developed a method for the study of deposition in which the diffusion to the deposition surface was both controllable and known. He achieved this by using the surface of a rotating disc[9] as the deposition surface and utilizing smooth plastic films as his deposition surface. By this means he was able to study the deposition of carbon black particles in a quantitative manner. However, he found that his experimental depositions were several orders of magnitude higher than those expected theoretically on the basis of a simple extension of the D.L.V.O. theory for sphere-plate interactions. These discrepancies may have been due to the failure of the hydrodynamic mass transfer equations to be applicable for diffusing particles of colloidal size. However, it was not possible for this matter to be checked in his system owing to the slow coagulation of his sol. (In his system it was essential to use detergents for the stabilization of his sol, and consequently it was virtually impossible to obtain oppositely charged surfaces without the sol becoming unstable). Other factors he considered to explain the discrepancies between theory and experiment were the effect of small surface roughness of his plastic films, and the fact that his "graphitized" carbon black particles were not geometric spheres but polygonal in character, a geometry that cannot be treated in the present state of the analytical equations

comprising the D.L.V.O. theory of colloid stability.

It is consequently evident that, if these uncertainties are to be resolved, the work of Marshall must be repeated with a model colloid of simple geometrical form. Furthermore, it is essential that the validity of the hydrodynamic mass transfer equations for colloidal particles in the rotating disc system be firmly established. In such a model system it should be possible to provide a stringent test of the D.L.V.O. theory for sphere-plate interactions. This test would perhaps be more testing than those performed for the coagulation of spherical particles, because in the rotating disc system individually deposited particles are actually determined directly, rather than by the effects of the particle-particle interactions on other physical parameters (e.g. light scattering). It is only in the case of fairly large particles that direct coagulation measurements have been made by the use of the Coulter counter, and it appears that the light-scattering and Coulter counter data for coagulating particles agree fairly well[10]. However, there are a number of simplifying assumptions in the light-scattering treatment of coagulation and even though they do not appear to have a significant effect for measurements on large particles, there will always remain a degree of uncertainty of interpretation for particle-particle interactions for much smaller particles. It is to be expected that the rotating disc system will provide a sufficiently severe test of the D.L.V.O. theory of colloid stability to indicate whether for small particles the discrepancies recorded by different workers[10,11] for

the Hamaker constant for polystyrene latex spheres from coagulation data are due to uncertainties in the interpretation of coagulation data or to the necessary simplifications in the analytical treatment of coagulation by the D.L.V.O. theory.

In the present investigation, the D.L.V.O. theory of colloid stability has been tested for the case of the deposition of polystyrene latex spheres on smooth plastic surfaces using the rotating disc technique. Polystyrene latex spheres appear in the electron micrographs to be perfectly spherical and can be prepared with a very narrow size distribution[12], which provides the ideal model colloid system. For a complete test of the hydrodynamic mass transfer equations for the rotating disc, these latex particles can be prepared with a variety of surface charged groups, so that the resulting dispersion remains stable even in the absence of surface-active agents, in which case the complications experienced by Marshall can be avoided. The maximum deposition rate can be determined by using a positively charged plastic film as the deposition surface and this maximum rate can then be compared with the theoretical one.

1.1. References

(1) Hunter, R.J. and Alexander, A.E. J. Coll. Sci. 18, 820, (1963).

(2) Durham, K. ed., "Surface Activity and Detergency", Macmillan, London, (1961).

(3a) Derjaguin, B.V. and Zimon, A.D. Kolloidn.Zh. 23, 544, (1961).

(3b) Krupp, H. Adv. Coll. and Interface Sci. 1, 111, (1967).

(4) Thiessen, P.A. Z. Electrochem. 48, 675, (1942).

(5a) Derjaguin, B.V. and Landau, L. Acta Physicochim.URSS. 14, 633,(1941).

(5b) Verwey, E.J.W. and Overbeek, J.Th.G., "The Theory of the Stability of Lyophobic Colloids", Elsevier, Amsterdam, (1948).

(6) Durham, K. J. Appl. Chem. 6, 153, (1956).

(7a) Von Lange, H. Koll. Z. 154, 103, (1957).

(7b) Von Lange, H. Koll. Z. 156, 108, (1958).

(8a) Marshall, J.K. Ph.D. Thesis Univ. London, (1964).

(8b) Marshall, J.K. and Kitchener, J.A. J.Coll. and Interface Sci. 22, 342, (1966).

(9) Levich, V.G. "Physico-chemical Hydrodynamics", Prentice-Hall, New York pp. 60-78, (1962).

(10) Ottewill, R.H. and Shaw, J.N. Disc. Faraday Soc. 42, 154, (1966).

(11) Watillon, A. and Joseph-Petit, A.- M. Disc.Faraday Soc. 42, 143, (1966).

(12a) Ewart, R.H. and Carr, C.I. J. Phys. Chem. 58, 640, (1954).

(12b) Vanderhoff, J.W., Vituske, J.F., Bradford, E.B. and Alfrey Jr., T.A. J. Polymer Sci. 20, 225, (1956)

(12c) Ottewill, R.H. and Shaw, J.N. Koll.Z. 215, 161, (1967).

2.0. THE NATURE OF THE IONIC DOUBLE-LAYER

2.1. Introduction

When a solid is immersed in water, some of the ionogenic groups present on its surface ionize, and the surface of the body consequently becomes charged. This charged surface influences the distribution of ions in solution near the surface, forming an ionic double-layer. The interaction of two double-layers of like sign results in the mutual repulsion between the bodies bearing them. Before considering the nature of this double-layer interaction, it is necessary to examine the structure of an isolated double-layer.

The structure of the double-layer has been covered in detail in the standard works[1], and consequently only a condensed review will be given here. The following symbols will be used without further definition, and considerations will apply to hydrophobic surfaces.

x is the perpendicular distance from the surface.

z is the valency of an ion.

e is the electronic charge.

ϵ is the bulk dielectric constant of the liquid medium.

κ is the Debye-Hückel reciprocal thickness parameter ($1/d$), defined by

$$\kappa^2 = \frac{4\pi e^2}{\epsilon kT} \sum z_i^2 n_{io}.$$

ψ_o is the potential at the surface.

ψ is the potential at a distance x from the surface.

k is the Boltzmann constant.

T is the absolute temperature.

d is the double-layer thickness.

n_o is the bulk concentration of ions in solution per ml.

n is the concentration of ions at a distance x from the surface.

a is the radius of the particles.

σ is the surface charge density.

ρ is the charge density per unit volume in the diffuse part of the double-layer.

2.2. The Theory of the Ionic Double-Layer

Helmholtz[2] considered the double-layer as a layer of counter-ions close to a charged interface, and Perrin[3] compared this to a condenser with separation between the plates of d, in which the potential gradient was linear. These approaches were an over-simplification and a complete analysis of the double-layer was given by Gouy[4] and independently by Chapman[5]. They considered the charged surface to consist of a uniform charge, and the potential distribution around this surface to be described by the Poisson equation,

$$\nabla^2\psi = -\frac{4\pi}{\epsilon}\rho \qquad (1)$$

and the distribution of ions (considered as point charges) about its charged surface to be described by the Boltzmann relation.

$$\sum n = \sum n_o \exp(-ze\psi/kT) \qquad (2)$$

On combining equations (1) and (2) the well-known Poisson-Boltzmann equation is obtained.

$$\nabla^2\psi = \frac{-4\pi}{\epsilon} \sum zen_o \exp(-ze\psi/kT) \qquad (3)$$

The Poisson-Boltzmann equation is the starting point for all double-layer calculations. This equation can be solved analytically for a flat double-layer. If the assumption of Gouy and Chapman is used, namely, that the surface can be treated as a mathematical plane of uniform "smeared out" charge, then the distribution of potential from the surface is given by

$$\kappa x = \ln \left\{ \frac{[\exp(ze\psi/2kT) + 1]}{[\exp(ze\psi/2kT) - 1]} \frac{[\exp(ze\psi_o/2kT) - 1]}{[\exp(ze\psi_o/2kT) + 1]} \right\} \qquad (4)$$

This equation is rather cumbersome to use; it may be reduced to,

$$\psi = \psi_o \exp(-\kappa x) \qquad (5)$$

for "small potentials", defined by $(ze\psi/kT) \ll 1$, showing that the potential falls exponentially, approaching zero over a distance of the

order of magnitude $1/\kappa$ (the "thickness" of the double-layer).

A number of corrections to the Poisson-Boltzmann equation have been made[6]. These arise from the many assumptions underlying the derivation of the equation. For instance, it is assumed that the dielectric constant of water has the same value in the double-layer as for bulk water. The polarizability effects of the charged surface on the liquid medium are completely neglected. The ionic volume of the ions in solution has also been neglected, though Stern[7] later provided a useful correction for the layer of ions next to the charged surface. He considered that the first layer of ions formed a rigid layer, of finite dimensions, next to the surface, over which the potential drop was linear (i.e. a parallel plate type condenser), and that outside this layer the potential and ion concentrations were of such values that the assumption of ions as point charges could be applied.

More recently, Levine and Bell[8] have considered corrections taking into account the "discreteness-of-charge" of the surface and its neighbouring ions. All of the corrections that have been applied to the double-layer are applicable only for specific conditions, and consequently no complete quantitative treatment for the double-layer is available. However, the modifications that are available can be used to give an indication of the direction and magnitude of the various corrections to the double-layer theory. Bolt[9] has shown that, provided the surface potentials and ionic concentrations are not too high (< 60mV and $< 10^{-2}$M respectively), then the corrections, fortunately,

become insignificant by a process of partial self-compensation. If, however, the potentials and ionic concentrations are high, the corrections rapidly increase in significance, and at 10^{-1}M electrolyte concentration and any value of the surface potential they may become greater than 20%.

The Poisson-Boltzmann equation can be solved for spherical double-layers as well as plane double-layers, though it can be solved analytically only for "small" surface potentials ($ze\psi/kT \ll 1$), which yields a solution of the same form as the well known Debye-Hückel equation[10].

$$\Psi = \Psi_0 \frac{a}{(x + a)} \exp(-\chi x) \qquad (6)$$

From this the potential is seen to fall off, for small particles, more rapidly than the purely exponential case for the plane double-layer.

In the case where the potential is "high" ($ze\psi/kT \gg 1$) there is no analytical expression for the potential distribution around a spherical particle and the distribution is obtained by numerical integration of the Poisson-Boltzmann equation. Müller[11] was the first to attempt the numerical integration. He showed that the approximate expression (eq. 6) was sufficiently accurate up to $ze\psi/kT = 4$ and $\chi a = 2$. However Hoskin[12], repeating the calculations for a wider range of potential and χa, found that only for $ze\psi/kT < 1$ did the approximate equation correspond to the accurate

numerical analysis at any value if χa. On increasing χa and the potential, the divergence increased rapidly. More recently, Loeb, Wiersema and Overbeek[13] have performed a complete analysis for a very large number of values of potential and χa and have confirmed the results of Hoskin. Using the tables in ref.(13) it is now possible to calculate the potential distribution for all practical cases.

2.3. Surface Charge Density and the Origin of Surface Charge

The surface charge density can be evaluated from the Poisson-Boltzmann equation for double-layers by using the equation

$$\sigma = - \int_0^\infty \rho \, dx \qquad (7)$$

Hence, the general expression for a plane double-layer is given by,

$$\sigma = \sqrt{\frac{2n\epsilon kT}{\pi}} \sinh \frac{ze\psi_0}{2kT} \qquad (8)$$

For small enough potentials for the exponentials to be expanded,

$$\sigma = \frac{\epsilon \chi \psi_0}{4\pi} \qquad (9)$$

From these equations a determination of the surface potential ψ_0 yields a value of the surface charge density. However, in practice only the

zeta-potential (ζ) can be determined. In most cases the zeta-potential is oonsidered equivalent to the Stern potential (ψ_δ), i.e. the potential at the edge of the Stern rigid layer of ions or the innermost edge of the diffuse part of the double-layer. As the Stern layer is the site of specifically adsorbed ions, which control the value of the Stern potential by the charge that these ions carry, it is usual to consider the Stern potential as being synonymous with the effective surface potential, and hence calculated surface charge densities from zeta-potential measurements are for the charge density at the Stern plane.

In the case of spherical double-layers, the surface charge density can be evaluated completely from the Poisson-Boltzmann equation only by numerical integration. These values have been tabulated by Loeb, Wiersema and Overbeek[13], and are usable for all practical cases where zeta-potentials can be evaluated. Two useful approximate equations, however, are available.

$$\sigma = \frac{\epsilon \psi_o}{4\pi} \left(\frac{1 + \kappa a}{a\kappa} \right) \qquad (10)$$

which is valid only for small potentials ($ze\psi/kT \ll 1$), and

$$\sigma = \sqrt{\frac{N\epsilon kT}{2000} \sum c_i \left[\exp(-z_i e\psi_o/kT) - 1 \right]} \qquad (11)$$

where c is the molar concentration of ions in solution. Equation (12),

however, is applicable only for large values of κa at any potential.

The surface charge may arise from either (or both) of two different processes.

(a) The ionizable groups on the surface may dissociated to yield a charged site, or

(b) specific adsorption of ions from solution may occur, yielding a surface charge density dependent upon the "adsorption potential" and concentration of adsorbing ions.

The latter case is prominent with surface-active agents.

2.4. References

(1) Overbeek, J.th.G. in "Colloid Science Vol.1". ed. Kruyt, H.R. (Elsevier) Amsterdam, pp. 127-144, (1952).

(2) Helmholtz, H. Ann. Phys. 7, 337, (1879).

(3) Perrin, J. J. Chim. Phys. 2, 601, (1904).

(4a) Gouy, G. J. Phys. 4, 9, (1910).

(4b) Gouy, G. Ann. Phys. 9, 129, (1917).

(5) Chapman, D.L. Phil. Mag. 6, 25, 475, (1913).

(6a) Bikermann, J.J. Phil. Mag. 33, 384, (1942).

(6b) Grahame, D.C. J. Chem. Phys. 18, 903, (1950).

(6c) Bockris, J. O'M., Ammour, I.A. and Conway, B.E. Trans. Faraday Soc. 47, 756, (1951).

(6d) Sparnaaj, M.J. Rec. Trav. Chim. 77, 872, (1958).

(6e) Levine, S. and Bell, G.M. J. Phys. Chem. 64, 1188, (1960).

(7) Stern, O. Z. Electrochem. 30, 508, (1924).

(8) Levine, S. and Bell, G.M. J. Phys. Chem. 67, 1408, (1963).

(9) Bolt, G.H. J. Coll. Sci. 10, 206, (1955).

(10) Debye, P. and Hückel, E. Z. Phys. 25, 204, (1924).

(11) Müller, H. Kolloid-Beihefte, 26, 257, (1928).

(12a) Hoskin, N.E. Trans. Faraday Soc. 49, 1471, (1953).

(12b) Hoskin, N.E. and Levine, S. Phil.Trans.Proc.Roy.Soc. A248, 433, (1956).

(13) Loeb, A.L., Wiersema, P.H. and Overbeek, J.th.G., "The Electrical Double-Layer around a Spherical Particle". The M.I.T. press, Cambridge, Mass. (1961).

3.0. THE POTENTIAL ENERGY OF INTERACTION OF TWO DOUBLE LAYERS

3.1. Introduction

When two particles bearing a surface charge approach one another they are subject to a repulsion if the charges are of the same sign. This repulsion is due to the interaction of the diffuse double-layers surrounding the particles and from the theory of the double-layer it is possible to evaluate the potential energy of interaction. In their classical monograph, Verwey and Overbeek[1] presented a complete mathematical treatment of this problem and consequently, only the results of this treatment and their limitations will be summarized in this chapter.

3.2. The Interaction of Two Plane-Parallel Double-Layers

The simplest case is that for two plane parallel double-layers.

When two plane parallel double-layers, bearing the same sign, approach one another, the two diffuse double-layers begin to interfere and neither of them can develop fully. As a consequence, the potential nowhere reaches the level it has at large distances from the surface. This last mentioned level is usually taken as zero potential. It is assumed that the surface potentials are maintained constant during interaction of the bodies by rapid equilibration of the "potential-determining ions".

Consideration of symmetry shows that the minimum value of the potential will be reached half-way between the plate surfaces. Thus the value of this minimum potential can be evaluated from the Poisson-Boltzmann equation with the adjustment of the necessary boundary conditions. The energy of interaction is obtained from considerations of the work done against the forces of interaction of the two double-layers when the two surfaces approach one another from infinity. The repulsive energy (V_R) for two like plane-parallel double-layers was given by Verwey and Overbeek[1] as,

$$\frac{z^2}{\chi} V_R = f(U.Z) \qquad (1)$$

where $\underline{U}$ is given by $ze\psi_d/kT$, in which ψ_d is the potential minimum between the two plates at a distance $\underline{d}$ from the surface of either and $\underline{Z}$ is given by $ze\psi_o/kT$. $f(U.Z)$ and $\underline{U}$ are described by complicated elliptic functions, the values of which can be evaluated from tables of elliptic integrals. Because this is a tedious procedure it is much more convenient to use approximate equations for the free energy of interaction of double-layers.

Derjaguin[2] developed a simple approximate expression for the repulsive energy between two plane parallel double-layers by considering that the gradient of the hydrostatic pressure and the force on the space charge balance each other at any point in the liquid phase when the whole system is in equilibrium. From this consideration he obtained the force between two flat double-layers as,

$$P = 2nkT \left[\cosh (ze\psi_d/kT) - 1 \right] \qquad (2),$$

from which the energy is readily obtained using the approximate expression, valid only for small potentials.

$$ze\psi_d/kT = 8\gamma \exp(-\kappa d) \qquad (3).$$

The energy is given by,

$$V_R = \frac{64nkT}{\kappa} \gamma^2 \exp(-2\kappa d) \qquad (4)$$

where γ is given by,

$$\gamma = \left[\frac{\exp(ze\psi_o/2kT) - 1}{\exp(ze\psi_o/2kT) + 1} \right]$$

Equation (4) is valid only if $\kappa d \gg 1$. Verwey and Overbeek[1] have shown that for $\kappa d < 1$ equation (4) rather over-estimates the interaction energy, the deviation from the accurate solution (eq.(1)) being larger the higher the value of the surface potential. A somewhat more accurate approximation has been given by Verwey and Overbeek[1] as,

$$V_R = \frac{32\, nkT}{\kappa} \gamma^2 \left[1 - \tanh(\kappa d) \right] \qquad (5)$$

3.3. The Interaction of Two Spherical Double-layers

It is impossible to solve the problem of the interaction of two spherical double-layers analytically because of mathematical difficulties. A purely numerical or graphical method seems unpromising because of the number of essential parameters (surface potential, thickness of the double-layer, radius of the particles and the distance between particles) are too large. However, by the application of diverse methods of approach, it is possible to cover the interaction of spherical double-layers almost completely.

Derjaguin[2,3] indicated and applied an ingenious method for deriving the interaction energy of spherical double-layers from that of infinitely large plane double-layers of the same composition. His method is applicable only when the range of interaction is small compared with the radius of the particle.

He considered the sphere to be composed of rings with their centres on the axis of symmetry. Then the interaction energy of each pair of plane parallel rings is summed over the surface of the sphere.

Considering two spheres of radius a and distance H apart, the spheres are divided into a number of rings of radius h and width dh. Then the interaction energy of each pair of rings is given by,

$$V_R = 2\pi h\, V(H)\, dh,$$

where V(H) is the interaction energy of plane double-layers at a

distance $\underline{H}$ apart. Consequently, the total energy of interaction of the two spherical double-layers is given by

$$V_R = 2\pi a \int_{H_o}^{H = \text{large}} \kappa V(H)dh \qquad (6)$$

where $(H_o + 2a)$ is the distance between the centres of the spheres. From the geometry of the system $\underline{hdh}$ can be expressed in terms of $\underline{H}$ for,

$$hdh = \frac{a}{2}\sqrt{1 - h^2/a^2}\, dH$$

and if $h^2/a^2 \longrightarrow 0$, then $hdh \longrightarrow adH/2$, and H = large may be replaced by infinity. Hence,

$$V_R = \pi a \int_{H_o}^{\infty} V(H)dH \qquad (7)$$

This simplification is valid only if the range of interaction is small, i.e. $\kappa a >> 1$. Moreover, unless the potentials are also very small, even with large κa, to maintain $h^2/a^2 \longrightarrow 0$, it is necessary that $H >> 1$. These conditions are inherent in this method of analysis despite the expressions for the energy of interaction for plane double-layers used in equation (7). If the approximate expressions for plane double-layer interaction are used, then the condition $\kappa H >> 1$ is inherent in their use regardless of this method of analysis.

By this treatment the most accurate expression for the

interaction of spherical double-layers is given by,

$$V_R = \frac{a}{z^2} G\,(ze\psi_o/kT, \chi H_o) \qquad (8)$$

in which $G(ze\,\psi_o/kT, \chi H_o)$ is an elliptic function, the values of which can be evaluated from tables of elliptic integrals.

For small surface potentials, using the approximate equation (5), the interaction potential for spherical double-layers is

$$V_R = \frac{\varepsilon a \psi_o^2}{2} \ln\left[1 + \exp(-\chi H_o)\right] \qquad (9)$$

When, however, the distance of separation is of the same order as the radius of the particles equation (9) is rather inaccurate and must be replaced by,

$$V_R = \frac{\varepsilon a \psi_o^2}{2} \ln\left[1 + \frac{2a}{2a + H_o} \exp(-\chi H_o)\right] \qquad (10)$$

3.3.1. The Interaction of a Spherical Double-layer and an Infinitely Large Plane Double-layer

The case of the interaction energy of a spherical double-layer and a plane double-layer is treated in the same manner as for two spherical double-layers. In this case the geometry is slightly different, changing equation (7) to

$$V_{s-p} = 2\pi a \int_{H_o}^{\infty} V(H)dH \qquad (11)$$

in which the same restrictions as for two spherical double-layers apply.

Comparison of equation (7) and (11) shows that the repulsive energy for the sphere-plate system is twice that for the sphere-sphere system.

3.4. Interaction at Constant Surface Charge

In the preceding treatment the repulsive energy of interacting double-layers was considered for the case of constant potential. Consequently, to maintain thermodynamic equilibrium, the surface charge must change with interaction. It is quite conceivable that this change of charge, which implies movement of charge carriers from one part of the system to the other, is a process much slower than the time of a Brownian encounter of two particles. In that case during the interaction of the double-layers not the surface potential but the surface charge must be regarded as constant.

Frens[4] has recently examined the case for constant surface charge and has found that for plane double-layers the use of constant charge expressions become significant only below $\kappa d < 0.5$. In this range, the repulsive potential was found to be greater at constant charge than at constant potential, the differences increasing the higher the value of the surface potential.

3.5. Heterocoagulation

In the preceding sections the interaction of double-layers bearing identical surface potentials have been considered. However, in many cases it is of interest to know the repulsion between double-layers of unequal potential.

This situation was first examined by Derjaguin[5], who showed that under certain circumstances unequal potentials of the same sign could lead to an electrostatic attraction. Later, Bierman[6] examined the interaction between non-identical particles from a different stand-point and arrived at the same general conclusions. His approach was from a consideration of the change in charge of the two surfaces, during interaction of two double-layers, by unequal adsorption of ions on the two surfaces, on the assumption that the electro-chemical potentials at the surface and in the medium were equal (i.e. at equilibrium).

Derjaguin[5] also showed that because of the presence of an electrostatic attraction between non-identical plane double-layers of like sign, there would necessarily result a force barrier and, furthermore, the magnitude of this force barrier was dependent only on the surface of lower potential. These general effects of the interaction of two plane double-layers are presented in Figs. (3.1-2).

The evaluation of the energies of interaction of non-identical double-layers are accurately done by numerical integration. For plane double-layers, Devereux and de Bruyn[7] have tabulated a complete set of numerical computations, from which the interaction energies can be

FIG(3·1) POTENTIAL ENERGY CURVES AT CONSTANT. $\psi_{02} = 10{\cdot}35$ mV FOR PLANE PARALLEL DOUBLE LAYERS. [TABLES DEVEREUX AND DE BRUYN]

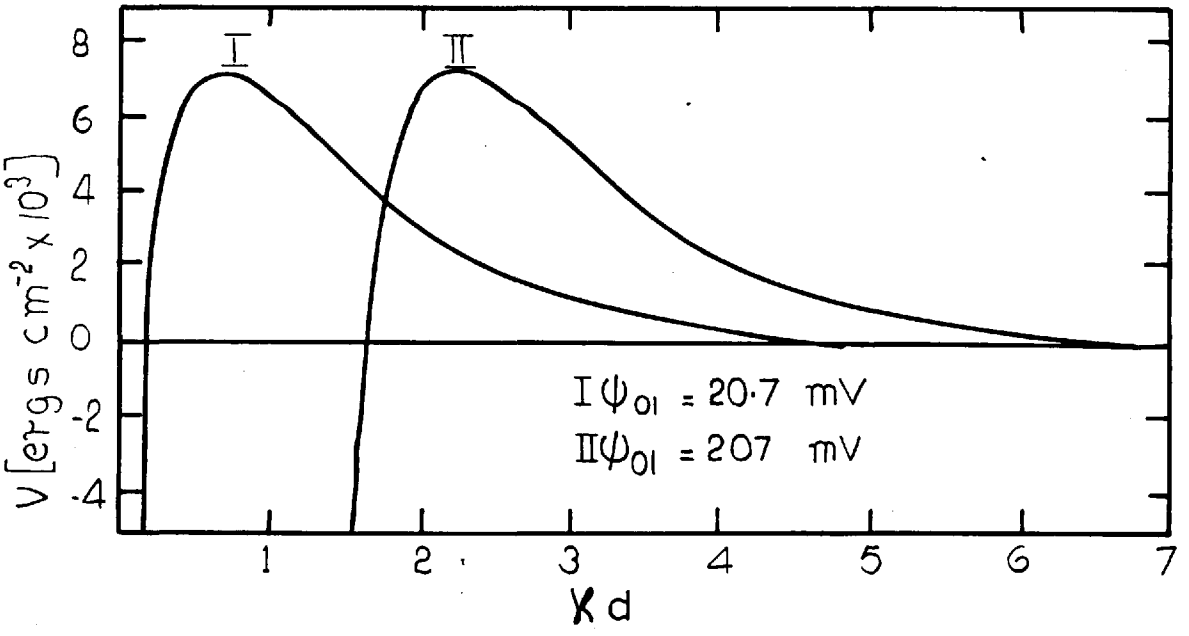

FIG (3·2) POTENTIAL ENERGY MAXIMUM FOR THE CASE OF NON-IDENTICAL PLANE PARALLEL DOUBLE LAYERS TO EQ (12)

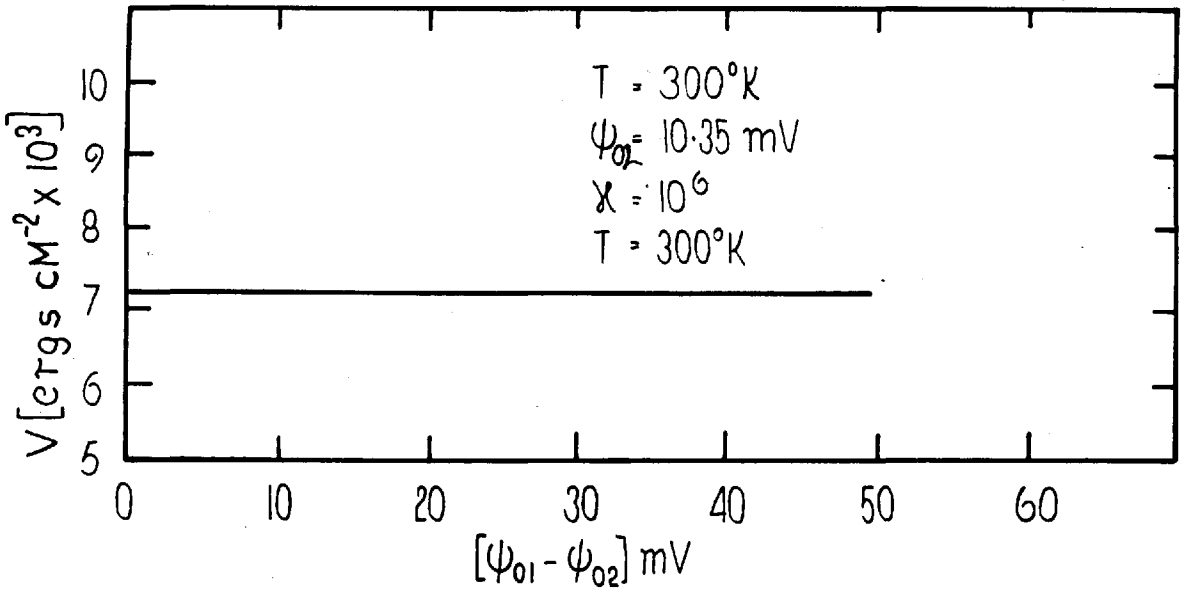

readily obtained, and they have shown that both a force barrier and an energy barrier exist and are dependent only upon the surface of lower potential. However, no such computations for sphere-sphere interactions have been made. Recently, Hogg, Healy and Fuerstenau[8] have derived some simple expressions for the interaction energies of non-identical plane parallel double-layers and spherical double-layers. Their expression for plane double-layers is,

$$V_R = \frac{\varepsilon \kappa}{8\pi}\left[\left(\psi_{01}^2 + \psi_{02}^2\right)(1 - \coth \kappa H) + 2\psi_{01}\psi_{02}\,\operatorname{cosech} \kappa H\right] \quad (12)$$

This is strictly valid only if ψ_{01} and ψ_{02} are small $\kappa H >> 1$. However, they have compared equation (12) with the results tabulated by Devereux and de Bruyn[7] and have shown that equation (12) is usable up to surface potentials of 70 mV. With equation (12) they have used the same treatment as Derjaguin[3] to obtain the interaction energies of non-identical spherical double-layers. Their final expression is

$$V_R = \frac{\varepsilon a_1 a_2 \left(\psi_{01}^2 + \psi_{02}^2\right)}{4(a_1 + a_2)}\left[\frac{2\psi_{01}\psi_{02}}{\left(\psi_{01}^2 + \psi_{02}^2\right)} \ln\left(\frac{1 + \exp(-\kappa H_0)}{1 - \exp(-\kappa H_0)}\right) + \ln(1 - \exp(-2\kappa H_0))\right] \quad (13)$$

This is valid only for $\kappa a >> 1$, $\kappa H_0 >> 1$ and $H_0 << a_1$ and a_2. It is of interest to consider equation (13) when $\psi_{01} = \psi_{02} = \psi_0$ and $a_1 = a_2 = a$; then equation (13) reduces to

$$V_R = \varepsilon a \psi_0^2 \ln (1 + \exp(-\chi H_0) \qquad (9)$$

which is identical with that derived by Derjaguin for spherical particles of surface potential ψ_0. Therefore, it appears that equation (9) is the limiting case of the more general equation (13).

In Figs. (3.3-4) is shown the potential energy curves for the interaction of spherical double-layers according to equation (13). From these graphs it is evident that the potential energy maximum is <u>not</u> invariably dependent <u>only</u> upon the lower potential. Calculations show that for the interaction of plane double-layers (eq.12) the energy maximum is indeed dependent only upon the lower potential in accord with theory. Consequently, this deviation of the energy maximum from lower potential dependency must arise in going from equation (12) to (13).

In Fig. (3.5) is shown the deviation of the energy maximum from lower potential dependency as a function of the difference in the particle surface potentials for various values of the lower surface potential. The curves in Fig.(3.5) can conveniently be combined into a single curve by changing the variable $(\psi_{01} - \psi_{02})$ to the dimensionless variable $(\psi_{01} - \psi_{02})/\psi_{02}$, (Fig.3.6.). This deviation of the energy maximum from lower potential dependency can be calculated theoretically from comparison between the maximum energy in equation (13) with the energy at contact ($\chi H = 0$) for equal lower potentials from equation (9), and is given by,

fig.(3·4) POTENTIAL ENERGY CURVES AT CONSTANT ψ_{02}=10mV. FOR SPHERICAL DOUBLE-LAYERS.

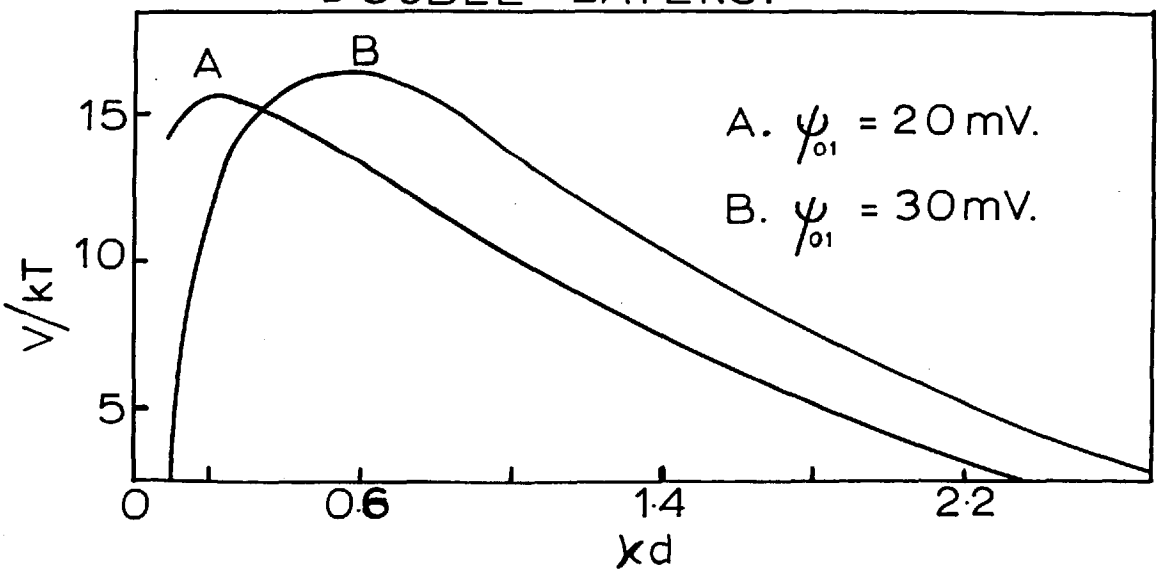

fig.(3·3) POTENTIAL ENERGY MAXIMUM FOR NON-IDENTICAL SPHERICAL DOUBLE-LAYERS.

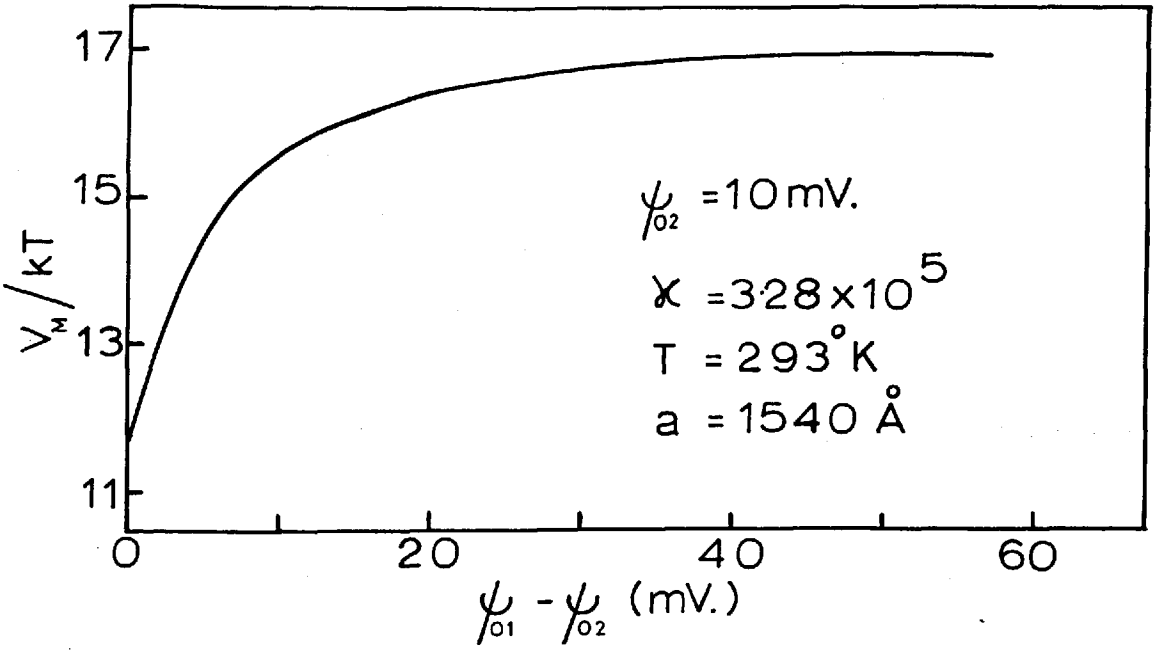

fig.(3.5) THE CHANGE IN MAXIMUM POTENTIAL ENERGY WITH DIFFERENCE IN SURFACE POTENTIAL FOR SPHERICAL DOUBLE LAYERS ACCORDING TO EQ.(10).

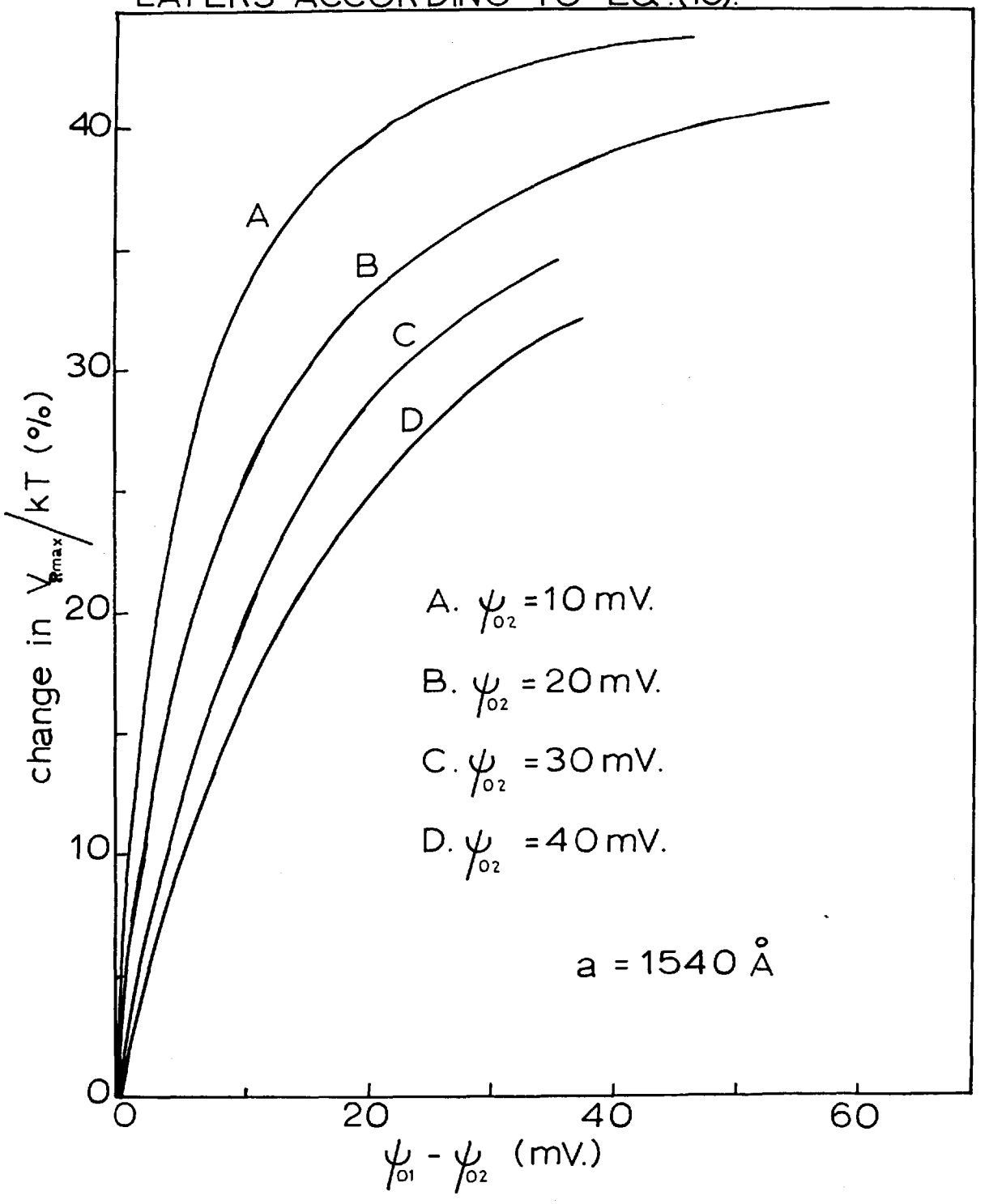

$$\text{change in maximum energy (\%)} = 36.136 \left[(x+2)^2 \ln\left(\frac{(x+2)^2}{(x^2+2x+2)}\right) + x^2 \ln\left(\frac{x^2}{x^2+2x+2}\right) \right] - 1 \qquad (14)$$

where x is the dimensionless variable $(\psi_{01} - \psi_{02})/\psi_{02}$. A much simpler approximate equation for this deviation has been computed and is,

$$\text{change in maximum energy (\%)} = \frac{0.0066 + 108.68x + 1.76x^2}{1 + 2.36x} \qquad (15)$$

Thus using equation (15), and assuming that this deviation is constant over the entire potential energy curve, a dimensionless correction factor can be calculated for the potential energy of interaction of two non-identical double-layers. The potential energy is then given by,

$$V_R = \frac{\varepsilon a_1 a_2}{4(a_1 + a_2)} (\psi_{01}^2 + \psi_{02}^2) \left[\frac{2\psi_{01}\psi_{02}}{\psi_{01}^2 + \psi_{02}^2} \ln\left(\frac{1 + \exp(-\kappa H_0)}{1 - \exp(-\kappa H_0)}\right) + \ln\left(1 - \exp(-2\kappa H_0)\right) \right] \left[1 \Big/ 1 + \frac{(0.0066 + 108.68x + 1.76x^2)}{100(1 + 2.36x)} \right] \qquad (16)$$

Comparisons between equations (13) and (16) are shown in Fig.(3.6).

It is assumed that equation (16) is applicable over the whole range of χH values. However, it is probable that at large distances of separation, the error is minimal and the energy is given by equation (13). The dotted curve in Fig.(3.7) is a likely possibility for the repulsive potential energy curve. Though the only sure value that is known is that of the potential energy maximum and until an accurate numerical analysis has been done on this system, uncertainties, though in general fairly small, will always be present.

All calculations, carried out for the interaction of non-identical double-layers, have been done on the basis of maintaining constant surface potential during interaction. As has been stated in section (3.4) this can only be maintained by the change in adsorption of counter-ions during interaction. If the potential energy is to pass through a maximum and eventually change sign, then it must be accompanied by the charge of one of the interacting surfaces changing sign. Thus the potential energy maximum must represent the point at which ions, oppositely charged to the surface, are adsorbing. It is difficult to see how this could happen in practice, and it is more likely that the interaction of constant surface charge rather than potential must be considered. Frens[4] has shown for identical double-layers that the calculation of their interaction potential energy must be done on the basis of constant surface charge for distances of approach of $\chi H < 1$. In Fig.(3.4),

FIG(3·6) THE CHANGE IN MAXIMUM POTENTIAL ENERGY AS A FUNCTION OF $(\psi_{01} - \psi_{02})/\psi_{02}$ FOR SPHERICAL DOUBLE LAYERS.

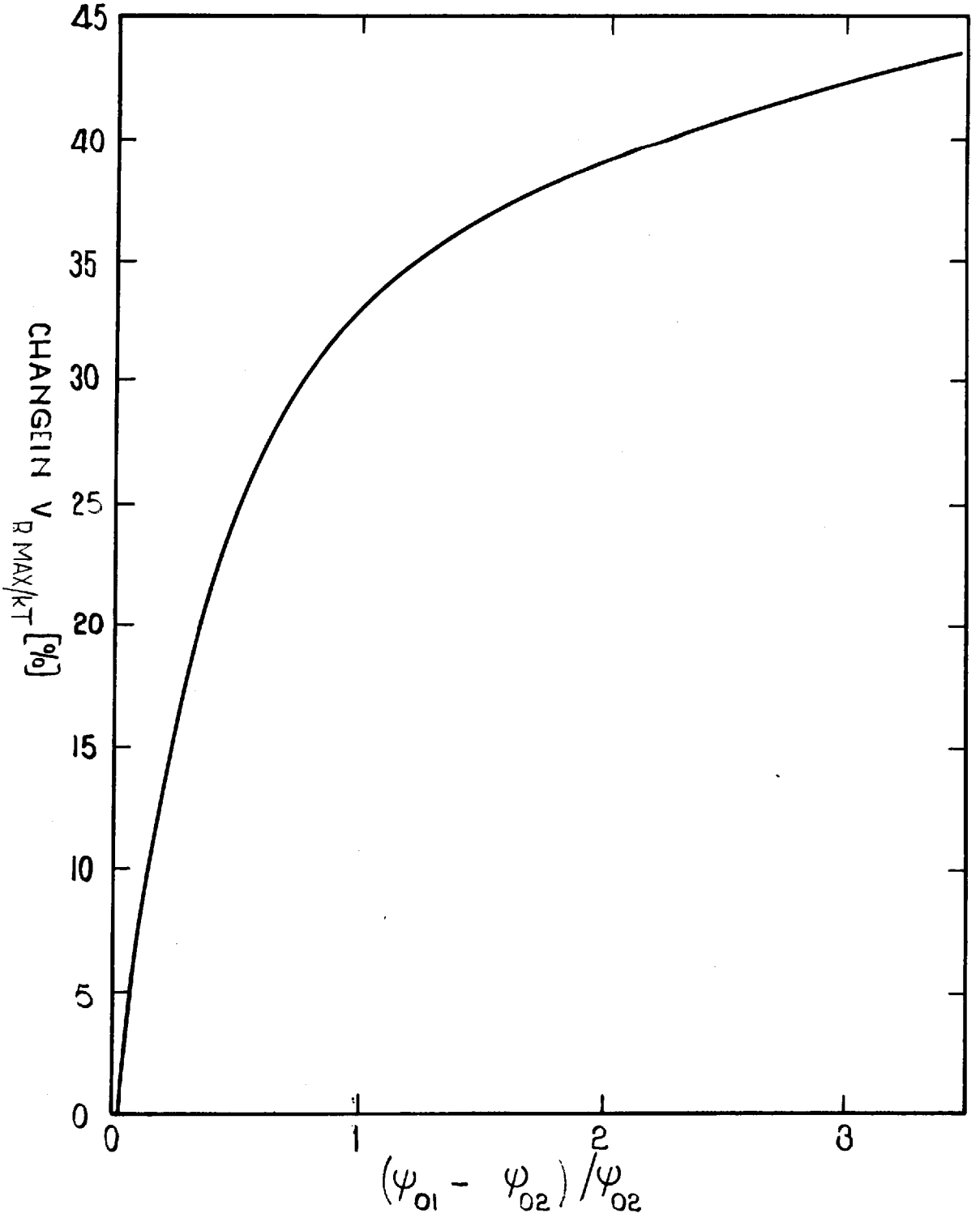

FIG. (3·7) THE INTERACTION OF NON-IDENTICAL SPHERICAL DOUBLE-LAYERS. $\psi_{01} = 30$ mV. $\psi_{02} = 10$ mV.

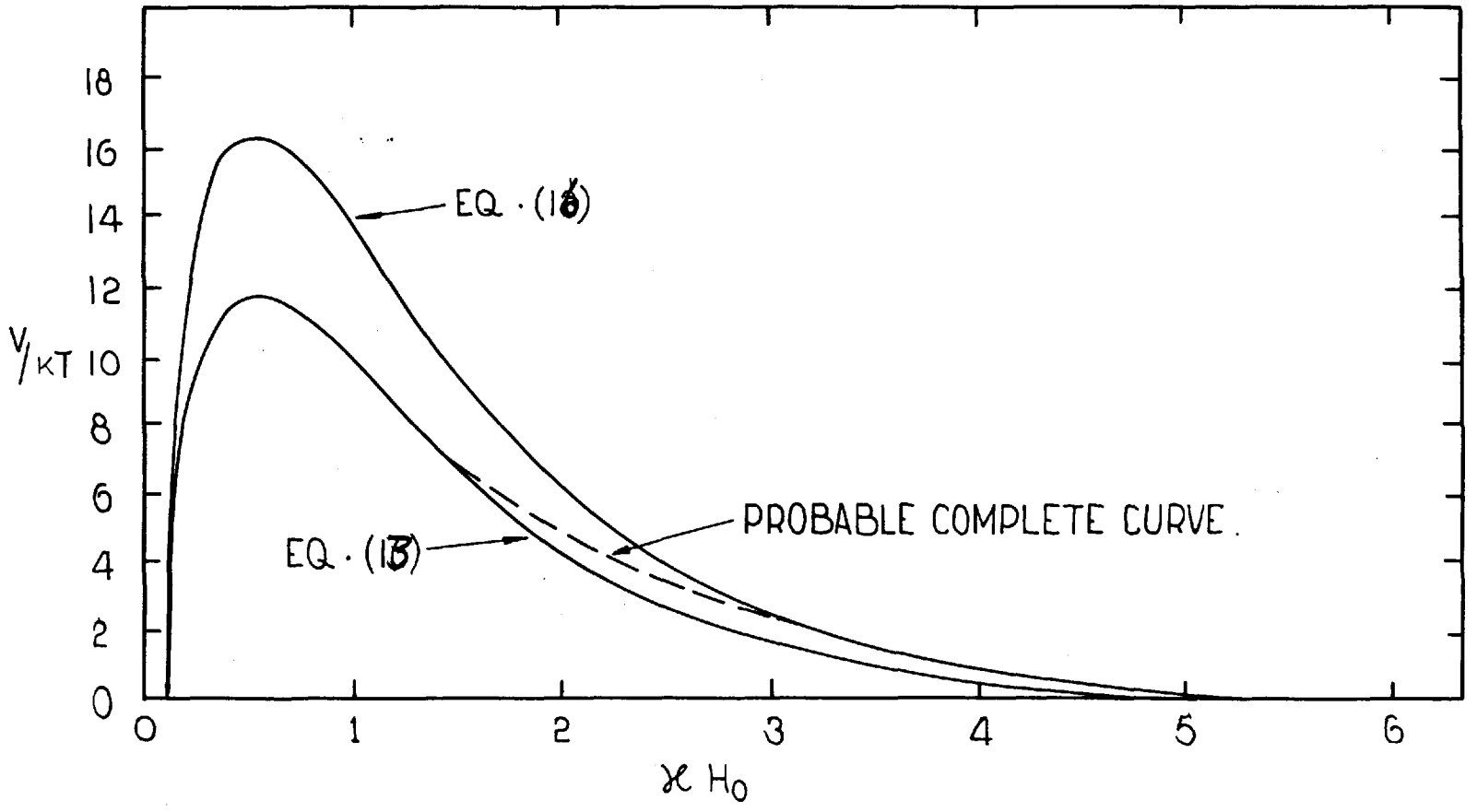

it can be seen that the potential energy maximum occurs at distances of separation of less than $\varkappa H = 1$, and it has also been found from calculations that this maximum never occurs at distances of separation greater than $\varkappa H = 4$. It thus seems reasonable that for distances of approach of $\varkappa H < 10$ the repulsion energy should be calculated on the basis of maintaining constant charge, in which case the electrostatic potential energy maximum would never occur. Thus equations (13) and (16) probably give too low a value for the repulsion potential energy, but in the absence of correct values of the repulsion energy, equation (13) will be used for all subsequent calculations.

3.6. References

(1) Verwey, E.J.W. and Overbeek, J. th. G. "Theory and Stability of Lyophobic Colloids", Elsevier, Amsterdam, (1948).

(2) Derjaguin, B.V. Trans. Faraday Soc. 36, 203, (1940).

(3) Derjaguin, B.V. Koll. Z. 69, 155, (1934).

(4) Frens, G. Thesis, University of Utrecht, The Netherlands, (1968).

(5) Derjaguin, B.V. Disc. Faraday Soc. 18, 85, (1954).

(6) Bierman, A. J. Coll. Sci. 10, 231, (1955).

(7) Devereux, O.F. and de Bruyn, P.L. "Interactions of Parallel Plane Double-layers". M.I.T. Press, Cambridge, Mass. (1963).

(8) Hogg, R., Healy, T.W. and Fuerstenau, D.W. Trans. Faraday Soc. 62, 1638, (1966).

4.0. THE STABILITY OF COLLOIDS

4.1. Introduction

The stability of "lyophobic " colloids is explained by the Derjaguin-Landau-Verwey-Overbeek theory (DLVO)[1,2]. The basis of this theory is the competition between the electrostatic repulsive forces between the particles due to the interaction of their double-layers and the long-range attractive forces between the particles. Before the total potential energy curves can be discussed, it is necessary to consider the nature of the long-range attractive forces between particles.

4.2. The London-van der Waals Energy between Bodies

The attraction between neutral atoms was introduced in 1873 by van der Waals[3]. Later London[4] placed this attraction on a sound quantum-mechanical foundation. The energy was considered to arise from the rapidly fluctuating dipole moment generated in the neutral atom by the zero point energy of the electrons. The fluctuating dipole in one atom momentarily polarizes the other one in the direction that the two atoms attract each other. London showed that this energy of attraction varies inversely as the sixth power of their distance of separation, and is (to a first approximation) independent of the interaction with other atoms. Therefore, for a large number of atoms in a condensed body the total energy may be found by simple

summation, which for some cases may be replaced by an integration.

Using the method of integration of atom-atom attractive energies, the attraction energy between two infinite flat plates may be derived. The energy between plates is given by

$$V_A = \frac{-A}{48\pi}\left[\frac{1}{d^2} + \frac{1}{(d+\delta)^2} - \frac{2}{(d+\delta/2)^2}\right] \qquad (1)$$

in which A is the "Hamaker constant" defined by

$$A = \pi^2 q^2 \lambda \qquad (2)$$

where λ is the wavelength characteristic of the atom dipole fluctuations, and q is the number of atoms per cm^3 of material in the body. δ is the thickness of the plate. For thick plates (where $d \ll \delta$) equation (1) reduces to

$$V_A = \frac{-A}{48\pi d^2} \qquad (3).$$

This attraction decays comparatively slowly with increasing distance, a property explaining the long-range character of the London-van der Waals forces between colloidal particles.

Hamaker[5] solved the problem of the energy of attraction between two spheres. He obtained

$$V_A = -\frac{A}{12}\left[\frac{y}{x^2 + xy + x} + \frac{y}{x^2 + xy + x + y} + 2\ln\left(\frac{x^2 + xy + x}{x^2 + xy + x + y}\right)\right] \qquad (4)$$

where $y = a_2/a_1$ and $x = H/2a_1$. For the special case of equal radius a equation (4) reduces to

$$V_A = -\frac{A}{6}\left[\frac{2a^2}{H(H + 4a)} + \frac{2a^2}{(H + 4a)^2} + \ln\left(\frac{H}{H + 4a}\right)\right] \qquad (5).$$

The attraction energy for the sphere-plate system may be obtained from equation (4) by putting $a_2 \to \infty$. However, a better derivation for the sphere-plate system has been given by Clayfield and Lumb[6]. They obtained the following expression for the van der Waals energy for the sphere-plate system

$$V_{s\text{-}p} = -\frac{A}{6}\left[\frac{2a(H + a)}{H(H + 2a)} + \ln\frac{H}{H + 2a} - \frac{a}{(H + t)} - \frac{a}{(H + 2a + t)} - \ln\left(\frac{H+t}{H+2a+t}\right)\right] \qquad (6)$$

where t is the thickness of the plate. When $t \gg a$ equation (6) reduces to

$$V_{s\text{-}p} = -\frac{A}{6}\left[\frac{2a(H + a)}{H(H + 2a)} + \ln\left(\frac{H}{H + 2a}\right)\right] \qquad (7).$$

As the plate will for most practical systems be very much greater in thickness than the radius of the colloidal particles, it can be regarded as infinitely thick and equation (7) can be used.

4.3. The Influence of "Retardation" on the London-van der Waals Forces

As the London-van der Waals forces are essentially of electrical origin, a certain time is necessary for their propagation, and it is expected that if the time of travel of an electromagnetic wave from one atom to another is of the same order or larger than the time of the electronic fluctuations (i.e. the wave-length of the London frequency is of the same order as the distance between atoms) then the London-van der Waals forces will be smaller than that given by London[4]. This problem was worked out by Casimir and Polder[7], who found that for large distances of separation the energy decreases as $1/d^7$ instead of $1/d^6$. The retarded energy may be represented as

$$V_{A_{ret}} = V_A f(p) \qquad (8)$$

where $p = 2\pi H/\lambda$.

Schenkel and Kitchener[8] derived an approximate expression for $f(p)$ usable from $0.5 < p < \infty$. Their expression is

$$f(p) = \frac{2.45}{p} - \frac{2.17}{p^2} + \frac{0.59}{p^3} \qquad (9)$$

With this expression it is possible to obtain an equation for the sphere-sphere interaction energy in the retarded case.

Clayfield and Lumb[9] have recently derived equations for both the sphere-sphere and sphere-plate systems in the retarded case employing equation (9). For the sphere-sphere case they obtained

$$V_{S\text{-}S_{ret}} = \frac{A}{\pi(H+2a)} \left\{ 0.04083 \left[a^2 \left(\frac{1}{(H+4a)^2} + \frac{2}{(H+2a)^2} + \frac{1}{H^2} \right) + 2a \left(\frac{1}{(H+4a)} - \frac{1}{H} \right) + \ln \frac{(H+2a)^2}{H(H+4a)} \right] \right.$$

$$- \frac{0.01808\lambda}{\pi} \left[\frac{a^2}{3} \left(\frac{1}{(H+4a)^3} + \frac{2}{(H+2a)^3} + \frac{1}{H^3} \right) + \frac{a}{3} \left(\frac{1}{(H+4a)^2} - \frac{1}{H^2} \right) + \frac{1}{6} \frac{1}{(H+4a)} - \frac{2}{(H+2a)} + \frac{1}{(H)} \right]$$

$$\left. + \frac{0.000351\lambda^2}{\pi^2} \left[a^2 \left(\frac{1}{(H+4a)^4} + \frac{2}{(H+2a)^4} + \frac{1}{H^4} \right) + \frac{2a}{3} \left(\frac{1}{(H+4a)^3} - \frac{1}{H^3} \right) + \frac{1}{6} \left(\frac{1}{(H+4a)^2} - \frac{2}{(H+2a)^2} + \frac{1}{H^2} \right) \right] \right\} \qquad (10)$$

and for the sphere-plate system

$$V_{S\text{-}P_{ret}} = -\frac{A\lambda}{\pi}\left\{ 0.04083\left(\frac{4a^3}{H^2(H+2a)^2}\right) - \frac{0.006028\lambda}{\pi}\left(\frac{8a^3(H+a)}{H^3(H+2a)^3}\right) + \frac{0.0009365^2}{\pi^2}\left(\frac{a^3(5H^2+10Ha+6a^2)}{H^4(H+2a)^4}\right)\right\} \qquad (11)$$

If the two bodies are composed of the same material and the medium between the bodies is not a vacuum, then the medium will have a "Hamaker constant" different from the solid bodies, and, in consequence, the total "Hamaker constant" will have a value intermediate between the bodies and the medium. Hamaker[4] showed that the value of the effective "Hamaker interaction constant" is given by

$$A = A_{11} - 2A_{12} + A_{22} \qquad (12)$$

where A_{11} is the "Hamaker constant" for the solid bodies and A_{22} is the "Hamaker constant" of the medium. A_{12} is the "Hamaker constant" for the interaction of the solid body with the medium, and is given approximately (provided the London frequencies are similar for the two materials) by

$$A_{12} = \sqrt{A_{11}\cdot A_{22}} \qquad (13).$$

Hence

$$A = \left(\sqrt{A_{11}} - \sqrt{A_{22}}\right)^2 \qquad (14).$$

If the two solid bodies are composed of different material, then the problem becomes more complicated; the total "Hamaker constant" for interaction becomes

$$A = A_{13} - A_{12} - A_{32} + A_{22} \qquad (15).$$

where A_{33} is the "Hamaker constant" for one of the solid bodies. In equation (15) only one of the four terms on the right-hand side is known and consequently for two bodies of different material interacting leads to uncertainties to the value of the "Hamaker constant" to use. Even for the case of equation (14) where both A_{11} and A_{22} are known, their values are by no means precisely known. For instance, the values of the "Hamaker constant" for polystyrene determined theoretically and experimentally[10-12] from coagulation data show wide differences in value (10^{-14} - 5×10^{-13}).

The foregoing method of calculating the van der Waals interaction energy between bodies has three major short comings. (1) The "Hamaker constant" is known only for a few pairs of atoms or molecules. (2) In the condensation to solids, the atoms or molecules may undergo such changes that the calculation of the van der Waals forces on the basis of free atoms or molecules is in error. (3) Retardation effects can be calculated only for a limited range of separation distances.

Lifshitz[13] developed a physically more satisfactory approach for calculating the interaction energy between bodies. He

started directly from the electronic properties of the interacting macroscopic bodies and calculated their van der Waals attraction from the imaginary parts of their complex dielectric constants. Owing to mathematical difficulties, only the case of parallel plate interactions has received any detailed study. In this treatment a constant $\hbar\bar{\omega}$ is obtained dependent only on the nature of the materials of the bodies. $\hbar\bar{\omega}$ is called the Lifshitz-van der Waals constant in which $\hbar$ is Planck's constant and $\bar{\omega}$ is given by

$$\bar{\omega} = \int_0^\infty \frac{\varepsilon_1(i\xi) - 1}{\varepsilon_1(i\xi) + 1} \cdot \frac{\varepsilon_2(i\xi) - 1}{\varepsilon_2(i\xi) + 1} \cdot d\xi \qquad (16)$$

where $\varepsilon_1(i\xi)$ is the imaginary part of the dielectric constant of body(1) and $\varepsilon_2(i\xi)$ is the imaginary part of the dielectric constant of body(2). Also $\hbar\bar{\omega}$ is related to the "Hamaker constant" by

$$\hbar\bar{\omega} = \frac{4}{3}\pi A \qquad (17).$$

For the case of a liquid medium between the two plates Dzyaloshinskii, Lifshitz and Pitaevskii[14] found that the Lifshitz-van der Waals constant is given by

$$\hbar\bar{\omega} = \int_0^\infty \frac{\varepsilon_1(i\xi) - \varepsilon_3(i\xi)}{\varepsilon_1(i\xi) + \varepsilon_3(i\xi)} \cdot \frac{\varepsilon_2(i\xi) - \varepsilon_3(i\xi)}{\varepsilon_2(i\xi) + \varepsilon_3(i\xi)} \cdot d\xi \qquad (18)$$

In principle $\hbar\bar{\omega}$ can be evaluated from direct physical measurements on the systems under investigation. However, the Lifshitz-

van der Waals constant has been worked out fully only for a few metals and non-metals in vacuo and for even fewer cases immersed in water[15]. Consequently, until more information is available, it will be necessary to rely on the values in existenoe of the "Hamaker constant".

4.4. The Total Potential Energy Curves and the Stability of Colloids

Total potential energy curves were presented by Verwey and Overbeek[2]. These curves were produced by the summation of the double-layer repulsion energy and the van der Waals attraction energy

$$V = V_R + V_A \qquad (19)$$

It is found that there exists a potential energy barrier, the magnitude of which, for a given Hamaker constant, depends upon both the surface potential of the colloidal particles and the conoentration of electrolyte. At high surface potential and low electrolyte concentration this energy barrier is high and hence the sol is stable. A reduction of potential and increase in eleotrolyte concentration or both reduces the height of the energy barrier till a state is reached where no barrier exists. In this case the resulting sol is completely unstable, and rapid coagulation oocurs. However, there is no sharp transition between stability and instability; as the potential energy

barrier increases the sol becomes more and more stable. In the region between instability and complete stability the sol is said to be in a state of "slow coagulation". The general form of the potential energy curves is shown in Fig.(4.1).

Verwey and Overbeek[2] also showed that at large distances of separation and for fairly large particles there is a further potential energy minimum, called the "secondary minimum", which arises from the fact that the double-layer repulsion energy falls off more rapidly than the van der Waals attraction energy. If this "secondary minimum" is a few kT units deep, it is expected that coagulation of the sol particles into this minimum would occur. As there is no energy barrier to coagulation, the coagulation into this minimum is reversible and hence "slow coagulation" results. Also on dilution of the coagulated sol, or reduction in electrolyte concentration (which leads to a higher repulsion energy and disappearance of the "secondary minimum") the sol should spontaneously re-disperse.

4.5. The Kinetics of Coagulation

Von Smoluchowski[16] was the first to consider the problem of the kinetics of coagulation. His treatment concerned the case of rapid coagulation, in which every encounter between particles leads to a permanent contact. The rate of this coagulation is then solely controlled by Brownian diffusion. He found that the number of i-fold particles present after a time t (ν_i) is

fig.(4.1) THE GENERAL FORM OF THE TOTAL POTENTIAL ENERY CURVES FOR THE INTERACTION OF A PAIR OF SPHERICAL COLLOIDAL PARTICALS.

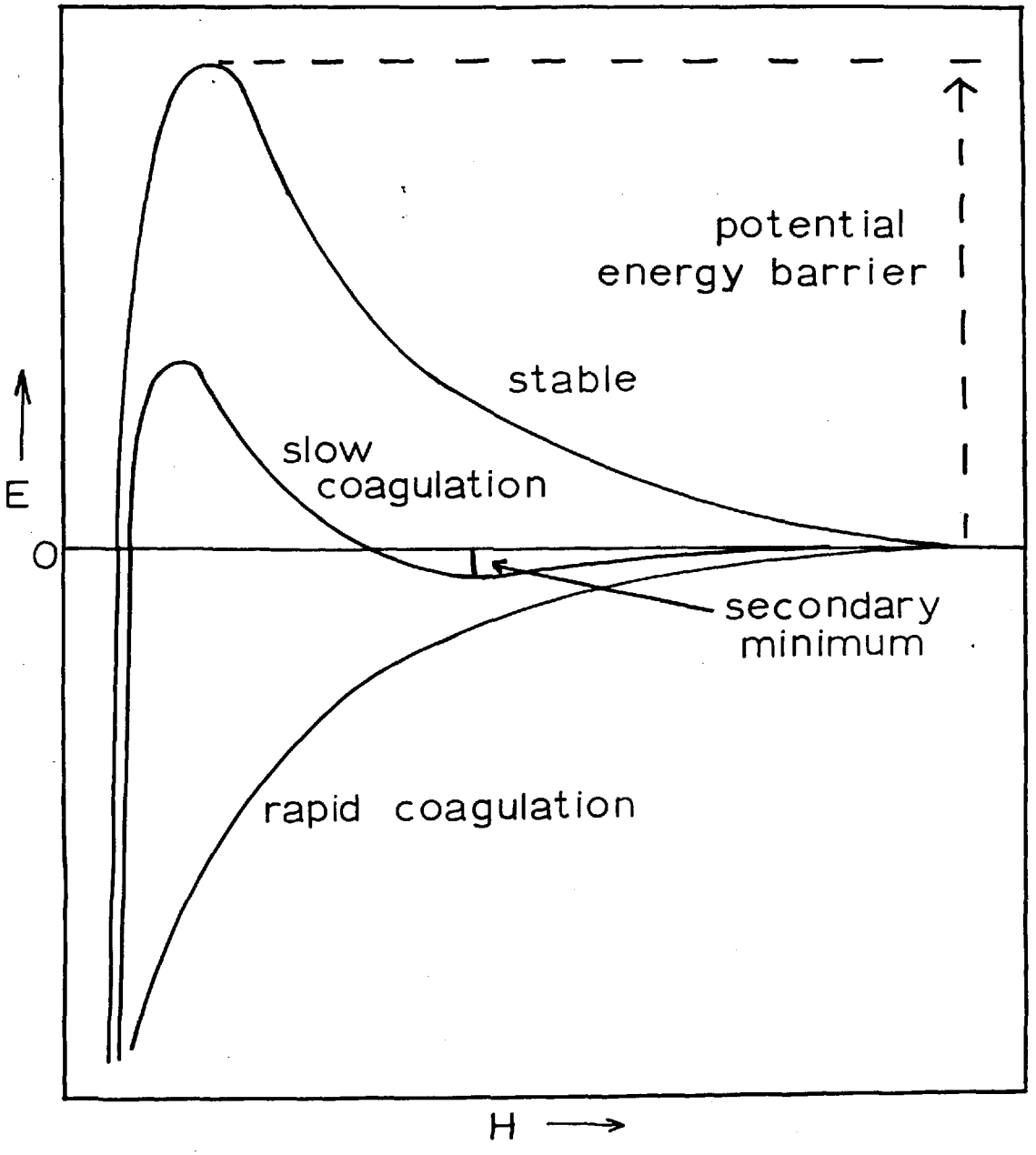

$$\sum_{i=1}^{\infty} i = \frac{\upsilon_0}{1 + t/T} \qquad (20)$$

where υ_0 is the original number of particles and $\underline{T}$ is called the coagulation time, giving the time in which the number of particles is just halved. $\underline{T}$ is given by

$$T = 1/4\pi Da\upsilon_0 \qquad (21)$$

where $\underline{D}$ is the diffusion coefficient of the particles, usually represented by the Stokes-Einstein equation,

$$D = kT/6\pi\eta a \qquad (22)$$

where η is the viscosity of the liquid.

Smoluchowski assumed that the differenoe between rapid and slow coagulation arose from the faot that in the former every encounter lead to contact whilst in the latter only a fraction $\underline{\alpha}$ of the encounters lead to contact. The oourse of coagulation is then fully desoribed by equation (20), and only the time of coagulation changes,

$$T = 1/4\pi Da\upsilon_0\alpha \qquad (23)$$

Consequently, he considered that all coagulation-time curves

should be transformable into each other simply by changing the time scale. However, there was no theory giving the relation between the factor α and the magnitude of double-layer potential etc.

Fuchs[17] analysed the problem of the kinetics of coagulation from a different standpoint. He considered, in the case of considerable interaction between particles, the diffusion equations determining their encounters should be solved for diffusion in a field of force. Using this method Derjaguin[18] derived an expression for the stability ratio of colloidal sols. The stability ratio is the ratio of the rate of rapid coagulation to the rate of slow coagulation, given by

$$W = 2a \int_{2a}^{\infty} \frac{\exp(V/kT)dH}{H^2} \qquad (24)$$

Equation (24) can be solved completely only by numerical integration, though a useful approximation is given by Verwey and Overbeek[2] as,

$$W = \frac{\exp(V_{max}/kT)}{2\chi a} \qquad (25)$$

where V_{max} is the value of the potential energy barrier. Thus with the use of equation (25), measurements of coagulation rates should give a value to the potential energy barrier, and with the knowledge of the values of surface potential, the Hamaker constant for the particles can be evaluated.

4.6. Empirical Stability Relations

Several empirical relations for colloid stability have been presented. Ostwald[19] postulated that the coagulation concentration of electrolyte corresponds to the same logarithm of the activity coefficient of the dissociating ions.

$$- \log f = \text{const.} \tag{26}$$

He claimed that the coagulation is proportional to a $^{1}/_{6}$th. power of the valency. This result has been confirmed from the D.L.V.O. theory of colloid stability, where the coagulating concentration (zero energy barrier) is given by

$$\frac{C}{100} = \frac{(107)^3 (kT)^5 \gamma^4}{A^2 Z^6 e^6 N} \tag{27}$$

Eilers and Korff[20] proposed that a critical zeta-potential is required for colloid stability, and suggested that,

$$\frac{\zeta}{\varphi_2} = 1/\text{const.} \tag{28}$$

and that providing the constant was greater than 0.5×10^{-2} the sol would be stable. Derjaguin[1] showed from the D.L.V.O. theory of colloid stability that an approximate expression connecting zeta potential and surface potential is

$$\frac{A\kappa}{\varepsilon\psi_o^2} = \text{const.} \qquad (29)$$

Reerink and Overbeek[21] have produced an empirical expression connecting the stability ratio and the coagulating concentration of electrolyte. Their expression is

$$-\ln W = k_1 \ln C_e + k_2 \qquad (30)$$

where k_1 and k_2 are constants and C_e is the electrolyte concentration for coagulation. They showed theoretically, using approximate equations from the D.L.V.O. theory of colloid stability, that

$$d \ln W/d \ln C_e = - 2.06 \times 10^7 (a\gamma^2/z^2) \qquad (31)$$

at 25°C. However, equation (31) can be correct only for $\kappa H_m = 1$ and H_m/a = a constant, where H_m is the distance of maximum potential from the surface. Consequently equation (31) should be applied only when $W \to 1$ (i.e. over a small range of W). By the same treatment the coagulating concentration (W = 1) is given by,

$$\kappa_{coag} = 2.04 \times 10^{-5} \gamma^2/Az^2 \qquad (32)$$

Equation (32) has been used extensively by Ottewill[10] for the determination of the Hamaker constant from coagulation data. For

really reliable values of Hamaker constant the complete set of potential energy curves should always be constructed, and values of Hamaker constant fitted for experimental stability ratios.

4.7. References

(1) Derjaguin, B.V. and Landau, L. Acta Physicochim. URSS 14, 633, (1941).

(2) Verwey, E.J.W. and Overbeek, J. th. G. "The Theory of the Stability of Lyophobic Colloids", Elsevier, (Amsterdam),(1948).

(3) Van der Waals, J.D. Thesis, University of Leyden, the Netherlands, (1873).

(4) London, F. Z. Phys. 63, 245, (1930).

(5) Hamaker, H.C. Physica 4, 1058, (1937).

(6) Clayfield, E.J. and Lumb, E.C. J. Coll and Interface Sci. 22, 269, (1966).

(7) Casimir, H.B.G. and Polder, D. Phys. Rev. 73, 360, (1948).

(8) Schenkel, J.H. and Kitohener, J.A. Trans. Faraday Soc. 56, 161, (1960).

(9) Clayfield, E.J. and Lumb, E.C. Proc. of the Vth International Congress of Surface Active Agents, Barcelona, (1968), in Press.

(10) Ottewill, R.H. and Shaw, J.N. Disc. Faraday Soc. 42, 154, (1966).

(11) Watillon, A. and Joseph-Petit, A.-M. Disc.Faraday Soc. 42, 143, (1966).

(12) Fowkes, F.M. Ind. Eng. Chem. 56, 40, (1964).

(13) Lifshitz, E.M. Soviet Phys. J.E.T.P., 2, 73, (1956).

(14) Dzyaloshinskii, I.E., Lifshitz, E.M. and Pitaevskii, L.P., Soviet Phys. J.E.T.P. 37, 161, (1960).

(15) Krupp, H. Adv. in Coll. and Interface Sci. 1, 111, (1967)

(16a) Von Smoluchowski, M. Z. Phys. 17, 557, 585, (1916).

(16b) Von Smoluchowski, M. Z. Phys. Chem. 92, 129, (1917).

(17) Fuchs, N. Z. Phys. 89, 736, (1934)

(18) Derjaguin, B.V. Trans. Faraday Soc. 36, 203, (1940).

(19a) Ostwald, Wo. Koll. Z. 73, 301, (1935).

(19b) Ostwald, Wo. Koll. Z. 83, 1, (1939).

(20) Eilers, H. and Korff, J. Trans. Faraday Soc. 36, 229, (1940).

(21) Reerink, H. and Overbeek, J. th. G. Disc. Faraday Soc. 18, 74, 1954).

5.0 PREPARATION OF MODEL COLLOIDS BY POLYMERISATION

5.1. Introduction

In order to employ or to verify the theory of colloid stability outlined in previous chapters, it is neoessary to prepare dispersions with well-defined particles of uniform size. It has been shown[1] that sols of narrow size range oan be prepared by the emulsion polymerisation technique. Also, by varying the conditions and reagents used in the polymerisation, the type and magnitude of the surface groupings oan be varied to produce different sol characteristics. For example, by using persulphate as initiator and long chain alkyl sulphates as stabilizers, polystyrene latex sols can be produoed which have sulphate surface groupings of sufficient number that the sols are completely stable in the absence of added detergent. In this case the deposition of these latexes (for example, on to positively charged surfaces) can be studied in the absence of added detergent, so that both surfaces can retain their charge characteristics during the deposition, without coagulation of the sol occurring. Such latex particles should be an ideal model system for the test of the D.L.V.O. theory of colloid stability.

In this chapter the preparation of a "monodisperse" polystyrene latex sol is described, and also the preparation of a positively charged plastic by the co-polymerisation of styrene with

vinyl-pyridine. To obtain a latex of narrow size-range, attention has to be given to the principles of emulsion polymerisation.

5.2. The Theory of Emulsion Polymerisation

A theory of emulsion polymerisation was presented by Harkins[2] in 1947. According to Harkins, with relatively insoluble monomers, nearly all of the polymer particle nucleii are initiated in the monomer solubilized in the interior of the micelles of the surface-active agent. In consequence, the total number of polymer particles produced depends upon the number of micelles present. As the polymer is formed the surface-active agent adsorbs on its surface and when the concentration of free surface-active agent is reduced to a level at which no micelles are present, then no more polymer particles are formed.

The micelles of the surface-active agent produce only an insignificant fraction of the polymer, which "grows" on the polymer thus initiated. This occurs by the polymerisation of the monomer present in the swollen polymer particle, the monomer being supplied by diffusion, from the monomer emulsion droplets, through the aqueous phase and into the polymer particle, forming monomer-polymer particles.[3] The emulsion droplets, therefore, serve only as a distributed reservoir of monomer and no particle formation occurs in them. For moderately soluble monomers (e.g. vinyl acetate) new polymer particles can readily be produced in the absence of micelles[4] in the presence of

"growing" polymer particles, whereas for an insoluble monomer (e.g. styrene) no new polymer particles are formed in this situation.

It has been shown[1b] that the rate of "growth" of the polymer particles is dependent upon the size of the "growing" polymer particles. Small particles "grow" faster than large ones, and, therefore, this differential rate tends to produce latexes in which the size distribution of the polymer particles is narrow.

A free-radical mechanism is proposed for the polymerisation of styrene.[5,1a] A common source of free-radicals is potassium persulphate

$$\overset{\ominus}{O} - SO_2 - O - O - SO_2 - \overset{\ominus}{O} \longrightarrow 2\,\overset{\ominus}{O} - SO_2 - O\bullet \qquad (1)$$

The polymerisation then proceeds by the following course of reactions:-

$$\overset{\ominus}{O} - SO_2 - O\bullet + ph - CH = CH_2 \longrightarrow ph - CH = CH\bullet + HSO_4^{\ominus} \qquad (2)$$

$$ph - \dot{C} = CH_2$$

$$ph - CH = CH\bullet + ph - CH = CH_2 \longrightarrow ph - (CH_2)_2 - \underset{ph}{CH} = CH\bullet \qquad (3)$$

or

$$ph - \dot{C} = CH_2 + ph - CH = CH_2 \longrightarrow ph - \underset{ph}{C} = CH\bullet \quad ph - CH - CH_3 \qquad (4)$$

The reaction is terminated by either a polymer free-radical interacting with a monomer free-radical,

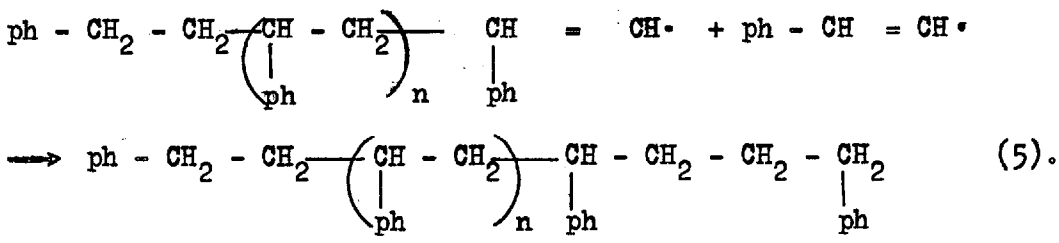

(5).

or by a polymer free-radical interacting with a sulphate free radical

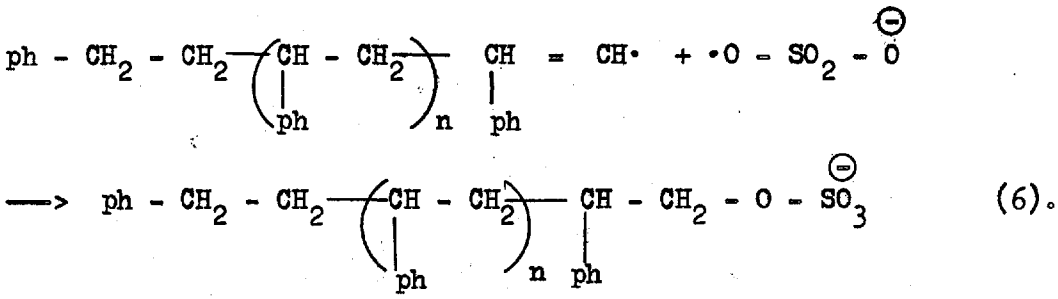

(6).

If the persulphate concentration is raised, the polymerisation rate increases and the rate of chain termination increases, yielding a low molecular weight polymer with a high density of terminal sulphate groups. It has also been shown[6] that if the persulphate concentration is high, chain branching can occur. However, this occurs only if the polymerisation is taken to high conversion values. In general, for the production of latexes for studies of colloid stability, the conversion rarely exceeds 70% and may be as low as 50%.

5.3. The Preparation of a "Monodisperse" Polystyrene Latex Sol by Emulsion Polymerisation

It was required that the polystyrene latex sol had a high surface charge density. Consequently, it was necessary for all polymerisations to be performed with fairly high concentrations of the initiator, potassium persulphate. To maintain only sulphate groups on the surface, the stabilizing surface-active agent used was an alkyl sulphate. Sodium octadecyl sulphate (SOS) was used because of its low c.m.c. ($\simeq 10^{-5}$M under the conditions used). It was expected that the amount of free SOS that would have to be eventually removed by dialysis would be small and could, consequently, be removed comparatively quickly.

The materials used were as follows. Styrene (Hopkins and Williams Ltd.) contained about 20 ppm of tert-butyl catechol as a stabilizer and consequently, the sample was freshly distilled at 42°C before each polymerisation. The sodium octadecyl sulphate was kindly supplied by Dr. G.A. Johnson of the Unilever Research Laboratories, Port Sunlight and the potassium persulphate was of "Analar" grade.

The first method of emulsion polymerisation tried was that used by Johnson[7] for polyvinyl acetate and was as follows:-

To 300 ml of 2 x 10^{-5}M sodium octadecyl sulphate solution, in a 500 ml round-bottomed flask, 5 g of potassium persulphate were added. Then 50 ml of freshly distilled styrene was added and the

mixture stirred vigorously to emulsify the styrene. The mixture was then placed in a water bath at 70°C, with constant stirring for six hours. The latex sol obtained was filtered through a Whatman No.541 filter paper to remove large aggregates. It was then dialysed at room temperature for two weeks against distilled water in a well-boiled "Visking" cellophane dialysis bag.

The resulting dialysed latex was examined under the electron microscope (Fig.5.1). It is seen that this sol is far from "monodisperse", and it was "grown" further. This was performed in the following manner.

50 ml of the "seed latex" (the one to be "grown" further) and 42 ml of freshly distilled styrene and 1.5 g potassium persulphate were added to 250 ml of distilled water contained in a 500 ml round-bottomed flask. The mixture was polymerised with constant stirring for 12 hrs at 65°C. No surface-active agent was added as the particles seemed sufficiently stable and without any surface-active agent no new particles should be formed. The resulting latex was dialysed against distilled water for two weeks.

The electron micrographs of this latex are shown in Fig.5.2. In this case the growth stage has evened out the size distribution of the large particles, as expected, but new particle formation has occurred. The large particles are about 2μ in diameter, and it has been found[8] that there appears to be an upper size limit for polystyrene latex particles. It thus appears that above a certain

FIG (5.1) ELECTRON-MICROGRAPH OF LATEX "A"

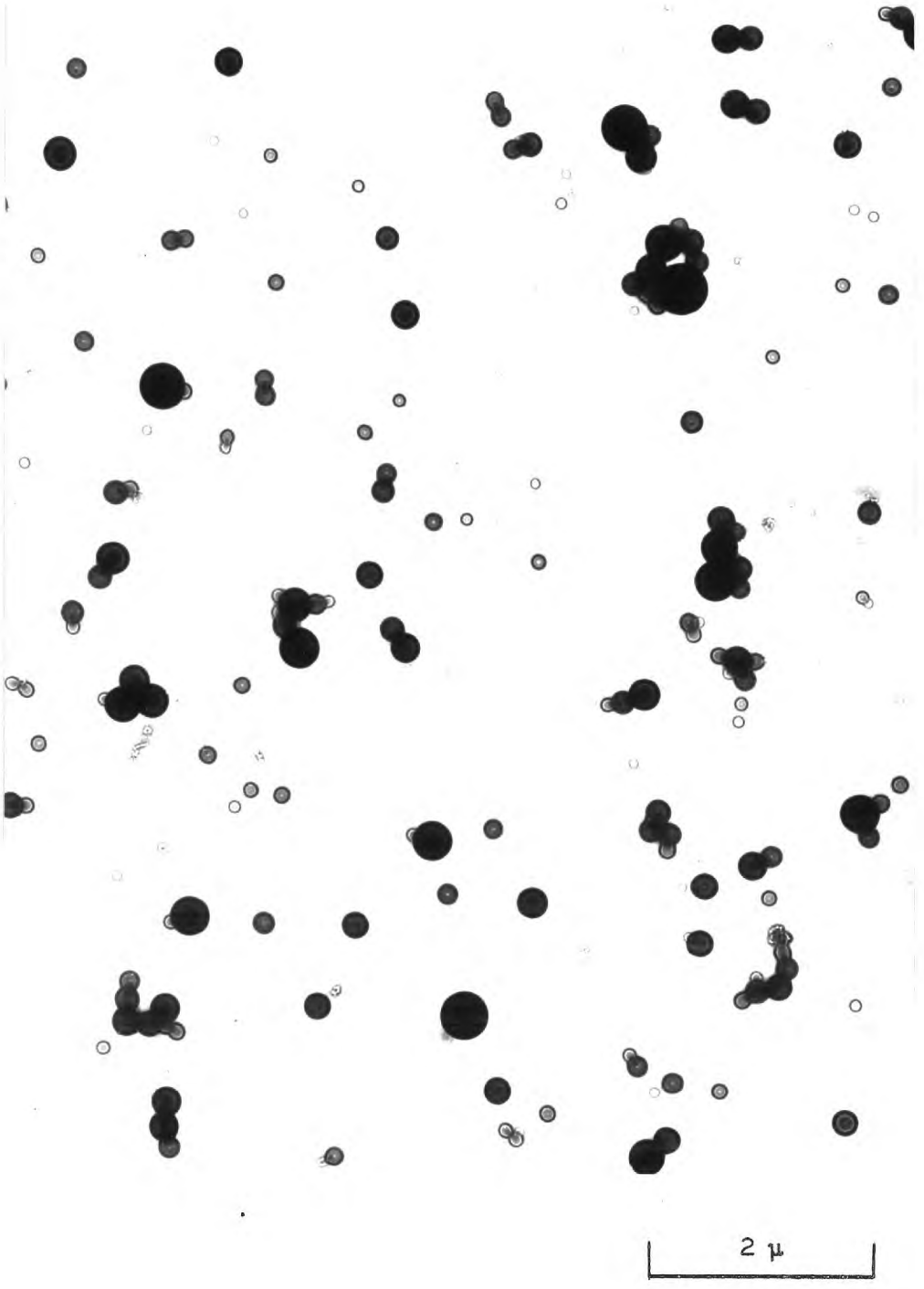

FIG (5.2) ELECTRON-MICROGRAPH OF LATEX "B"

size the probability of the initiation of a polymer free-radical is less than for monomer free-radical formation outside the polymer particle leading to new particle formation. Once formed these new particles will "grow" further and as their size increases, their size distribution gets more and more narrow. It would thus be expected that if a number of latex partioles have reached their maximum size and new particle growth has occurred, then a bi-modal distribution of particle size should occur. This is what is found (Fig.5.2). It was consequently concluded that a different approach to the preparation of the latex sol was required, with more stringent conditions.

5.3.1. Dialysis

During dialysis three components are removed from the latex sol; (a) the initiator, (b) the surface-active agent (only from the "seed" latex) and (c) any unreacted monomer styrene.

(a) Tests showed that the initiator was readily removed by dialysis at room temperature, the extent of removal being determined by the changes in conductivity of the water against which the dialysis was carried out. By dialysing against 10 l of distilled water with changes every 12 h, it required only three changes for the initiator to be completely removed.

(b) The surface-active agent (SOS) is sparingly soluble at room temperature, but very soluble at 70°C. It was, therefore, expected that at a concentration of 2×10^{-5}M at room temperature the surface-active agent would be colloidally dispersed, resulting in a very prolonged dialysis for removal. Therefore, dialysis was tried at 70°C, when the surface-active agent would be in solution and more readily removed. It was found that a week was required to reduce the concentration of the sodium octadecyl sulphate to a level below 10^{-6}M, with changes of water every 12 h. as indicated by foaming tests. As the seed sol (the only one stabilized) would be diluted by a factor of 6 in the growth stage, and by a further factor of from 500 to 50,000 in the deposition experiments, this surface-active agent level was considered suitable for experimental purposes.

(c) In no case was the polymerisation taken to completion and therefore a certain amount of monomer remained in the latex sol. The presence of monomer leads to softness of the particles and deformation in the electron microscope. This could be removed effectively from the sol only by dialysis at 70°C, which took from one to two weeks depending upon the stage of the "growth" of the particles. The extent of removal was followed by the colour changes produced by the reaction of the "free styrene" with alkaline permanganate solution. The colour after five minutes was as follows:-

Yellow	> 4×10^{-2}% styrene
Green	4×10^{-3}% styrene
Purple	< 8×10^{-4}% styrene.

Dialysis was, therefore, continued until a permanent purple colour was obtained for five minutes or longer, at which stage the sol was considered sufficiently free of monomer for experimental purposes.

The dialysis procedure subsequently used in all polymerisations was to dialyse at room temperature over-night to remove the initiator (at this temperature further polymerisation should be negligible), and then to complete the dialysis at 70°C.

5.3.2. Preparation of the Seed Latex (1)

The seed latex was prepared in order that the size of the particles was small, and "growth" could be carried out without approaching the optimum size limit. The procedure was as follows:

To 2×10^{-5}M sodium octadecyl sulphate (300 ml), in a 500 ml round-bottomed flask at 65°C, was added freshly distilled styrene (2 ml). This mixture was then emulsified by shaking and ultrasonic treatment for 30 minutes. The flask was then put into a water bath at 65°C, and nitrogen ("white spot" grade) bubbled through for ten minutes. Then potassium persulphate (0.5 g) was added and the polymerisation continued for three hours, using nitrogen bubbles for agitation. (Too high a rate of bubbling had to be avoided, as the system had a tendency to foam). The sol was then

dialysed fully as described previously.

The dialysed sol was examined in the electron microscope and the electron micrograph is shown in Fig.(5.3). The mean particle diameter was 0.192 $\pm$ 0.03μ, and their size distribution is shown in Fig.(5.5). These particles were too small for easy optical examination in deposition experiments and were thus "grown" further.

5.3.3. Preparation of Growth Latex (2)

In this stage it was considered essential for the latex particles to reach equilibrium with the monomer styrene before the initiator was added, so that most of the monomer styrene would be within the polymer particles, reducing the probability of new particle formation. Latex (1) was sufficiently stable that no further surface-active agent was required in this stage. The experimental procedure was as follows:-

Fully dialysed latex (1) (50 ml) was diluted to 300 ml with distilled water in a 500 ml round-bottomed flask. To this was added freshly distilled styrene (3 ml), and the mixture was shaken periodically at room temperature for one hour. Then the flask was placed in a water bath at 65^{o}C, with nitrogen passing through it for one hour. Potassium persulphate (0.3 g) was then added and the polymerisation carried out for three hours with nitrogen bubbles for agitation. The latex was then dialysed (as previously described) for two weeks.

FIG (5.3) ELECTRON-MICROGRAPH OF LATEX (1)

fig.(5.5) PARTICLE SIZE HISTOGRAM FOR LATEX (1).

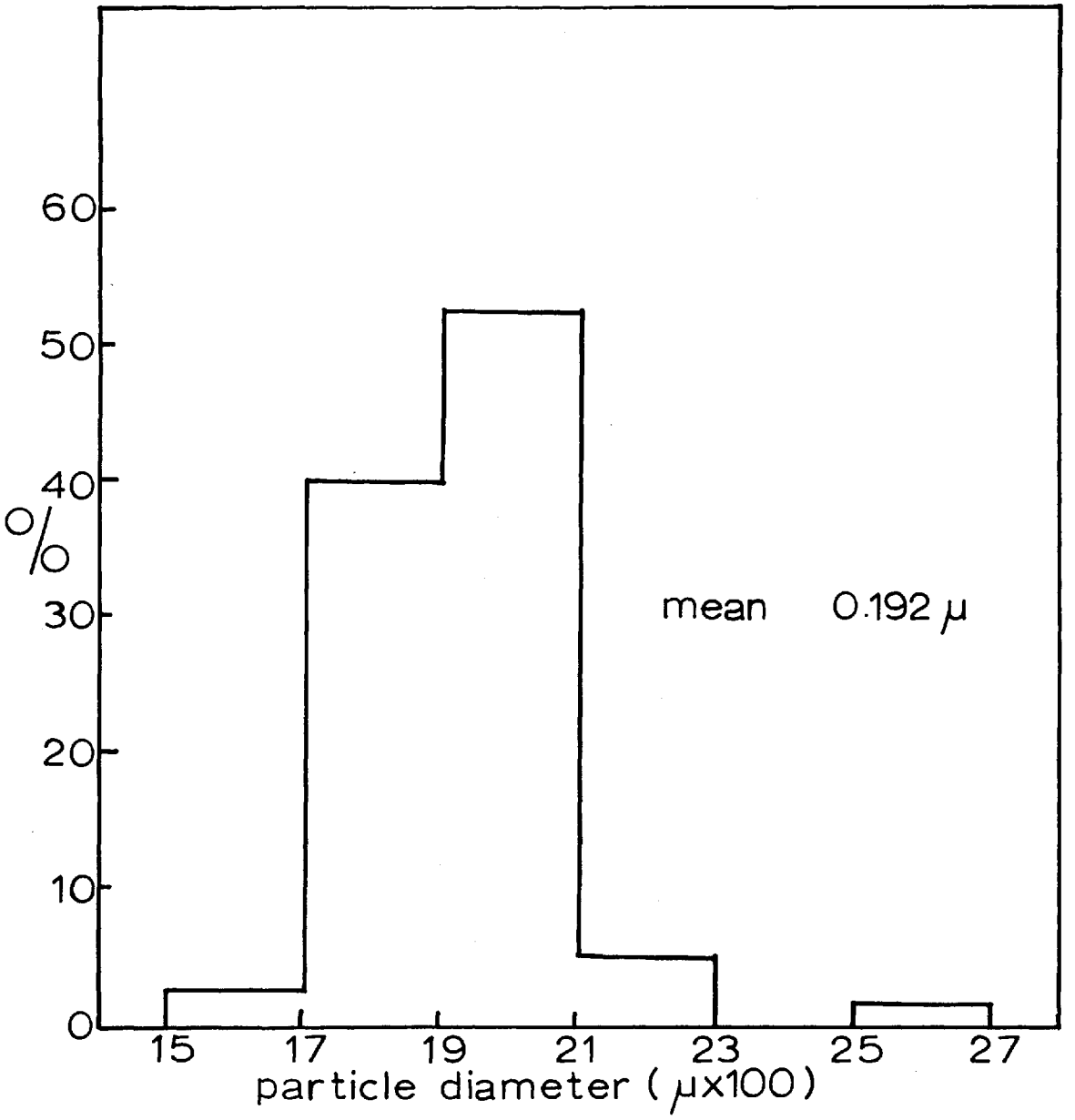

Latex (2) was examined in the the electron microscope, Fig.(5.4), and its size distribution determined Fig.(5.6). This sol was closely "monodisperse" with a mean diameter of 0.308 $\pm$ 0.001μ. This sol was used for all subsequent investigations.

5.3.4. The Determination of the Concentration of Latex (2)

The concentrated latex sol (which contained c. 10^{11} particles/ml) was kept with 0.1% potassium persulphate to act as a fungicide, for it was observed that with the first latexes produced, mould did form. The latex was dialysed and diluted as required. The working sol had a concentration from 10^9 to 10^{10} particles/ml. The determination of particle concentration was a tedious process and consequently after an initial determination the concentration of fresh sols was determined by turbidity measurements.

The latex sol as prepared was extremely stable, and it was not possible to determine the concentration by centrifugation and weighing of the solid content.

An attempt was made to measure the concentration gravimetrically by evaporating the sol to dryness, but as the weights involved were very small, it was not possible to make an accurate determination. Therefore, it was decided to determine the sol concentration by particle counting in a haemacytometer cell.

One of the major difficulties in this determination was the

FIG (5.4) ELECTRON-MICROGRAPH OF LATEX (2)

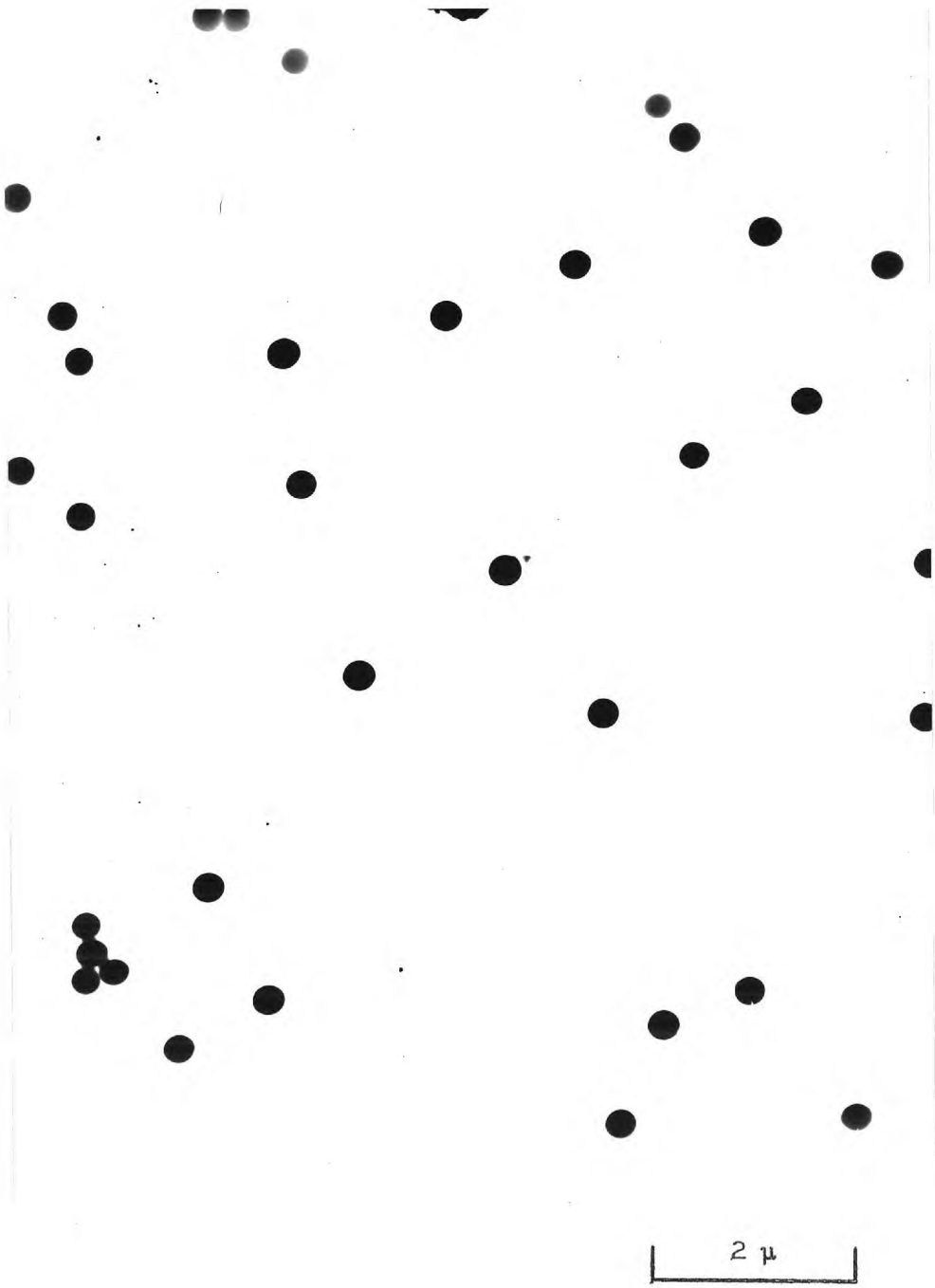

fig.(5.6) PARTICLE SIZE HISTOGRAM FOR LATEX (2).

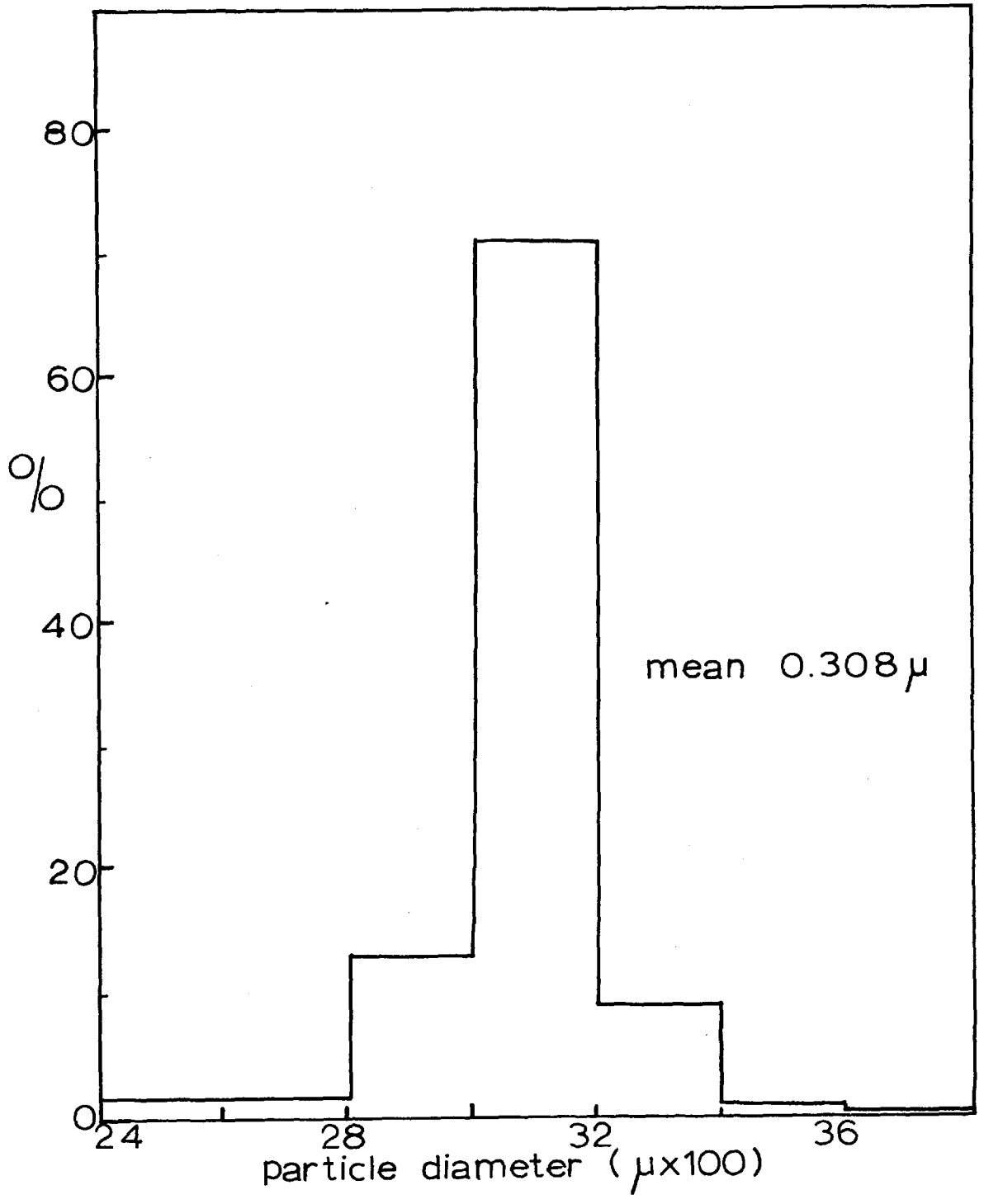

removal of deposited latex particles after each determination. The cleaning procedure used was to wash the cell and cover-slips in benzene and then to subject them to 30 minutes of an ultrasonic cleaning bath in an aqueous solution of a non-ionic detergent, finally rinsing well with distilled water. Eleven determinations, comprising counts over 200 squares in each determination, were made on a sol containing c. 10^8 particles/ml, and a mean value of $1.103 \pm 0.033 \times 10^8$ particles/ml was obtained. This is comparable to the approximate value obtained by the gravimetric technique of 1.06×10^8 particles/ml.

By dilution, the sol concentration as a function of turbidity was determined, Fig.(5.7), and from these data the particle concentration of the sol could be easily and quickly determined.

5.4. The Preparation of Poly-2-vinyl pyridine/styrene Copolymer

A plastic was required, having a fairly high positive surface charge so that maximum deposition rates of latex (2) on its surface could be studied. When conventional emulsion polymerisation was used, the negatively charged sulphate groups outweighed the positive charge effect of the pyridine nitrogen, even though cetyl trimethyl ammonium bromide was used as the stabilizer. It is probable that even with a weak initiator (H_2O_2), which would produce terminal carboxyl groups, that the plastic would be only weakly positive with perhaps areas of negative charge. Consequently, solution polymerisation was used for the preparation of Poly-2-vinyl pyridine/

fig.(5.7) TURBIDITY AS A FUNCTION OF SOI CONCENTRATION FOR LATEX(2)

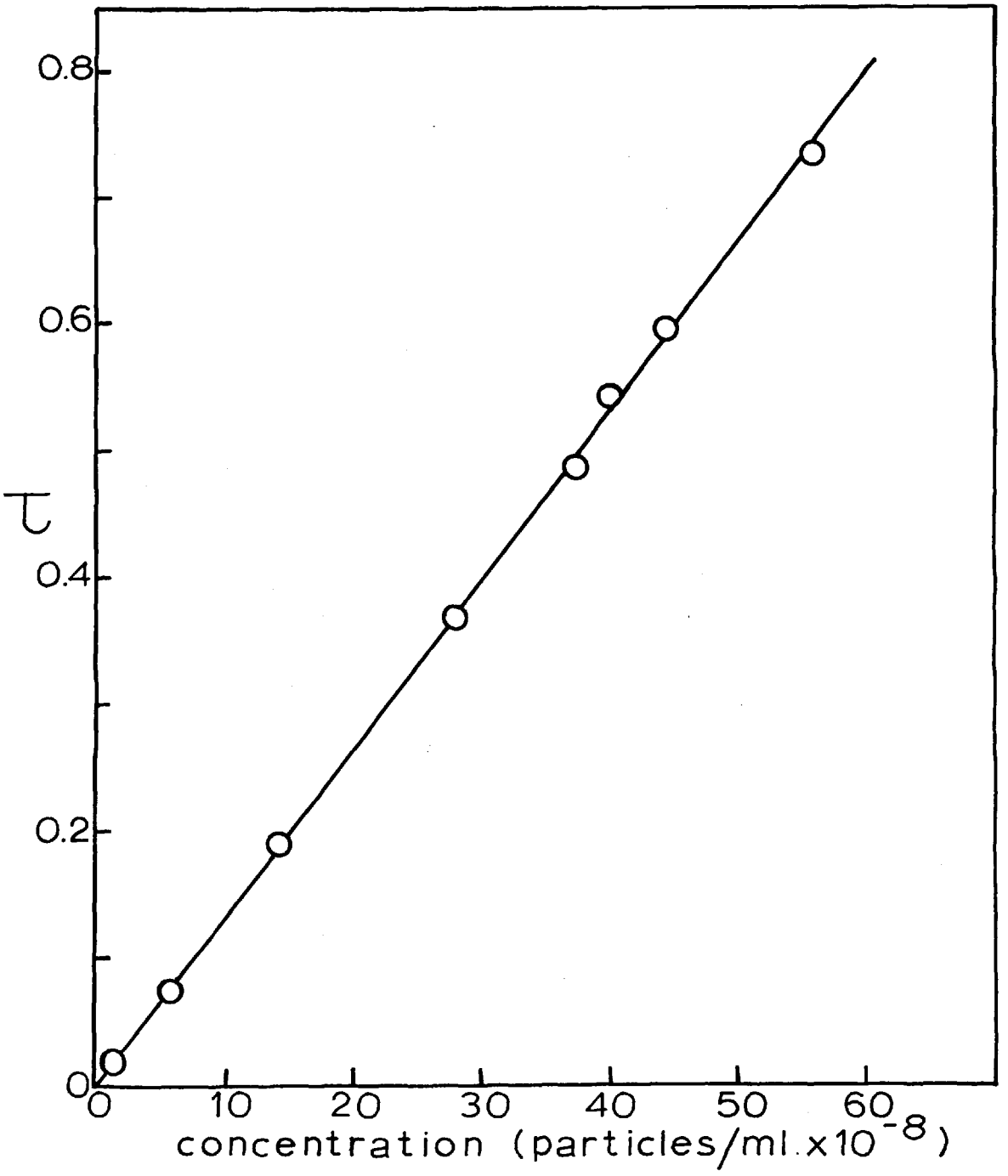

styrene copolymer. It was prepared in a similar manner to that described by Utsumi, Ida, Takahashi and Sugitomo,[9] namely, as follows:

To freshly distilled 2-vinyl pyridine (7.5 ml) (distilled at 70°C) and freshly distilled styrene (2 ml) in a 50 ml round-bottomed flask, methyl alcohol (2 ml) was added. Nitrogen was passed for one hour at room temperature and then benzoyl peroxide (0.1 g) was added. Nitrogen was bubbled through the mixture at room temperature for 12 h and the flask was wrapped in black paper to exclude light. By this time the viscosity of the solution had increased considerably and it was no longer feasible to pass nitrogen. The flask was then sealed and kept in the dark for two days at room temperature. At this stage the polymer was solid in the bottom of the flask and was clear golden brown in colour. The polymer was dissolved in chloroform and reprecipitated with ether to purify it. This procedure was performed twice. The polymer thus produced contained c.80% 2-vinyl pyridine and later gave a zeta-potential of +72 mV in distilled water. This polymer was used in subsequent investigations of maximum deposition rates.

A negatively charged substrate was prepared from the commercial polymer "Formvar" (polyvinylformaldehyde) of electron microscopy grade supplied by Schawinigan Ltd.

Both polymers are insoluble in water but readily soluble in chloroform.

5.5. References

(1a) Ewart, R.H. and Carr, C.I. J. Phys. Chem. 58, 640, (1954).

(1b) Vanderhoff, J.W., Vitkuske, J.F., Bradford, E.B. and Alfrey Jr. T.A. J. Polymer Sci. 20, 225, (1956).

(1c) Bradford, E.B. and Vanderhoff, J.W. J. Polymer Sci. Polymer Symposia No.3, 41, (1963).

(2a) Harkins, W.D. J.Amer.Chem.Soc. 69, 1428, (1947).

(2b) Harkins, W.D. J. Polymer Sci. 5, 217, (1950).

(3a) Smith, W.V. J.Amer.Chem.Soc. 70, 3695, (1948).

(3b) Corrin, M.L. and Harkins, W.D. J. Polymer Sci. 5, 207,(1950).

(4) Patsiga, R., Litt, M. and Stannett, V. J.Phys.Chem. 64, 801, (1960).

(5) Smith, W.V. and Ewart, R.H. J. Chem. Phys. 16, 592, (1948).

(6) Henrici-Olivé, G. and Olivé, S. J.Polymer Sci. 48, 329, (1960).

(7) Johnson, G.A. Unpublished data.

(8) Gregory, J. Unpublished data.

(9) Utsumi, I., Ida, T., Takahashi, S., and Sugitomo, N. J. Pharm. Sci. 50, 592, (1961).

6.0 THE ROTATING DISC

6.1. Introduction

The rotating disc electrode has been used extensively by electrochemists[5-10], because the hydrodynamic mass transfer equations for it have been solved completely. Moreover, the diffusion flux is constant over the entire disc surface, giving a large uniform reaction area.

Marshall[1] first used this technique for the study of the deposition of colloidal particles on plane surfaces and obtained reproducible deposition measurements with this technique. Unfortunately, owing to the particular system studied, he was unable to test fully the hydrodynamic mass transfer equations as applied to particles of colloidal size.

In this chapter a rigorous test of the hydrodynamic mass transfer equations for the rotating disc system for particles of colloidal size is presented.

6.2. The Theory of the Rotating Disc

The equations for convective diffusion assume their simplest form when the surface of a rotating disc is taken as the reaction surface. Von Kármán[2] and later Cochran[3] solved the hydrodynamics

of the case in which a liquid is entrained by a rotating disc whose axis is perpendicular to its plane surface. Cochran's exact solution provides the following picture of fluid motion. Far from the surface, the fluid moves towards the disc surface, and in a thin layer immediately adjacent to the disc surface, the liquid acquires a rotating motion. The angular velocity of the liquid increases until at the disc surface it acquires the angular velocity of the disc. Furthermore, the fluid acquires a radial velocity under the influence of the centrifugal force. The velocity profile is shown in Fig.(6.1).

The exact solution of Cochran for the velocity profile is,

$$\left.\begin{aligned} V_r &= r\omega F(\zeta) \\ V_\varphi &= r\omega G(\zeta) \\ V_y &= (r\omega)^{1/2} H(\zeta) \\ p &= -\rho\nu\omega P(\zeta) \end{aligned}\right\} \qquad (1)$$

where V_r, V_φ, and V_y are the radial, tangential and axial velocities respectively, and p is the hydrostatic pressure. $\underline{r}$ is the radius of the disc surface, and $\underline{\omega}$ is the angular velocity of rotation. ρ is the density of the liquid and $\underline{\nu}$ is the kinematic viscosity of the liquid. ζ is the dimensionless distance from the disc surface, defined by

$$\zeta = (\omega/\nu)^{1/2} y$$

fig.(6.1) STREAMLINES FOR FLOW TO THE SURFACE OF A ROTATING DISC.

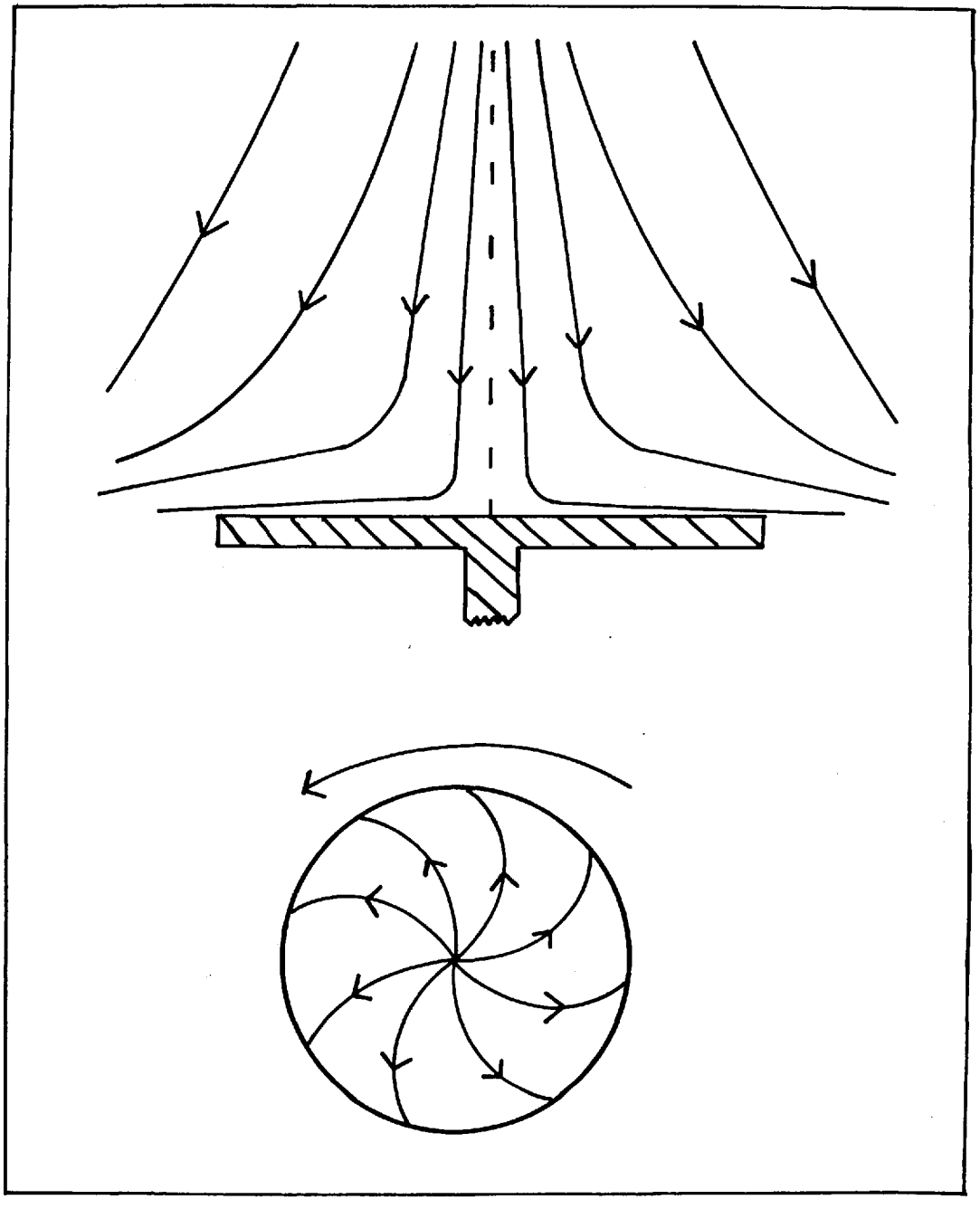

where y is the axial distance from the surface. The functions $F(\zeta)$, $G(\zeta)$, $H(\zeta)$ and $P(\zeta)$ were tabulated by Cochran. These velocity-distance relations will be considered in more detail later.

Levich[4], using the data of Cochran, solved the case for the convective diffusion to the surface of a rotating disc in an infinite volume of fluid. He found that the equivalent diffusion boundary layer is constant over the entire surface of the disc, hence the mass flux to the surface is constant over its entire surface. Levich's expression for the mass transfer is

$$j = 0.62\, D^{2/3} \upsilon^{-1/6} \omega^{1/2} C_o \qquad (2)$$

where $\underline{D}$ is the diffusion coefficient and C_o is the concentration of particles per ml in the external solution.

Equation (2) has certain restrictions governing its use; (1) it is valid only in the laminar flow regime, which occurs theoretically in the range

$$10 < R_e < 10^5$$

where R_e is the Reynolds number, defined by

$$R_e = U_o \ell / \upsilon \qquad (3)$$

where U_o is the linear velocity of the fluid and ℓ is a "characteristic

length", (which can be equated to R the radius of the disc). Thus equation (3) for a rotating disc is,

$$R_e = \frac{2\pi R^2}{60\nu} \times \text{r.p.m.} \qquad (4)$$

Riddiford[5] claimed that in practical systems, uncontrollable convective currents are present below Reynolds numbers of 100. However, recently Daguenet and Robert[6] have shown, for an electrolytic process, that the diffusion is governed by equation (2) provided

$$60 < R_e < 2.7 \times 10^5 \qquad (5)$$

(2) Only if $R >> \delta_o$ can the edge effects of the disc be neglected. δ_o is the hydrodynamic boundary layer, given by

$$\delta_o = 3.6\,(\nu/\omega)^{1/2} \qquad (6)$$

(3) According to Riddiford and Gregory,[7] at low values of the Prandtl number (ν/D) the Levich equation requires modification. Their expression is

$$j = \frac{0.62\, D^{2/3} \nu^{-1/6} \omega^{1/2} c_o}{\left[1 + 0.35\,(D/\nu)^{0.36}\right]} \qquad (7)$$

However, Kishinevskii and Denisova[8], from a study of the dissolution rates of benzoic acid in water, have shown that the mass transfer follows equation (2) if the Prandtl number is greater than 1000. Otherwise equation (7) must be used. With colloidal particles of radius 0.1μ in water, the Prandtl number is about 10^6, using the Stokes-Einstein equation for the evaluation of the diffusion coefficient for the particles.

$$D = kT/6\pi\eta a \qquad (8)$$

where k is the Boltzman constant and T is the absolute temperature; a is the radius of the particles and η is the viscosity of the liquid medium.

There is one other case where the mass transfer may not be described by equation (2). That is when deposition can occur by "impaction".

Impaction occurs when a particle leaves its streamlines owing to its own inertia and deposits; under such circumstances, a higher deposition rate than expected from equation (2) would be observed. Fuchs[12] showed that this does not occur if the Stokes number (Stk) is very much less than 1.2. The Stokes-number is given by

$$Stk = \frac{2R_e \rho a^2}{9\rho_0 R^2} \qquad (9)$$

which for the rotating disc system on substituting for the Reynolds number is

$$\text{Stk} = \frac{\pi \rho a^2 \times \text{r.p.m.}}{135\eta} \qquad (10)$$

where ρ_0 and ρ are the density of the fluid and of the particles respectively.

For particles of 0.154μ radius and a density of 1.06 g cm^{-3} in water with a disc speed of 360 r.p.m., the Stokes number has the value of 2×10^{-7}. Consequently, for any impaction to occur aggregation of the particles would have to take place so that the radius of the aggregates would be of the order of 1000 times the radius of the primary particles. In the present investigation this did not occur.

It might be considered that small protrusions on the surface of the disc would appreciably disturb the streamlines. In the present investigation the deposited particles would themselves constitute micro-protrusions. However, Rogers and Taylor[13] have shown that for protrusions of the order of 10μ there is no macroscopic effect on the laminar streamlines.

6.3. 0. Experimental Results

6.3.1. The Rotating Disc Apparatus

An improved apparatus based on the recommendations of Riddiford[5] was used, Fig.(6.2). Improvements over the apparatus employed by Marshall[1a] were a heavier mechanical construction and a spring transmission, both designed to reduce vibration. The body of the disc (4 cm diam.) was turned from polymethacrylate plastic and the working surface was ground flat and true in the actual collet chuck used in the apparatus. The plastic was coated with black paint to reduce the background reflections when the experimental surface was under optical examination (with the experimental surface, a coated cover-glass, in position).

The sol (500 ml) was contained in a glass dish of 12 cm diameter, which could be raised into a standard position for each experiment. The rate of rotation was accurately controlled by using synchronous motors with different reduction gears. Three different speeds were used (120, 240 and 360 r.p.m.).

6.3.2. The Deposition Surface

The substrate, onto which particles were to deposit, was prepared by coating a clean circular microscope cover-glass (22 mm diam.) with a polymer. The cover-glass was cleaned in hot chrome-sulphuric acid, well washed in distilled water and dried in a desiccator. A smooth coating was obtained from a chloroform

FIG (6.2a) THE ROTATING DISC APPARATUS

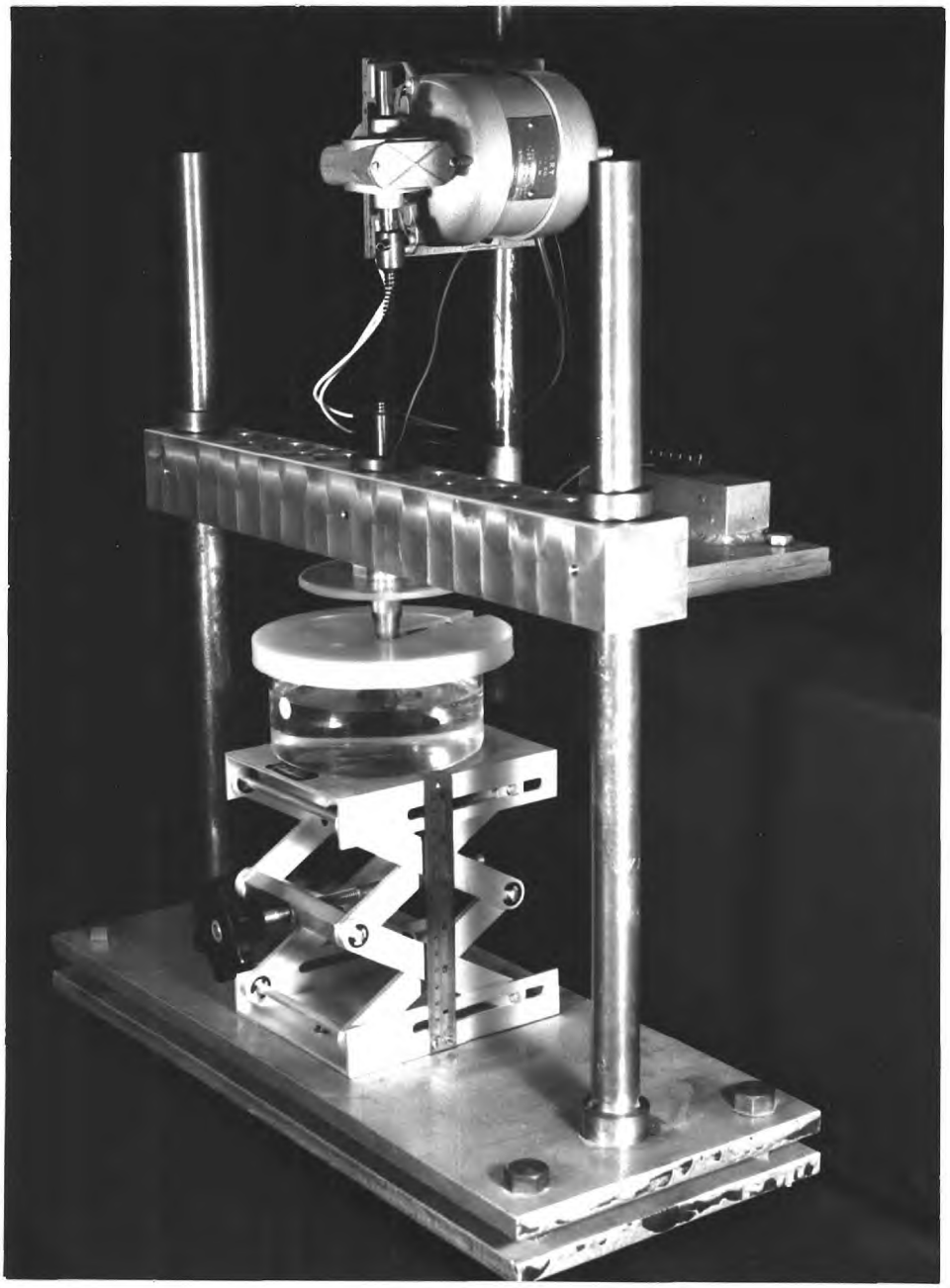

FIG(6·2) THE ROTATING DISC APPARATUS.

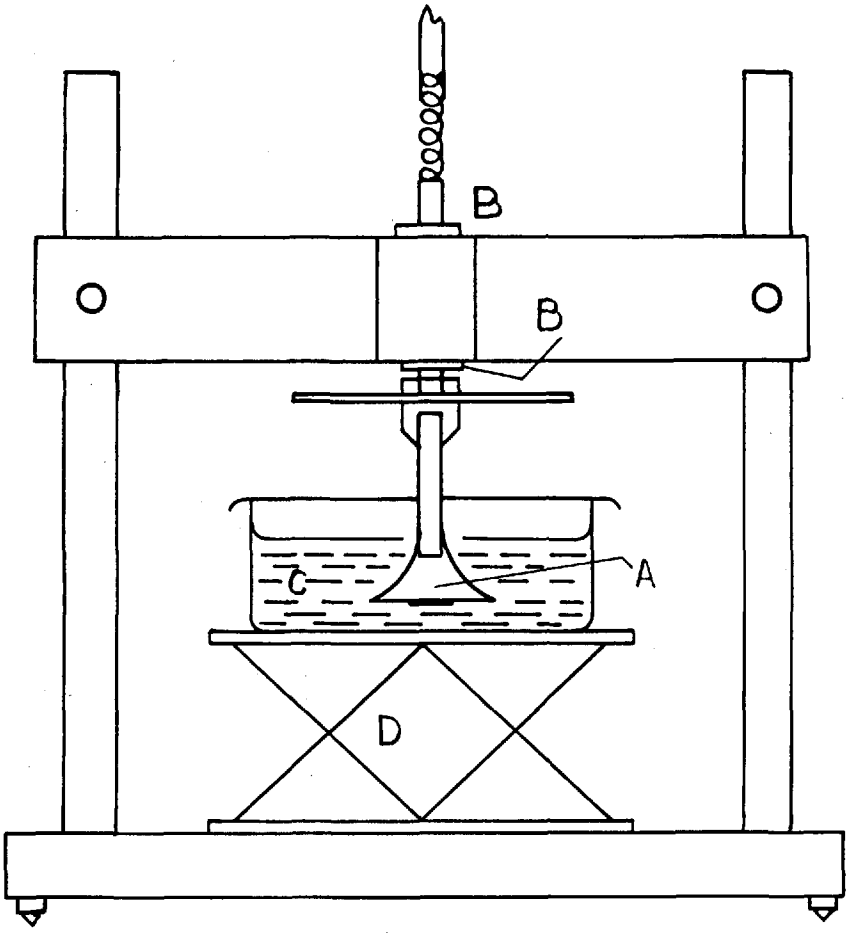

A PLASTIC DISC
B BALL BEARINGS
C DISPERSION
D ADJUSTABLE STAND

solution of the polymer by using the falling level technique that has been employed for preparing films for electron microscopy.[14] Such films are known to be very smooth and of uniform thickness. The coated cover-glasses were attached to the rotating disc with paraffin wax.

6.3.3. The Measurement of Deposition

Deposition experiments were carried out by rotating the disc for the required time in a diluted latex suspension of known particle concentration. This was followed by a 30 s rinse in distilled water. The disc, with the coated cover-glass still attached, was then dried in a desiccator. Finally, it was examined under a microscope at 400 times magnification. The surface of the disc was illuminated intensely at grazing incidence to reveal the particles as points of scattered light.[15] The surface density of particles was determined by counting over 400 squares covering four different areas of the surface. The mean deviation of the counts was about $\pm$ 3%. The results were conveniently expressed as N_d, the number of particles deposited per 10^4 sq.micron of surface.

6.4. The Test of the Levich Equation

In order to test fully the applicability of the Levich equation (equation (2)) for the mass transfer of colloidal particles to the surface of a rotating disc, it was essential that conditions were so arranged that every particle coming into contact with the disc

surface became firmly attached. This was ensured by using the negatively charged (-70mV) polystyrene latex particles and a film of the positively charged (found from the measurement of the electro-osmotic velocity within a micro-electrophoresis cell, coated with the polymer, to be + 72mV) co-polymer of 2-vinyl pyridine and styrene as the deposition surface in distilled water. Under these conditions the latex sol was completely stable and the deposited particles were strongly attached to the plastic surface by a combination of electrostatic and van der Waals attractive forces. Even quite vigorous washing in distilled water caused no measurable removal.

Deposition measurements were made for different sol concentrations and different times of rotation at three different speeds of rotation, Figs.(6.4, 6.5). It is readily seen that these curves are linear, in accord with the Levich theory. From these results it was found that the deposition was a linear function of the square-root of the speed of rotation, Fig.(6.6). Thus the results confirm the form of the Levich equation for the mass transfer of colloidal particles to the surface of a rotating disc.

As the deposition should be constant over the entire surface of the disc, the deposition should be uniform and randomly deposited. All deposits examined appeared uniformly random, but it was considered necessary to apply a strict test for the randomness of deposition. Consequently, from the mean of one of the deposition measurements, a Poisson distribution of the number of squares containing certain

fig.(6·3) THE DISTRIBUTION OF DEPOSITED PARTICLES COMPARED TO A POISSON DISTRIBUTION.

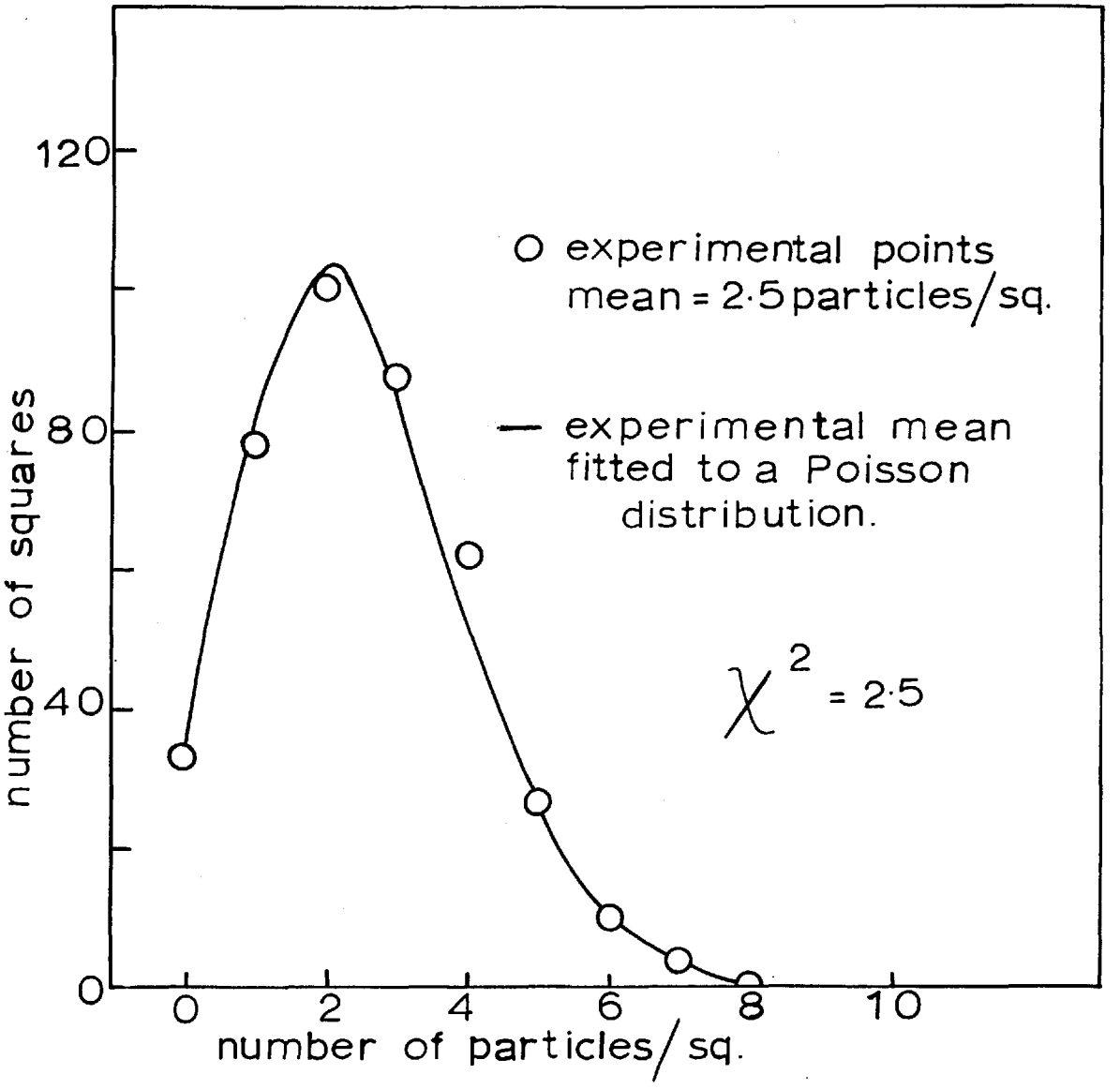

fig.(6.4) INFLUENCE OF SOL CONCENTRATION ON DEPOSITION

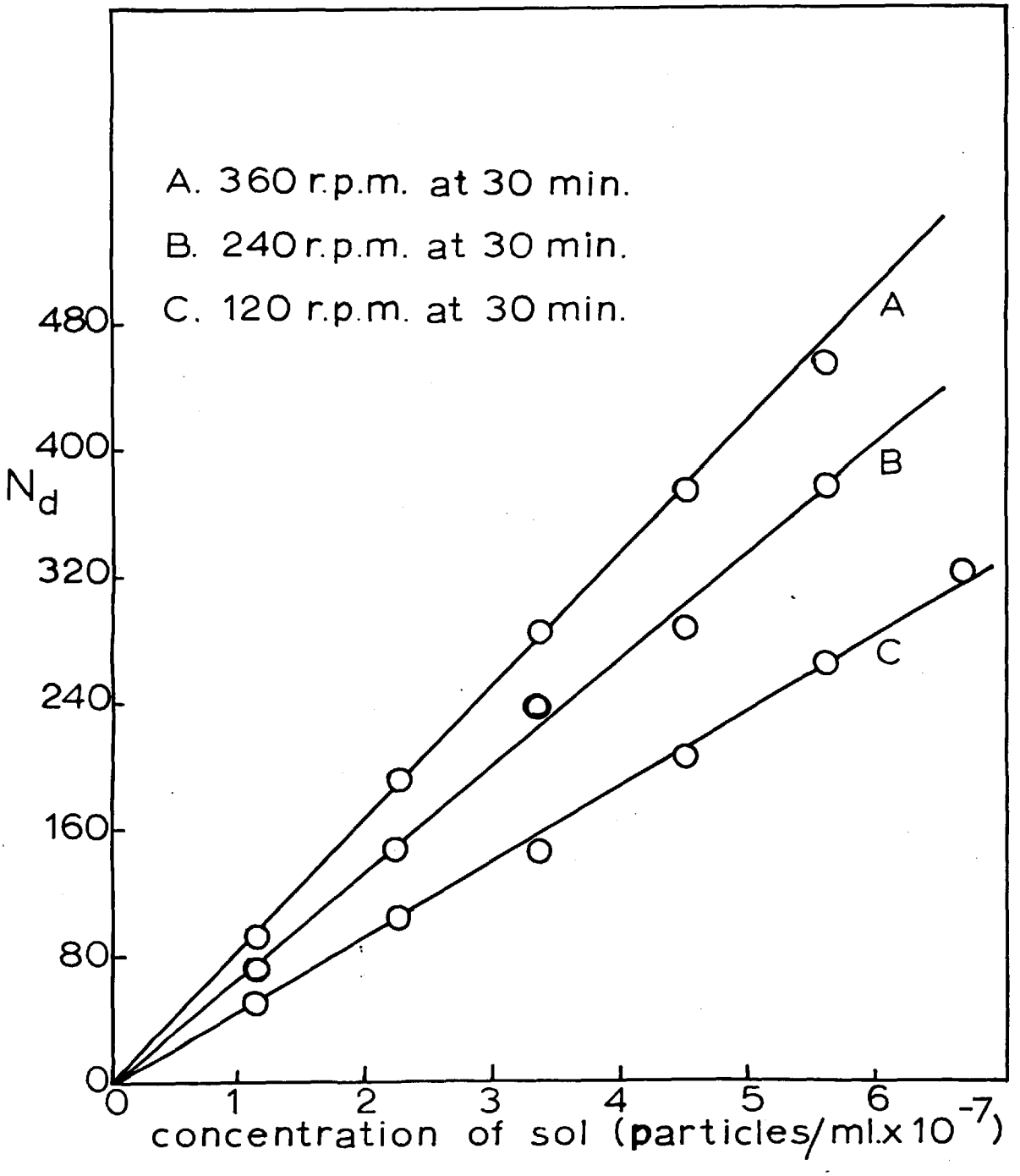

fig.(6:5) INFLUENCE OF TIME ON DEPOSITION

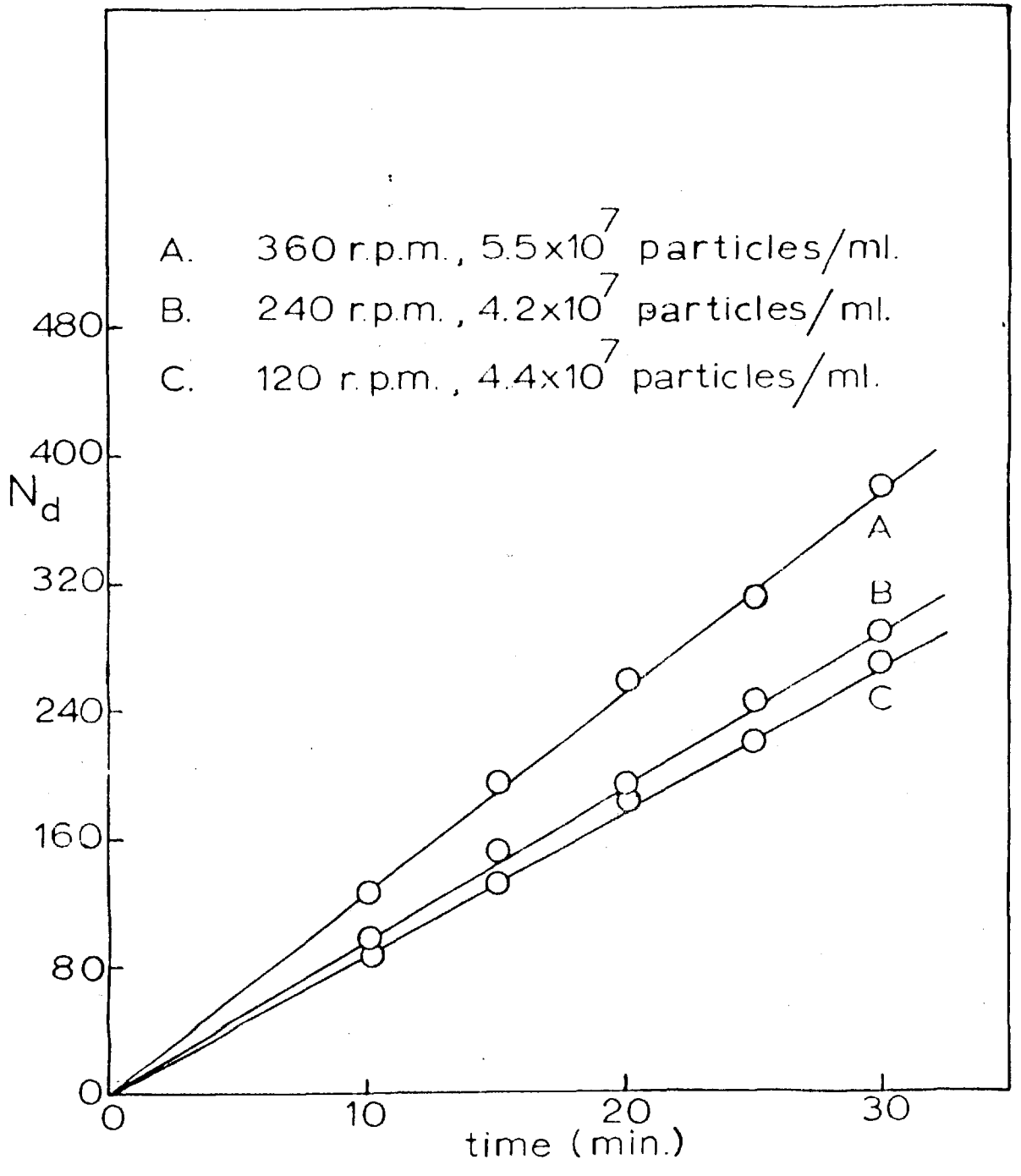

fig.(6.6) INFLUENCE OF SQUARE ROOT OF SPEED OF ROTATION ON DEPOSITION

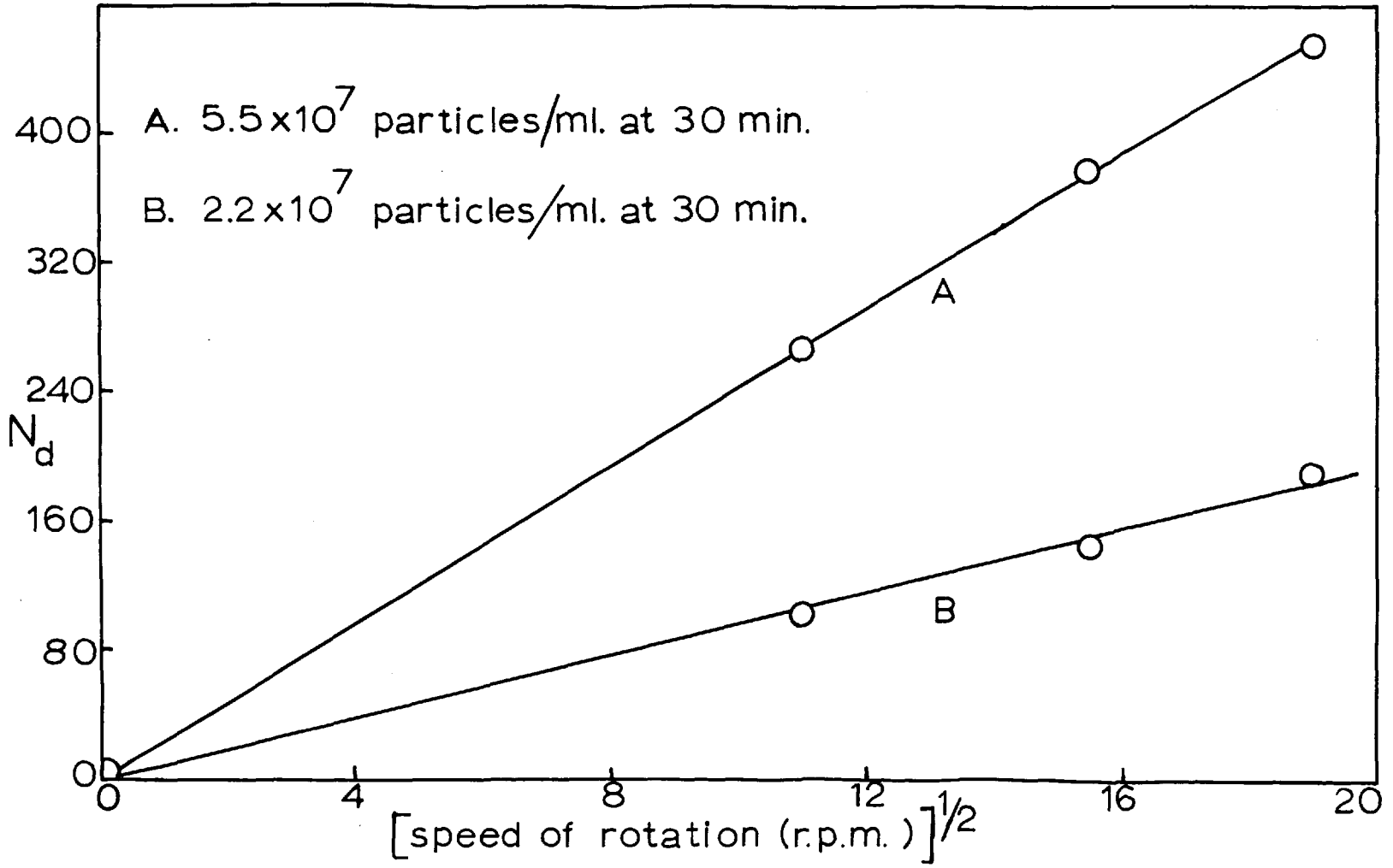

numbers of particles was constructed and compared with the experimentally determined distribution (Fig.6.3). As can be seen the agreement is very close. On application of the χ^2- test, it was found that the observed deposition was a Poisson distribution to within 98% confidence limits. Thus it can confidently be concluded that the deposition was uniform with the particles randomly deposited.

The Levich equation was derived from considerations of a disc rotating in an "infinite" volume of fluid. This condition is, of course, not met exactly in practical systems and consequently it was necessary to determine how critical is the position of the disc surface in the sol. Gregory and Riddiford[7] have shown that providing the disc surface is more than 0.5 cm from any bounding surface, then the streamlines can fully develop and the mass transfer is described by the Levich equation. This criterion was tested (Fig.6.7) and it was found to be correct under the experimental conditions of the present investigation. Therefore, it has been found that the position of the disc surface in the liquid is not at all critical.

All the above results were compared directly with the Levich equation by evaluating the "rate constant" $(j/\omega^{1/2} C_o)$ for each point and comparing it with the theoretical value, namely, $0.62 (kT/6\pi\eta a)^{2/3} \nu^{-1/6}$. The mean experimental value for the "rate constant" was $7.59 \pm 0.30 \times 10^{-6}$, which is in full agreement with the theoretical value of 7.66×10^{-6}, (Appendix I).

fig.(6.7) INFLUENCE OF DEPTH OF IMMERSION OF DISK SURFACE ON DEPOSITION

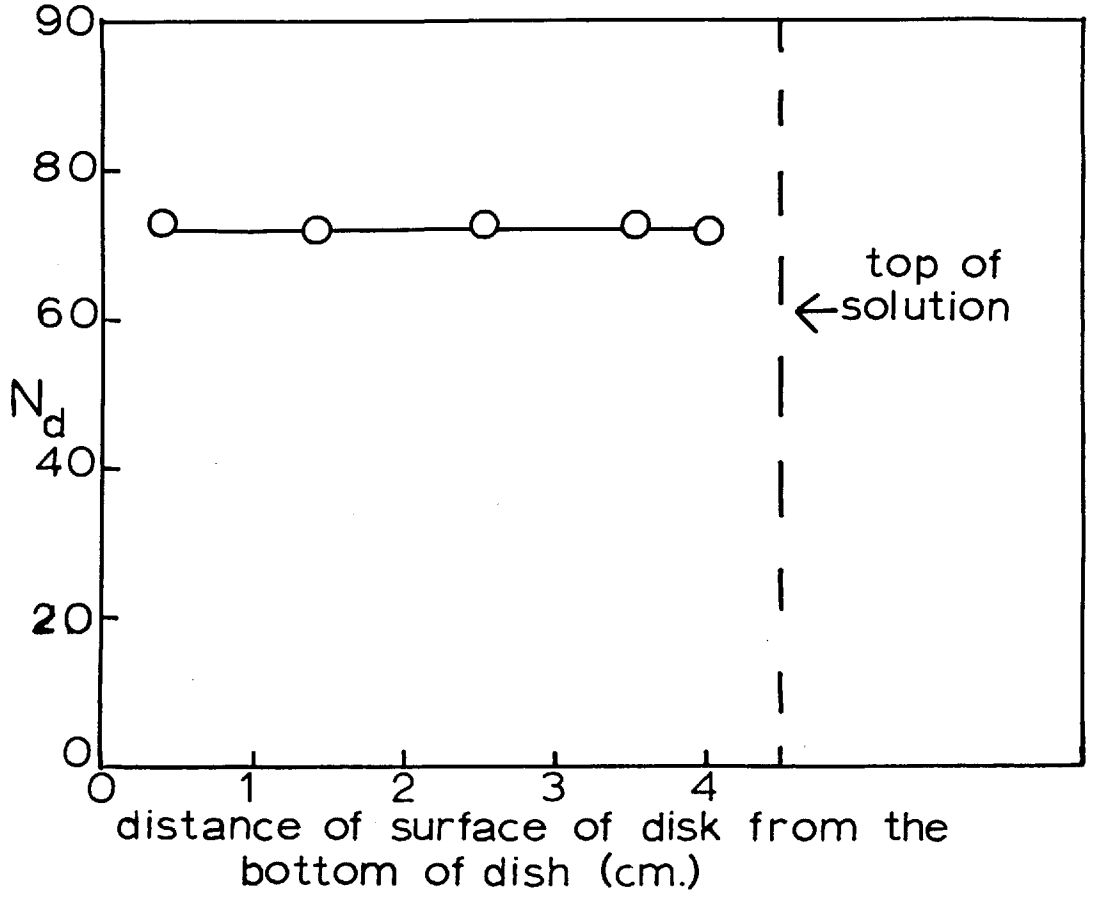

However, it is possible that the electroviscous effects of the particles may affect their diffusion coefficient and thus alter the experimental value of the "rate constant". This effect will now be considered.

6.4.1. The Effect of the Primary Electroviscous Effect on the Deposition Rate Constant

The viscosity of a suspension of spherical particles bearing no electrical double-layer was given by Einstein[16] as,

$$\eta_s = \eta_o (1 + 2.5\varphi) \qquad (11)$$

where η_s is the viscosity of the suspension and η_o is the viscosity of the liquid medium. φ is the volume fraction occupied by the spherical particles.

For spherical particles possessing an electrical double-layer the viscosity of the sol is greater as the movement of the particles causes a distortion of the double-layer, which increases the drag on the particles. Von Smoluchowski[17] presented the following expression for the viscosity of a suspension of spherical particles bearing a double-layer (though he gave no derivation),

$$\frac{\eta_s - \eta_o}{\eta_o \varphi} = 2.5\left[1 + \frac{1}{\lambda \eta_o a^2}\left(\frac{\varepsilon \zeta}{2\pi}\right)^2\right] \qquad (12)$$

where λ is the specific conductivity of the liquid medium, ζ is the zeta-potential of the particles and ε is the dielectric constant of the liquid medium.

Later Krasny-Ergen[18] published a derivation for the viscosity of a sol in which the particles possess a double-layer. His equation was almost identical to equation (12), the only modification being a factor of 3/2 multiplying the correcting term due to the electrokinetic potential. His derivation had the restriction that it applied only when the thickness of the double-layer was small compared to the particle radius.

Booth[19] re-examined this problem, but without the restriction on the double-layer thickness, and obtained the following expression,

$$\frac{\eta_s - \eta_o}{\eta_o \varphi} = 2.5\left[1 + q^* \left(\frac{e\zeta}{kT}\right)^2 (1 + \kappa a)^2 Z(\kappa a)\right] \qquad (13)$$

where $q^* = kT \sum n_i z_i \omega_i^{-1} \eta_o e^2 \sum n_i z_i^2$, ω_i is the mobility of an ion of species i and $Z(\kappa a)$ is a rather complicated function of κa which was expressed graphically by Booth.[19]

If the assumption is made that the ion mobilities are equal, then equation (14) may readily be transformed into a similar expression to the Smoluchowski equation, and is

$$\frac{\eta_s - \eta_o}{\eta_o \varphi} = 2.5\left[1 + \frac{1}{\lambda \eta_o a^2}\left(\frac{\varepsilon \zeta}{2\pi}\right)^2 \pi (\chi a)^2 (1+\chi a)^2 Z(\chi a)\right] \quad (14)$$

Several attempts have been made to determine experimentally the magnitude of the primary electroviscous effect. It is generally found[19-22] that the Smoluchowski equation yields values of η_s that are of several orders of magnitude too high. The Booth equation gives values of η_s of the same order of magnitude as found experimentally.[19-22] The lack of complete agreement[19-21] is probably due to the nature of the systems studied. Recently, Stone-Masui and Watillon,[22] using a well characterised series of "monodisperse" polystyrene latex sols, have shown their experimental results to be in complete accord with the Booth equation. Hence the Booth equation will be used to estimate the effect of the primary eleotroviscous effect on the mass transfer to the rotating disc.

The mass transfer equation for the rotating disc system contains two viscosity terms, namely

$$j = 0.62\left(\frac{kT}{6\pi\eta a}\right)^{2/3}\left(\frac{\rho}{\eta}\right)^{-1/6}\omega^{1/2} c_o.$$

Hence an increase in the viscosity of the sol due to the primary electroviscous effect would lead to a decrease in the mass flux to the surface of the rotating disc. For the conditions operative in the test of the mass transfer to the surface of a rotating disc, values of

electrophoretic zeta-potential, conductivity and κa can be inserted into equation (14). When this is done it is found that there is an increase in viscosity by a factor of $(1 + 6.5 \times 10^{-5})$ on pure water. On substitution into the Levich equation, it is found that the theoretical mass transfer is too large by a factor of $(1 + 4 \times 10^{-5})$. Consequently, it is unlikely that the primary electroviscous effect has any effect upon the theoretical deposition rates.

6.5. Conclusions

It has been shown that the Levich equation for the mass transfer of colloidal particles to the surface of a rotating disc is fully applicable. It has also been shown that the primary electroviscous effect has negligible effect upon the theoretical deposition rates. Thus, indirectly the use of the Stokes-Einstein equation for the calculation of the diffusion coefficient of colloidal particles has been confirmed.

6.6. References

(1a) Marshall, J.K. Ph. D. Thesis, Univ. London. (1964).

(1b) Marshall, J.K. and Kitchener, J.A. J. Coll. and Interface Sci. 22, 342, (1966).

(2) Von Kármán, T. Z. Agnew. Math. i Mech. 1, 244, (1921).

(3) Cochran, W.G. Proc. Camb. Phil. Soc. 30, 365, (1934).

(4a) Levich, V.G. Acta Physicochim URSS. 17, 257, (1942).

(4b) Levich, V.G. Acta Physicochim URSS. 18, 335, (1944).

(4c) Levich, V.G. "Physico-chemical Hydrodynamics", Prentice-Hall, (N.Y.) pp. 60-72, (1962).

(5) Riddiford, A.C. Advances in Electrochemistry and Electrochemical Engineering. 4, 77, (1966),

(6) Daguenet, M. and Robert, J. Compt. rend (AB) 1125, (1966).

(7) Riddiford, A.C., and Gregory, D.P. J. Chem. Soc. 3756, (1956).

(8) Kishinevskii, M. Kh. and Denisova, T.B. J. Appl.Chem. URSS 37, 1533, (1964).

(9) Riddiford, A.C. and Gregory, D.P. J. Electrochem. Soc. 107, 950, (1960).

(10) Hsueh, L. and Newman, J. Electrochim. Acta. 12, 429, (1967).

(11) Newman, J. J. Electrochem. Soc. 114, 239, (1967).

(12) Fuchs, N.A. "The Mechanism of Aerosols" (Pergamon Press) pp. 137-180, (1964).

(13) Rogers, G.T. and Taylor, K.J. Nature 200, 1062, (1963).

(14) Revell, R.S.M. and Agar, A.W. Brit. J. Appl. Phys. 6, 23, (1955).

(15) Visser, J. Unpublished work.

(16a) Einstein, A. Ann. Phys. 19, 289, (1906).

(16b) Einstein, A. Ann. Phys. 34, 591, (1911).

(17) Von Smoluchowski, M. Koll. Z. 18, 194, (1916).

(18) Krasny-Ergen, W. Koll Z. 74, 172, (1936).

(19) Booth, F. Proc. Roy. Soc. A203, 533, (1950).

(20) Chan, F.S. and Goring, D.A.I. J.Coll. and Interface Sci. 22, 371, (1966).

(21) Schaller, E.J. and Humphrey, A.E. J.Coll. and Interface Sci. 22, 573, (1966).

(22) Stone-Masui, J. and Watillon, A. J.Coll. and Interface Sci. 28, 187, (1968).

7.0 ELECTROPHORESIS

7.1. Theory

The theory of electrophoresis was first treated by Helmholtz[1] in 1879. Later his treatment was extended and improved by von Smoluchowski[2], without appreciably altering the form of the equations. For streamlined flow and from the considerations of the electrical and frictional forces, the electrophoretic velocity $\underline{V}$ of the colloidal particles was obtained as,

$$V = \frac{\varepsilon \zeta X}{4\pi\eta} \qquad (1)$$

where ε is the dielectric constant and η is the viscosity of the liquid medium. ζ is the zeta-potential and $\underline{X}$ is the applied field strength.

Underlying the derivation of equation (1) are several assumptions, namely.

(1) The particle is rigid and insulating.

(2) The applied electric field although distorted by the presence of the particle can simply be added to the field of the double-layer.

(3) The conductivity, dielectric constant and viscosity of the liquid medium have the same values in the double-layer as outside it.

(4) The particle radius is large in comparison to the thickness of the double-layer.

(5) The liquid at the particle surface has the velocity of the particle, and the velocity gradient begins at the surface. (By the surface of the particle is meant the shear plane outside the Stern layer. This point was discussed in Chapter 2).

From von Smoluchowski's treatment, the electrophoretic velocity is found to be dependent upon the potential of the particle (rather than its charge) and independent of shape or size.

In 1924 Hückel[3] applied the Debye-Hückel theory[4] of the conductance of strong electrolytes to colloidal particles, and obtained the following expression for the electrophoretic velocity of colloidal particles,

$$v = \frac{\varepsilon \zeta x}{6\pi\eta} \qquad (2)$$

which is essentially the same as the Helmholtz-Smoluchowski equation, but with a factor of 1/6 instead of 1/4. Since Hückel used the same assumptions as Smoluchowski, but did not indicate the source of error in the latter's analysis, there remained a doubt to which expression was applicable. This remained until 1931 when Henry[5] renewed the analysis and showed that the two expressions were applicable under appropriate conditions.

In Henry's analysis the deformation of the applied electric field by the particle and its associated double-layer was taken into account. He showed that the effect of the particle on the electric field was dependent upon the shape of the particle, its size and the thickness of the double-layer. For his complete analysis he considered only spherical particles, though he did indicate the form of shape correction factors for other geometries.

For spherical particles the electrophoretic velocity was given by Henry by two discontinuous functions, usable for different parts of the range of $\underline{\kappa a}$ values for the particles.

For $\underline{\kappa a} > 25$

$$V = \frac{\varepsilon X}{4\pi\eta}\left\{ f(1+\lambda) + 3\lambda a^3 \left(5a^2 \int_{\infty}^{a} \frac{\partial\psi . dr}{\partial r . r^6} - 2\int_{\infty}^{a} \frac{\partial\psi dr}{\partial r . r^4} \right) \right\} \quad (3)$$

and for $\underline{\kappa a} < 5$

$$V = \frac{\varepsilon X}{6\pi\eta}\left\{ f + \lambda a^3 \left(3a^2 \int_{\infty}^{a} \frac{\partial\psi dr}{\partial r . r^5} - 2\int_{\infty}^{a} \frac{\partial\psi dr}{\partial r . r^3} \right) \right\} \quad (4)$$

where $\underline{\lambda}$ is a factor taking into account the conductivity of the particles and is given by

$$\lambda = \frac{6_s - 6_o}{2 6_s - 6_o} \quad (5)$$

where σ_s is the specific conductivity of the electrolyte solution, and σ_o is the specific conductivity of the particles. For an insulating particle λ has the value $\frac{1}{2}$.

By using the Debye-Hückel[4] linear approximation of the Poisson-Boltzman equation for the potential distribution about a spherical particle (small potentials), Henry obtained the following expressions for an insulating particle from equations (3) and (4) respectively.

$$V = \frac{\varepsilon \zeta X}{4\pi\eta} \left\{ 1 - \frac{3}{\kappa a} + \frac{25}{(\kappa a)^2} - \frac{220}{(\kappa a)^3} \right\} \Bigg|_{25 = \kappa a}^{\infty = \kappa a} \qquad (6)$$

and

$$V = \frac{\varepsilon \zeta X}{6\pi\eta} \left\{ 1 + \frac{(\kappa a)^2}{16} - \frac{5(\kappa a)^3}{48} - \frac{(\kappa a)^4}{96} - \frac{(\kappa a)^5}{96} - \frac{11}{96} \exp(\kappa a) \int_{\infty}^{a} \frac{e^{-t}}{t}\, dt \right\} \Bigg|_{0 = \kappa a}^{5 = \kappa a} \qquad (7)$$

from which it is readily seen that at large κa, equation (6) reduces to the Smoluchowski equation,

$$V = \varepsilon \zeta X / 4\pi\eta \qquad (1)$$

and at small κa, equation (7) reduces to the Hückel equation,

$$v = \frac{\varepsilon \zeta x}{6\pi\eta} \qquad (2).$$

These approximate equations do not cover the complete range of κa values for the evaluation of zeta-potential from electrophoretic velocity determinations. However, the values of the electrophoretic velocity for the intermediate κa values can readily be obtained by interpolation between the functions in equations (6) and (7).

Later Henry[6] and independently Booth[7] extended equations (3) and (4) to take into account the effect of the surface conductance of the particles on the applied field.

Surface conductance arises because owing to the double-layer surrounding the particles, there is a higher concentration of ions in the double-layer than in the bulk solution. Generally the correction factors are not large for large particles and large values of κa, but increase in importance as κa decreases and the particle size decreases. However, as the effect of surface conductance is taken into account in the following treatments, it need not be considered in detail.

7.1.1. The Relaxation Effect

In all the preceding theories of electrophoresis the double-layer is assumed to move entirely with the particle without

deformation. In the theory of ionic conduction in an alternating field, Debye and Hückel[4] have shown that the "ion atmosphere" lags behind the ion, as the applied field induces the "ion atmosphere" to move in the opposite direction to the ion. Consequently, there is required a certain finite time for the distorted ion-atmosphere to regain spherical symmetry. This time is known as the relaxation time and the distortion of the "ion-atmosphere" has the effect of retarding the movement of the ion. In a similar manner it is expected that the double-layer surrounding the migrating colloidal particle undergoes relaxation, as the charge sign is opposite that on the particle. Consequently, in circumstances where the double-layer is thick, a considerable slowing up of the particle due to relaxation could take place. It is expected that, for a given $\underline{\kappa}$ value, the magnitude of the retardation to be a function of the zeta-potential of the particle. For the higher the zeta-potential the higher is the charge in the double-layer and hence the greater the deformation of the double-layer with particle migration.

This problem has been examined by Overbeek[8] and independently by Booth[9]. They both showed that for intermediate values of $\underline{\kappa a}$ the electrophoretic velocity of colloidal particles varies as a power series in zeta-potential. Owing to the laborious nature of the computations the series was calculated only for a few terms, and is thus still only exactly applicable for low potentials. For symmetrical electrolytes the expression derived by Overbeek for the electrophoretic velocity is,

$$V = \frac{\varepsilon \zeta X}{6\pi\eta}\left\{ f_1(\kappa a) - z^2\left(\frac{e\zeta}{kT}\right)^2 f_3(\kappa a) - \left(\frac{\rho_+ + \rho_-}{2e}\right)\frac{\varepsilon kT}{6\pi\eta e}\left(\frac{e\zeta}{kT}\right)^2 f_4(\kappa a)\right\} \tag{8}$$

where the functions $f_1(\kappa a)$, $f_3(\kappa a)$ and $f_4(\kappa a)$ have been tabulated by Overbeek[10]. ρ_+ and ρ_- are the frictional constants of the ions and are given by,

$$\rho_{\pm} = \frac{Ne^2 Z_{\pm}}{\lambda^o_{\pm}} \tag{9}$$

where $\lambda^o_{\pm}$ is the limiting equivalent conductance of the ions. N is the Avagadro's number and Z is the ion valency.

Recently, Wiersema, Loeb and Overbeek[11] have re-examined and extended the treatments of Overbeek[8] and Booth[9] by numerical methods using a computer, and employing more accurate expressions for the potential distribution about a spherical particle.[12] Their computations were carried out only for the range $0.2 < \kappa a < 50$, but it is seen in Fig.(7.1) that at the limits of this range the approximate expression by Overbeek (eq.7) is approximately equivalent to the numerical values, and consequently, would be valid even for high zeta-potentials outside this range. E in this graph is the dimensionless electrophoretic mobility given by,

$$E = \frac{6\pi\eta e}{kT}\,\frac{V}{X} \tag{10}$$

FIG.(7·1) THE ELECTROPHORETIC MOBILITY AS A FUNCTION OF κa FOR VARIOUS RELAXATION EQUATIONS.

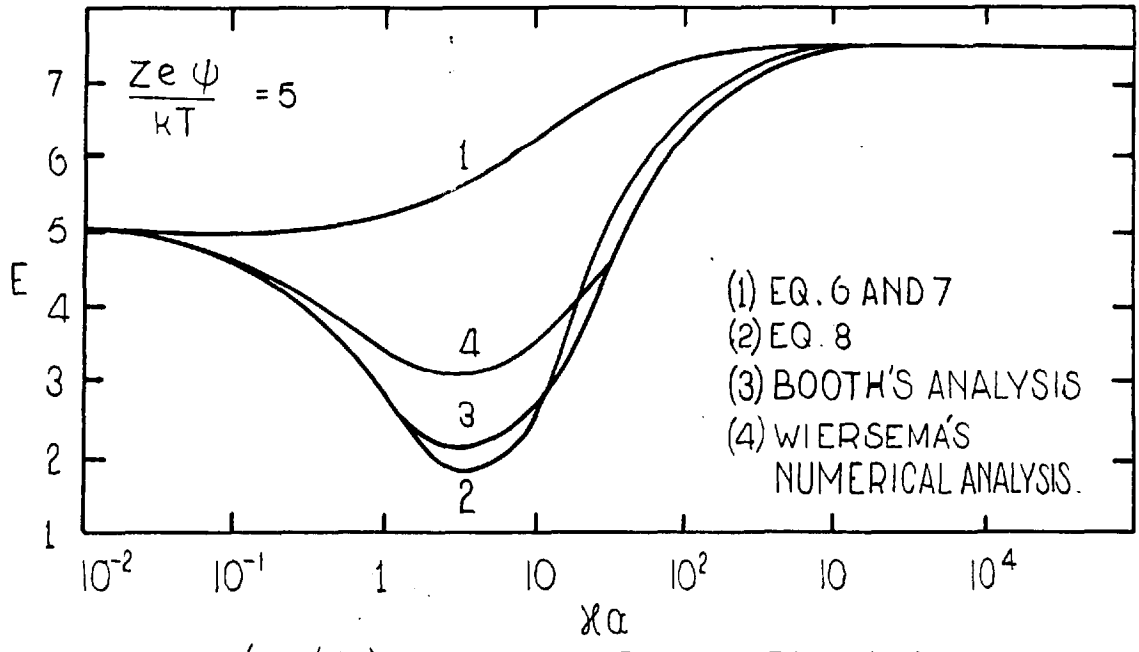

(FIG(7·2) THE LIMITS OF APPLICABILITY OF ANALYTICAL APPROXIMATIONS

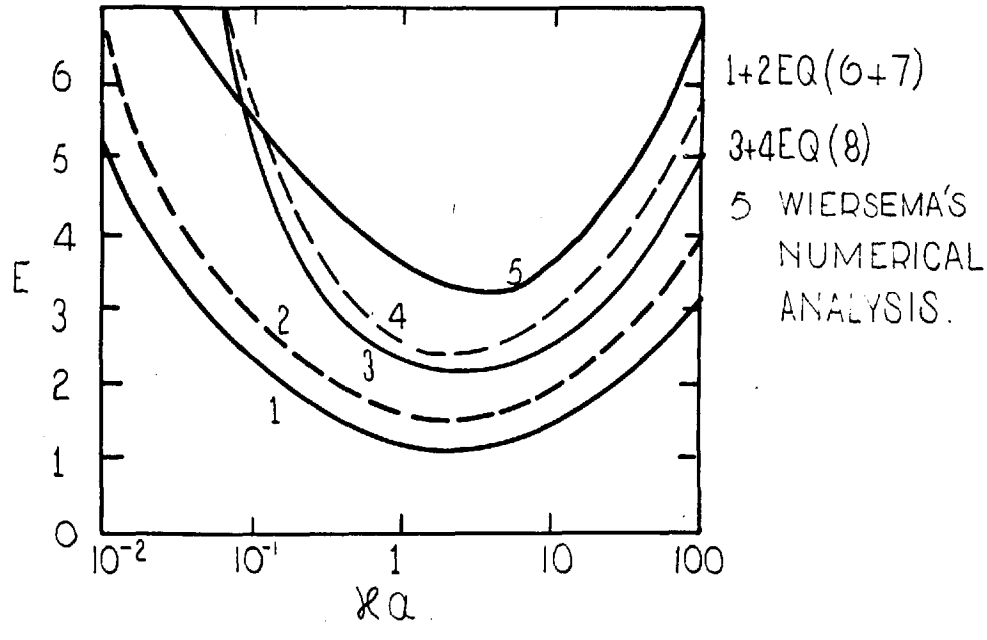

In Fig.(7.2) is shown the limits of applicability of the various approximate equations. The limits for the numerical computations are fixed either because the computations were not taken to high enough potentials ($ze\zeta/kT = 6$), or because the function $E = \phi(e\zeta/kT)$ passes through a maximum. This latter case occurs for $1 < \kappa a < 10$, and indicates that for this range of κa no value of mobility greater than 3.5 should be possible. Cases of mobility greater than those possible from this theory are rare but recently a number of cases have been found to occur with the synthetic latices[13-15], showing that the numerical computations still do not give a fully accurate description of electrophoretic behaviour.

7.2. The Electrophoresis Apparatus

The electrophoretic mobilities of the polystyrene latex particles were determined in a modified flat microscope electrophoresis cell. The detailed construction of which has been fully described by Shergold, Mellgren and Kitchener.[16] In essence, this apparatus consists of a glass cell fitting into two "Perspex" electrode compartments, as shown in Fig.(7.3). The glass cell is demountable from its electrode compartments, which is of advantage in the present work, for, apart from being much easier to clean than the conventional apparatus, the cell walls can easily be coated with plastic films, so that in the same apparatus the electrophoretic velocity of the particles and the electro-osmotic velocity of the liquid along the cell walls can be measured. The determination of the zeta-potential

FIG (7.3) MICRO-ELECTROPHORESIS APPARATUS

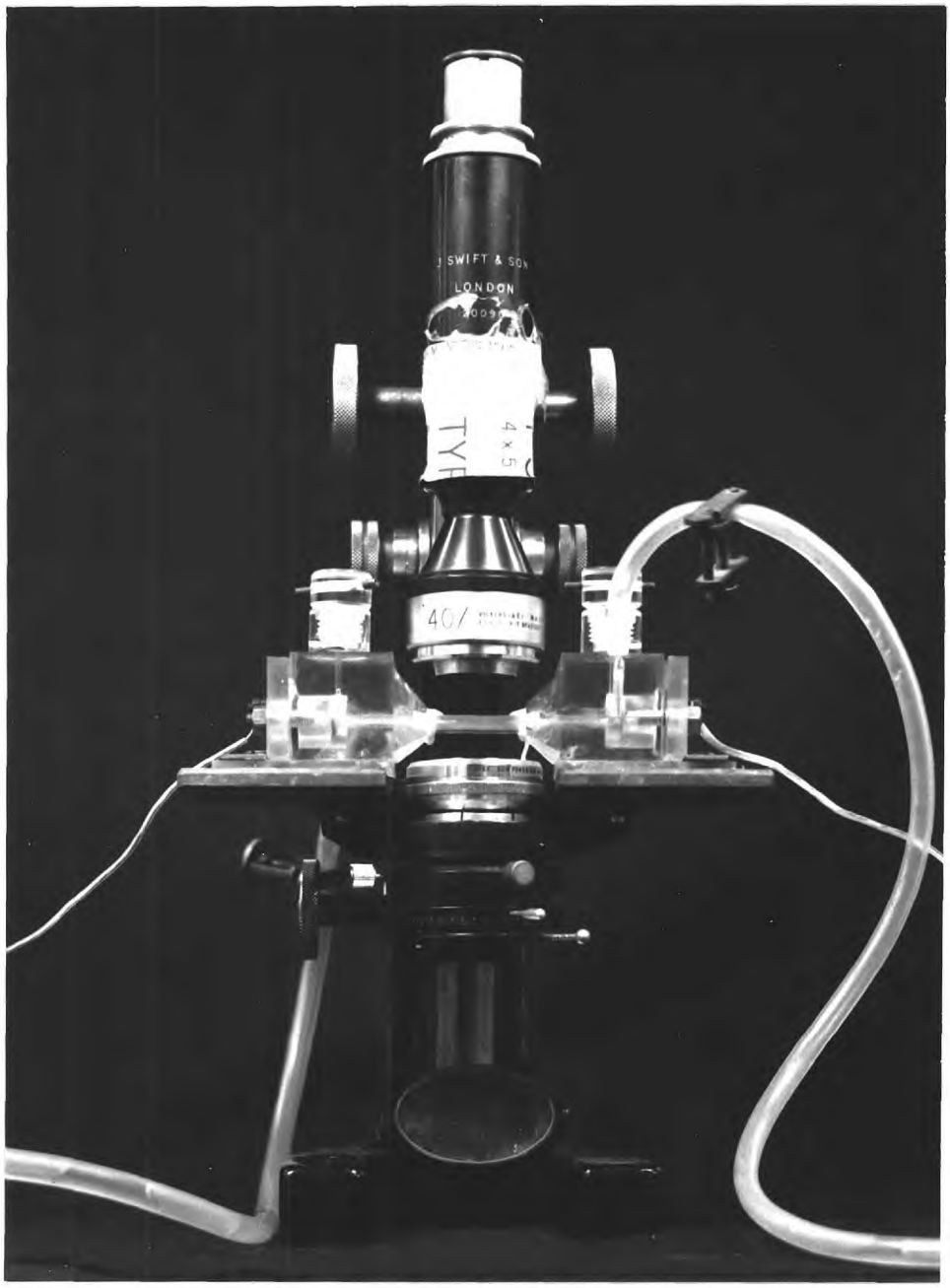

of the plastic substrates from electro-osmotic flow in this apparatus is of importance for the measurements are made on the plastic films in the same physical state as they are in the deposition measurements.

The glass cell (supplied by Tintometer Sales Ltd.) was a 1 mm standard spectrophotometer cell 60 mm long and 15 mm wide constructed without ends. In use the cell was sealed to the "Perspex" electrode compartments with silicone moulding paste and clamped to the microscope state.

The optical system of the microscope consisted of a dark field sub-stage condenser (Cooke, low-power dark ground, numerical aperture 0.70 - 0.80), a X40 long working distance objective (Vickers, A.E.I., numerical aperture, 0.57) capable of focusing on any level within the glass cell, and a X8 eyepiece. Heat from the light source was removed by a heat filter and a dilute copper sulphate solution cell.

The electrodes were of platinized platinum, and the voltage applied across the cell was supplied by a stabilized d.c. power supply unit. The circuit used with this apparatus is shown in Fig.(7.4).

7.2.1. The Theory of the Microscopic Method

In this method the electrophoretic velocity is measured by timing the movement of individual particles over a set distance at a given applied field strength. However, the electro-osmotic streaming of the liquid past the cell walls cannot be eliminated or

fig.(7·4) CIRCUIT DIAGRAM FOR THE MEASUREMENT OF ELECTROPHORETIC MOBILITY.

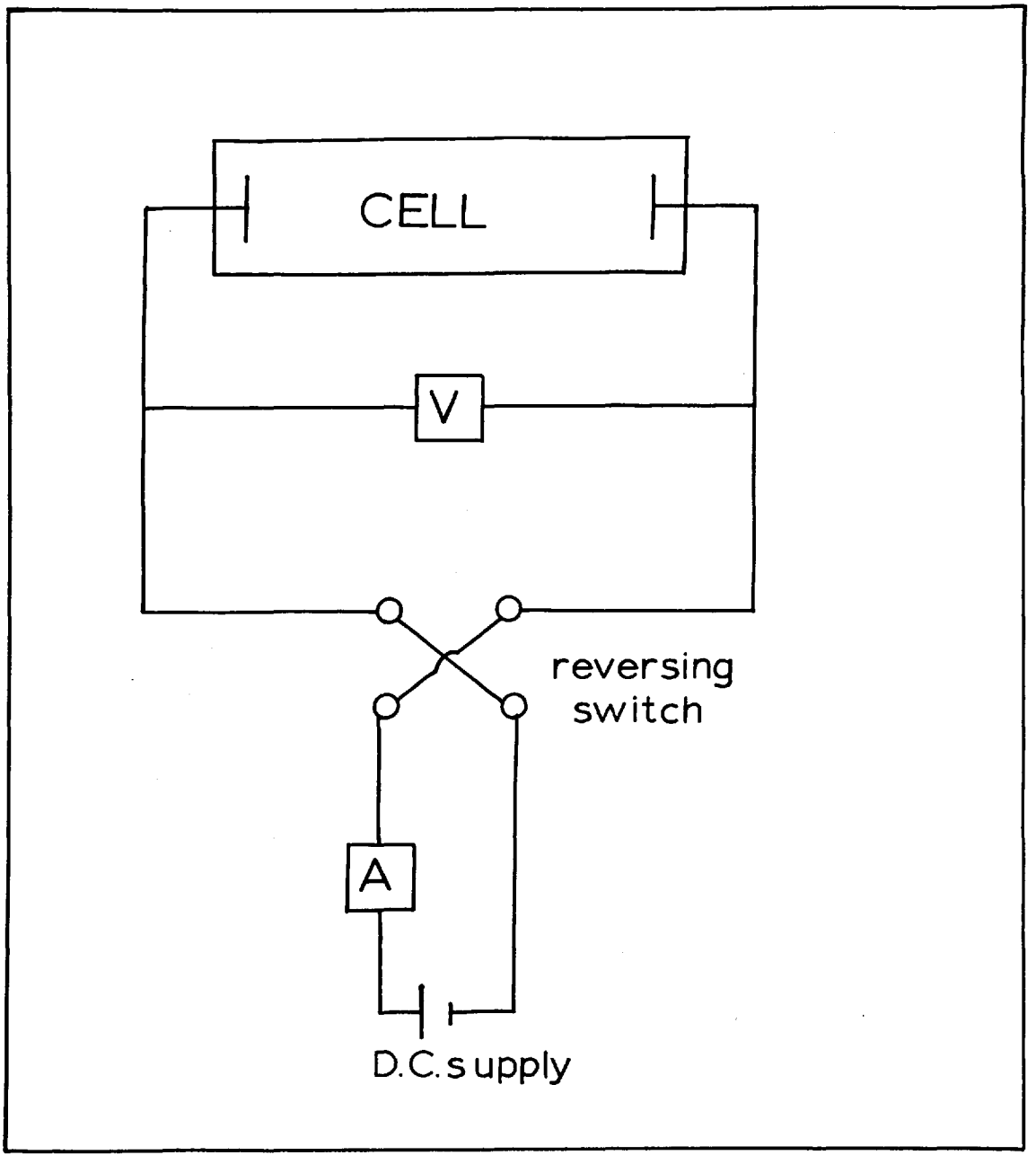

counteracted by any known method and must be taken into account if the true electrophoretic velocity is to be measured. Since the system is closed, and, therefore, the nett flow of liquid through the cell must be zero, the flow of liquid along the walls is counterbalanced by a flow in the opposite direction in the centre of the cell. Therefore, the velocity of the liquid varies with the depth of the cell.

It has been shown[17] that the electro-osmotic velocity is related to the liquid velocity at any position within the cell by the equation

$$V_w = \frac{U}{2}\left(\frac{3h^2}{a^2} - 1\right) \qquad (11)$$

where V_w is the velocity of the liquid at level $\underline{h}$, $\underline{U}$ is the electro-osmotic velocity at the wall, $\underline{h}$ is the distance from the centre of the cell, and $\underline{2a}$ is the total depth of the cell. (This equation is a parabola, symmetrical about the centre of the cell). Consequently, from equation (11) putting $V_w = 0$ it is found that the velocity of the liquid is zero at a distance of $\pm$ 0.578a measured from the centre of the cell. As the measured velocity of the particles is given by,

$$V_{obs} = V_E + V_w \qquad (12)$$

where V_E is the electrophoretic velocity, then at the depth where $V_w = 0$ the observed velocity of the particles is their true electrophoretic velocity. These positions within the cell are known as the

stationary levels.

If the velocity of the particles is measured at the stationary levels and also at the top of the parabola (h = 0), then the value of the electro-osmotic velocity of the liquid can be calculated, being related to the observed velocity by the equation

$$V_{obs} = V_E = U/2 \qquad (13).$$

Equation (11), however, is correct only for cells in which the width is large compared to the thickness. Komogata[18] has studied the more general case where the width is not great compared to the thickness. If the ratio of the cell width to thickness is K, and if a_o is the position of the stationary levels in terms of fractional depth from the top of the cell, then

$$a_o = \frac{1}{2} + \sqrt{\frac{1}{12} + \frac{32}{\pi^5 K}} \qquad (14).$$

Thus for the particular cell used where K = 10, the stationary levels occur at 0.194 and 0.806 of the total depth of the cell.

7.3. The Experimental Results

The usual method of determining the field strength by measuring the current flowing through the cell and the conductivity of the sol could not be used in this investigation with any degree of accuracy. There were two possible reasons for this state of

affairs.

(1) With the electrolyte conditions used for testing the parabolic profile for this apparatus (10^{-6}M sodium hexadecyl sulphate) by using different applied voltages, it was necessary to change the current scale on the ammeter. It was found that there were differences of accuracy between the two scales by comparing with another meter, and by the determination of the resistance of a standard resistor at different applied voltages.

(2) It was just possible that at these very low ionic strengths, surface conductance along the walls of the cell also lead to erroneous values of the current passing through the cell. It was, therefore, decided to determine the effective distance between the electrodes, and thence by measuring the applied potential across the cell, the field strength could be readily calculated.

The effective distance between the electrodes was determined by measuring the current at given applied voltages for various sodium chloride concentrations, and from the values of the conductivity of these salt solutions the distance between the electrodes could be calculated. Determinations were made with both 'Formvar'-coated cells and plain glass cells with applied voltages of between 10 and 50 V. Sodium chloride concentrations of 10^{-5}, 10^{-4} and 10^{-3}M were used. From these determinations a mean distance between the electrodes of 83.2 $\pm$ 0.4 mm was recorded. Using this value reproducible values of electrophoretic mobility were obtained.

In a glass cell (uncoated walls) the velocity profile at two values of the applied potential was determined for polystyrene latex particles in 10^{-6}M sodium hexadecyl sulphate solution, Fig.(7.5). It is seen that the profile is truly parabolic and symmetrical about the centre of the cell. Also, the agreement for the two different applied voltages is quite good. Consequently, this cell was used for all subsequent electrophoresis measurements.

The electrophoretic mobility for polystyrene latex particles in 10^{-6}M sodium hexadecyl sulphate and various sodium chloride concentrations was measured (see Chapter 8), and converted into zeta-potentials by the methods of von Smoluchowski[2] and Wiersema, Loeb and Overbeek[11]. These results are represented in Fig.(7.6). From the corrections for relaxation by the Wiersema method[11] on this data it is evident that the relaxation effect for these particles is very large. Moreover, there was a small range of salt concentrations ($5 < \kappa a < 10$), where the zeta-potentials could not be determined by the Wiersema method, because the experimentally determined electrophoretic mobilities were too high. According to the numerical computations of Wiersema[11] it should not be possible to obtain electrophoretic mobilities greater than 3.76μ/volt/sec at $\kappa a = 5$ as the function $E = \phi\ (e\zeta/kT)$ passes through a maximum at this value of mobility. However, the experimentally determined mobility was 4.13μ/volt/sec, which is considerably higher than the maximum for $E = \phi(e\zeta/kT)$. There has recently been reported such high mobilities for "monodisperse" polystyrene latex particles[13-15], and Wiersema[11]

fig.(7·5) THE ELECTROPHORETIC MOBILITY OF POLYSTYRENE LATEX PARTICLES IN 10^{-6} M SODIUM HEXADECYL SULPHATE AS A FUNCTION OF CELL DEPTH.

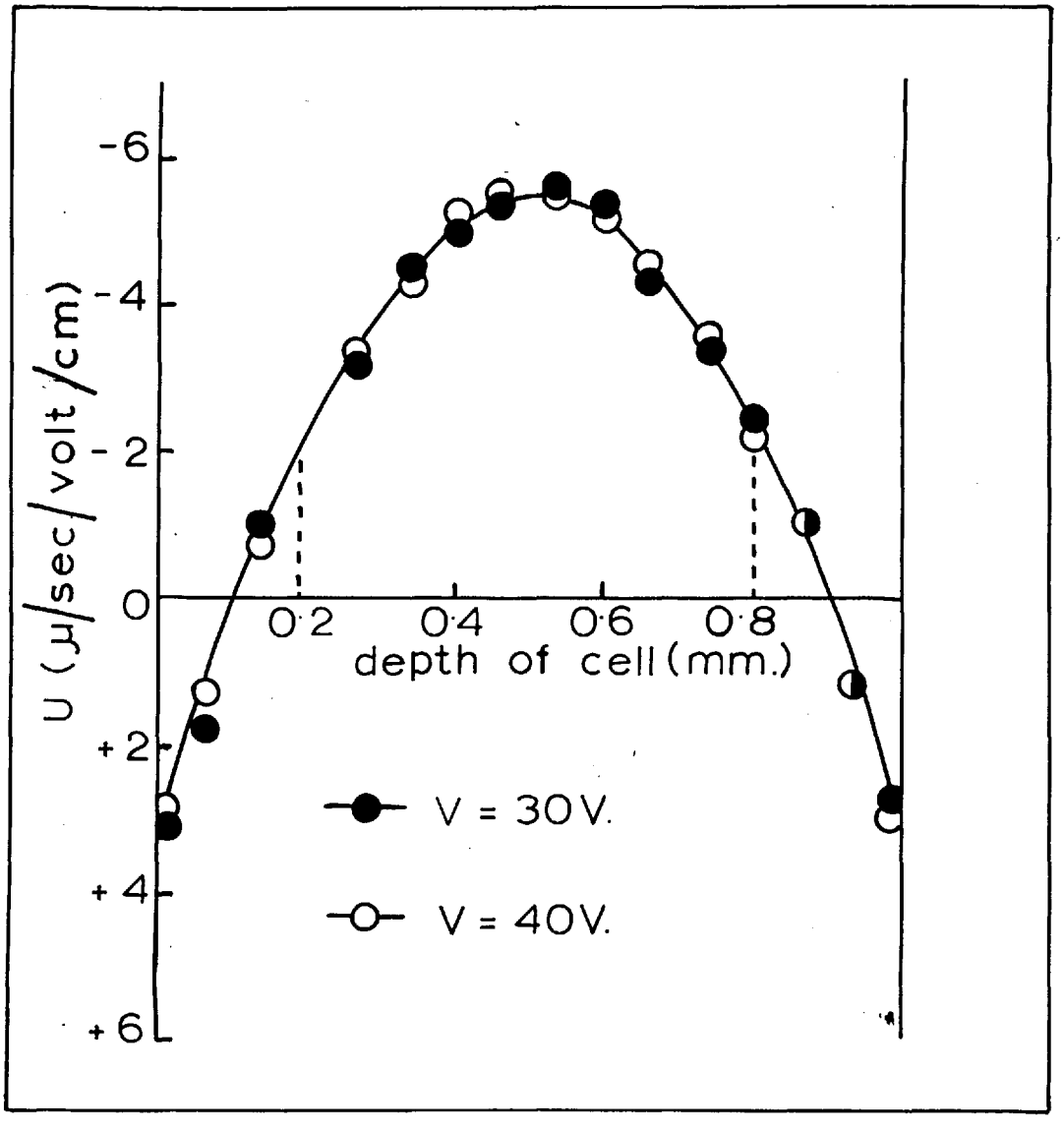

FIG(7·6) ZETA POTENTIAL FOR POLYSTYRENE LATEX PARTICLES AS A FUNCTION OF Na Cl CONCENTRATION IN 10^{-6}M SODIUM HEXADECYL SULPHATE.

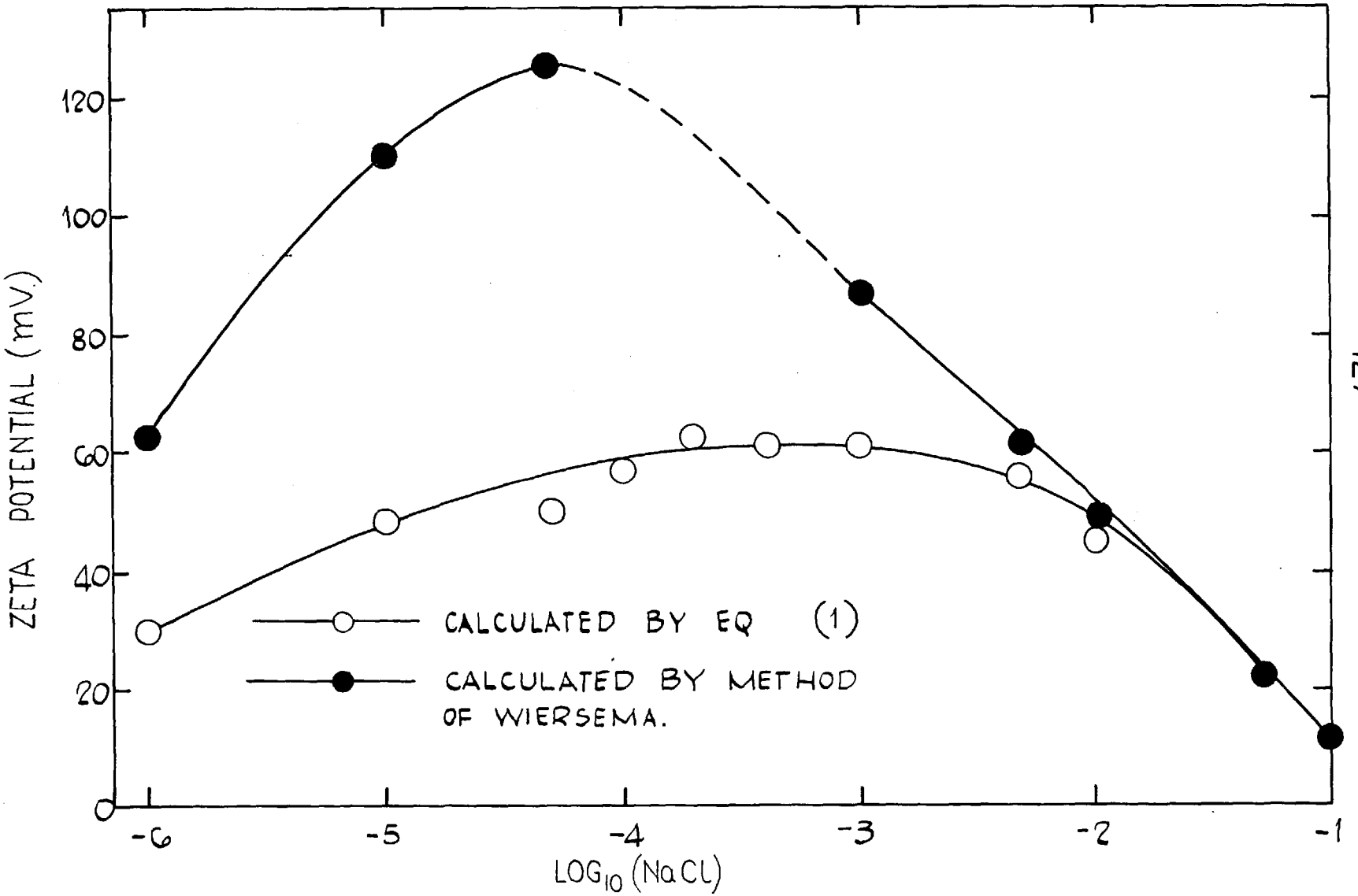

in his paper quotes anomalous results for silver iodide sols. Consequently, it appears that the numerical computations still yield too low a value for the electrophoretic mobility. Unfortunately, in the absence of a more complete description of the relation between the relaxation effect and electrophoretic mobility, the numerical values as tabulated by Wiersema, Loeb and Overbeek will have to be used, with the realization that these values may be too low. In the present case, sufficient data could be obtained on either side of the "critical" ζa range so that interpolation for this region could be obtained fairly confidently, though the inadequacy of the theory in the "critical" range also throws doubt on the accuracy in adjoining ranges.

It is of interest to note that the zeta-potential as a function of electrolyte concentration still passes through a maximum on adjustment for relaxation. This effect is probably due to the effect of the salt concentration upon the extent of adsorption of the sodium hexadecyl sulphate, though it has been suggested by Levine and Bell[19] that the zeta-potential should pass through a maximum due to the "discreteness-of-charge effect". Which of these two factors is responsible for the maximum is uncertain, though it seems unlikely that the salt concentration could change the amount of adsorption of such a small concentration of surface-active agent so that the zeta-potential is just about doubled. Consequently, it is possible that both factors are operative together.

In Figs.(7.7 and 7.8) are shown the zeta-potentials of the

FIG(7·7) THE ZETA POTENTIAL OF POLYSTYRENE PARTICLES AS A FUNCTION OF SODIUM CHLORIDE CONCENTRATION . (a) 4×10^{-4} M S.D.S.

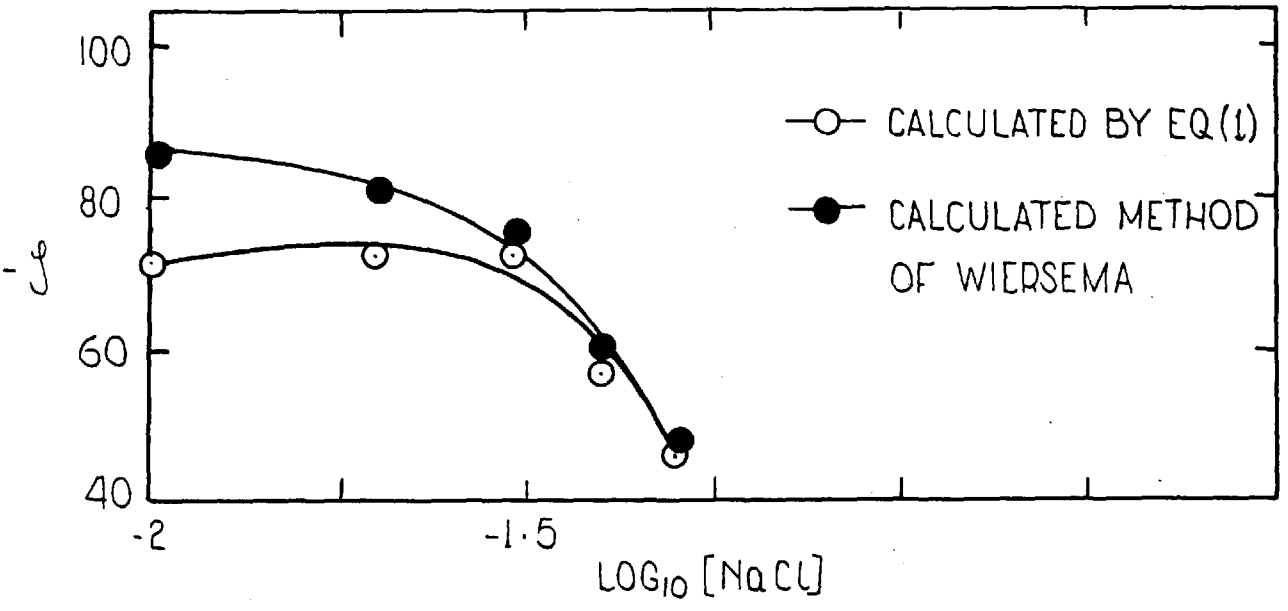

(b) 2×10^{-4} M S.D.S. AND 10^{-4} M S.D.S.

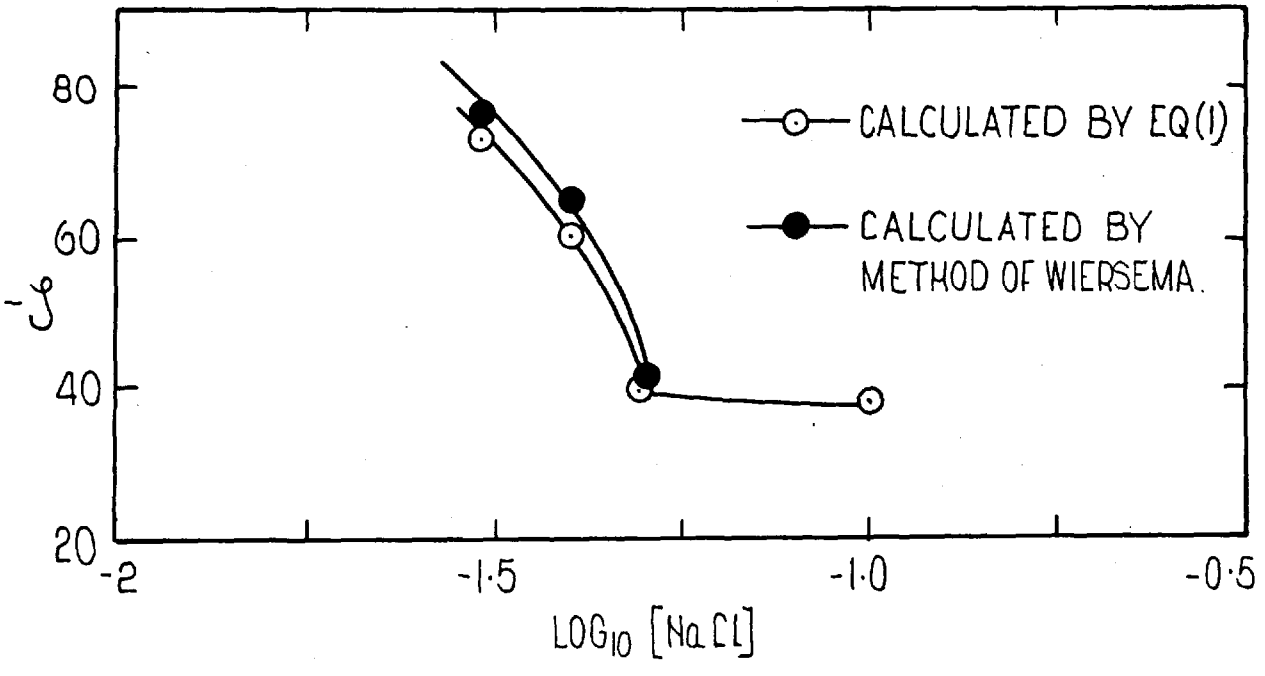

FIG (7·8) THE ZETA-POTENTIAL OF A "FORMVAR" FILM AS A FUNCTION OF SODIUM CHLORIDE CONCENTRATION.

(a) 4×10^{-4} M S.D.S.

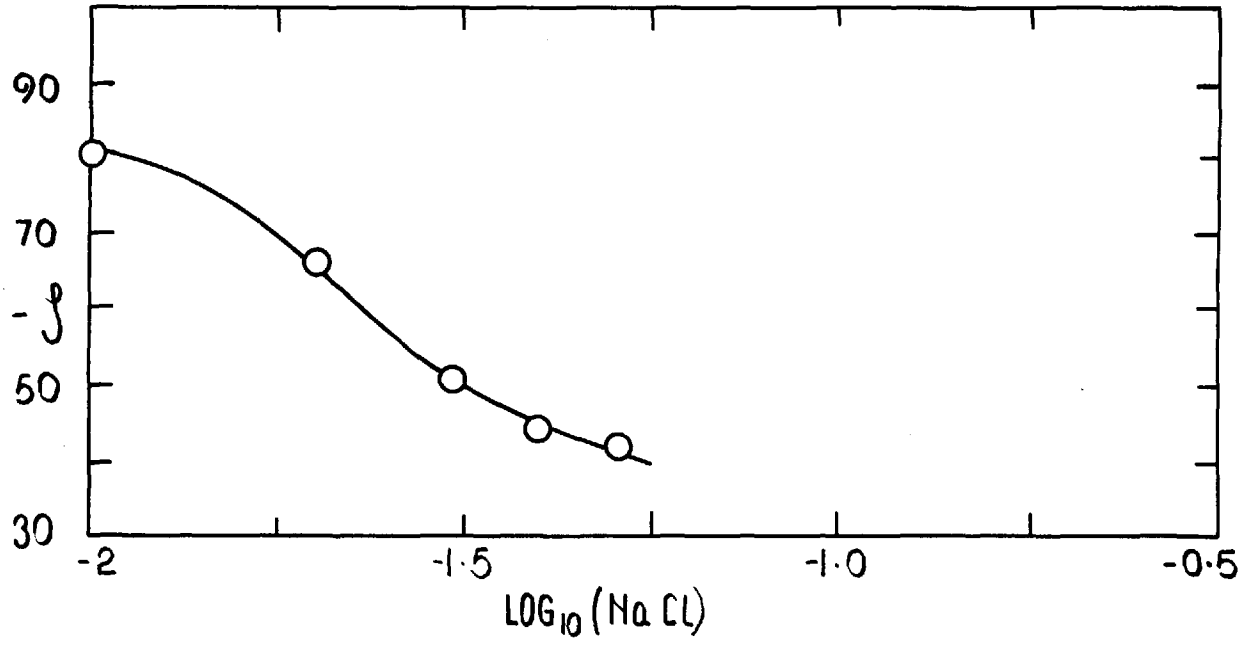

(G) 2×10^{-4} AND 10^{-4} M S.D.S.

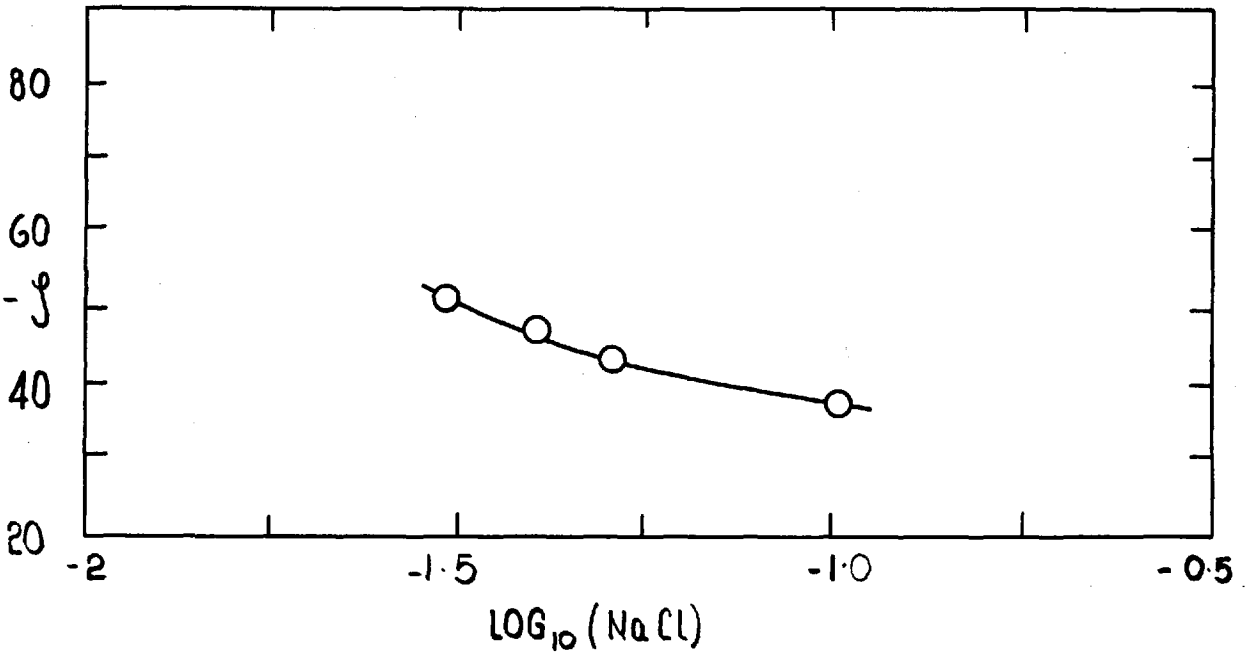

'Formvar' surface and the polystyrene latex particles at the high ionic strengths found to be necessary for uniform reproducible deposition measurements. At the high ionic strength (0.1M) the measurement of the electrophoretic mobility was difficult because of the tendency of gassing to occur at the electrodes. Thus for this determination after one particle had been timed for a set distance in both directions, the cell was flushed with sol and the measurement repeated. Values of the electrophoretic mobility (Appendix 2) are the mean of 40 separate determinations.

It is of interest to note that even at these high ionic strengths, the treatment of Wiersema[11] yields small corrections, presumably because the zeta-potentials involved are high. The values of the zeta-potentials thus determined were subsequently used for the calculation of potential energy curves for the interaction of spherical polystyrene particles with the plane 'Formvar' surface.

7.4. References

(1) Helmholtz, H. Ann. Phys. 7, 337, (1879).

(2) von Smoluchowski, M. Z. Phys. Chem. 92, 129, (1918).

(3) Hückel, E. Z. Phys. 25, 204, (1924).

(4) Debye, P. and Hückel, E. Z. Phys. 24, 185, (1923).

(5) Henry, D.C. Proc. Roy. Soc. A.83, 106, (1931).

(6) Henry, D.C. Trans. Faraday Soc. 44, 1021, (1948).

(7) Booth, F. Trans. Faraday Soc. 44, 955, (1948).

(8) Overbeek, J. th. G. Kolloid-Beihefte 54, 287, (1943).

(9) Booth, F. Proc. Roy. Soc. A.203, 514, (1950).

(10) Overbeek, J. th.G. Adv. in Colloid Sci. 3, 97, (1950).

(11) Wiersema, P.H., Loeb, A.L. and Overbeek, J.th.G. J. Coll. and Interface Sci. 22, 78, (1966).

(12) Loeb, A.L., Wiersema, P.H. and Overbeek, J.th.G. "The Electrical Double-Layer around a Spherical Particle". The M.I.T. Press, Cambridge, Mass. (1961).

(13) Shaw, J.N. and Ottewill, R.H. Nature, 208, 573, (1966).

(14) Schaller, E.J. and Humphrey, A.E. J. Coll. and Interface Sci. 22, 573, (1966).

(15) Stone-Masui, J. and Watillon, A. J. Coll. and Interface Sci. 28, 187, (1968).

(16a) Shergold, H.L., Mellgren, O. and Kitchener, J.A. Trans.Instn. Min. Metall. (Sect.C), 75, 331, (1966).

(16b) Shergold, H.L. Ph.D.Thesis, Univ. of London, (1968).

(17) von Smoluchowski, M. in "Handbuch der Elektrizität und des Magnetismus". Vol. 2. p. 366. Barth. Leipzig. (1921).

(18) Komagata, S. Researches Electrotech. Lab. Japan No.348, p. 8, (1933).

(19) Levine, S. and Bell, G.M. J.Phys. Chem. 67, 1408, (1963).

8.0 DEPOSITION AGAINST A POTENTIAL ENERGY BARRIER

8.1. Experimental Procedure

In preliminary experiments, deposition measurements of polystyrene latex particles on "negatively" charged plastic films were made in exactly the same way as has been described for the deposition on a "positively" charged plastic film (Chap.6). However, in this case the sol concentration and time of deposition were increased, for measurable deposition, because of the presence of a potential energy barrier to deposition.

Two plastic films were used in these measurements, (1) polystyrene (prepared in the same way as the latex sol and precipitated with ethanol) and, (2) electron microscopy grade "Formvar" (polyvinyl-formaldehyde). With both of these substrates in 10^{-5}M sodium chloride solution, the sol concentration was about 10^{9} particles/ml and the time of deposition 60 minutes for a measurable deposition to be obtained.

It was found with both these substrates that the deposition was not uniform, in contrast to the case with the positively charged substrates (Chap.6). Different samples of polystyrene were prepared and all showed the same non-uniform deposition. In 10^{-5}M sodium chloride solution the deposition was very much less with the polystyrene than with the "Formvar", and perhaps because the deposition

was higher with the latter, the non-uniformity of the deposition was much more pronounced. In Fig.(8.1) is shown depositions of polystyrene latex spheres on a "Formvar" surface in 10^{-5}M sodium chloride solution, all photographs being taken from the same disc. It, therefore, became evident that before any meaningful deposition measurements could be made, the origin of this non-uniform deposition had to be investigated and a means of obtaining a uniform deposition sought. All further work was carried out on "Formvar" films only.

8.2. The Origin of the Non-Uniform Deposition

It seemed possible that the non-uniform deposition was caused by irregularities in the plastic film due to the "Formvar" containing "small" particles of a component insoluble in chloroform. Indeed, the chloroform solution of "Formvar" showed a Tyndall beam, which indicated that such particles were present. Consequently, the "Formvar" solution was filtered through a 0.2μ membrane filter. This treatment gave a solution optically much clearer, and the faint Tyndall beam observed was probably due to the polymer itself and not insoluble particulate matter. However, subsequent deposition measurements on a film prepared from this solution still showed a non-uniform deposition. Therefore, it did not seem that the nature of the polymer solution was the cause of the uneven deposition.

Another possible cause was that, during the film preparation, the evaporation of chloroform led to condensation of water droplets on

FIG (8.1) DEPOSITS OF POLYSTYRENE LATEX SPHERES ON 'FORMVAR' IN 10^{-5}M NaCl

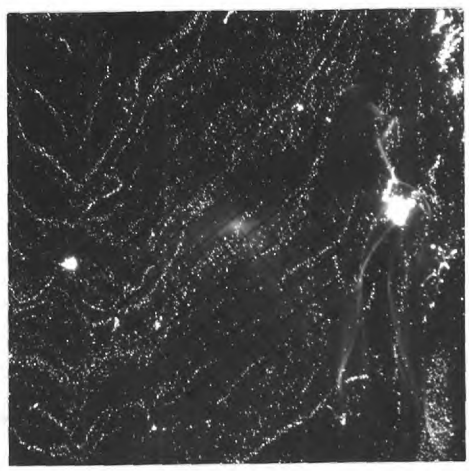

(a)

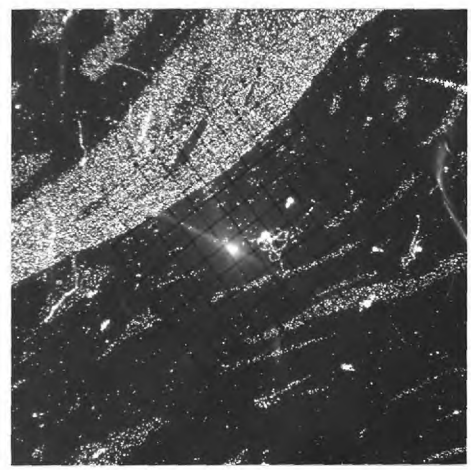

(b)

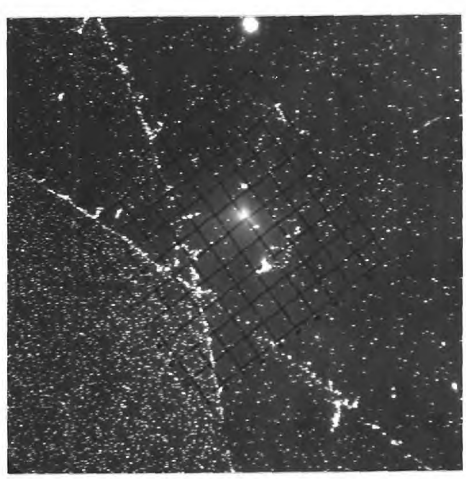

(c)

(d)

(e)

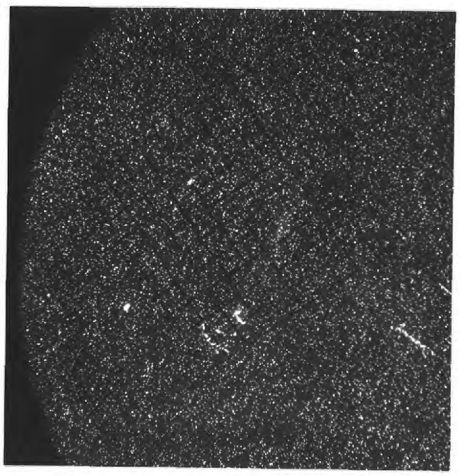

(f)

the film during formation, the net result of which would be to produce a two-phase system leading, on complete "drying" to an incomplete polymer film, where areas of the underlying glass surface would be available for deposition. Such incomplete films have, in fact, been produced in this way[1]. Consequently, it was decided to prepare the plastic films in a desiccant atmosphere. This was achieved by using a slight modification of the apparatus described by Revell and Agar[2]; it is shown in Fig.(8.2). However, the use of this new apparatus did not remove the non-uniformity of deposition, indicating that little moisture condensation was occurring during film preparation, and therefore the non-uniform deposition was due to another cause. Nevertheless, all subsequent films were prepared in this apparatus to ensure that no variation in the relative humidity of the laboratory could effect the morphology of the prepared films.

In Fig.(8.1) it can be seen that some of the deposits resemble a "ripple pattern" that could be formed by the flow of liquid with non-uniform drainage rates, which could have occurred during the film preparation. For, during film preparation, a thin film of polymer solution is formed on the disc, which drains to a uniform thickness, the solvent evaporating off leaving a uniformly thin polymer film. Revell and Agar[2] used microscope slides, which being rectangular, would lead to a uniform laminar drainage of the film in the vertical direction. However, with a circular cover-slip of 22 mm diameter it might be expected that both edge effects due to

FIG(8·2). APPARATUS FOR PREPARING SMOOTH PLASTIC FILMS.

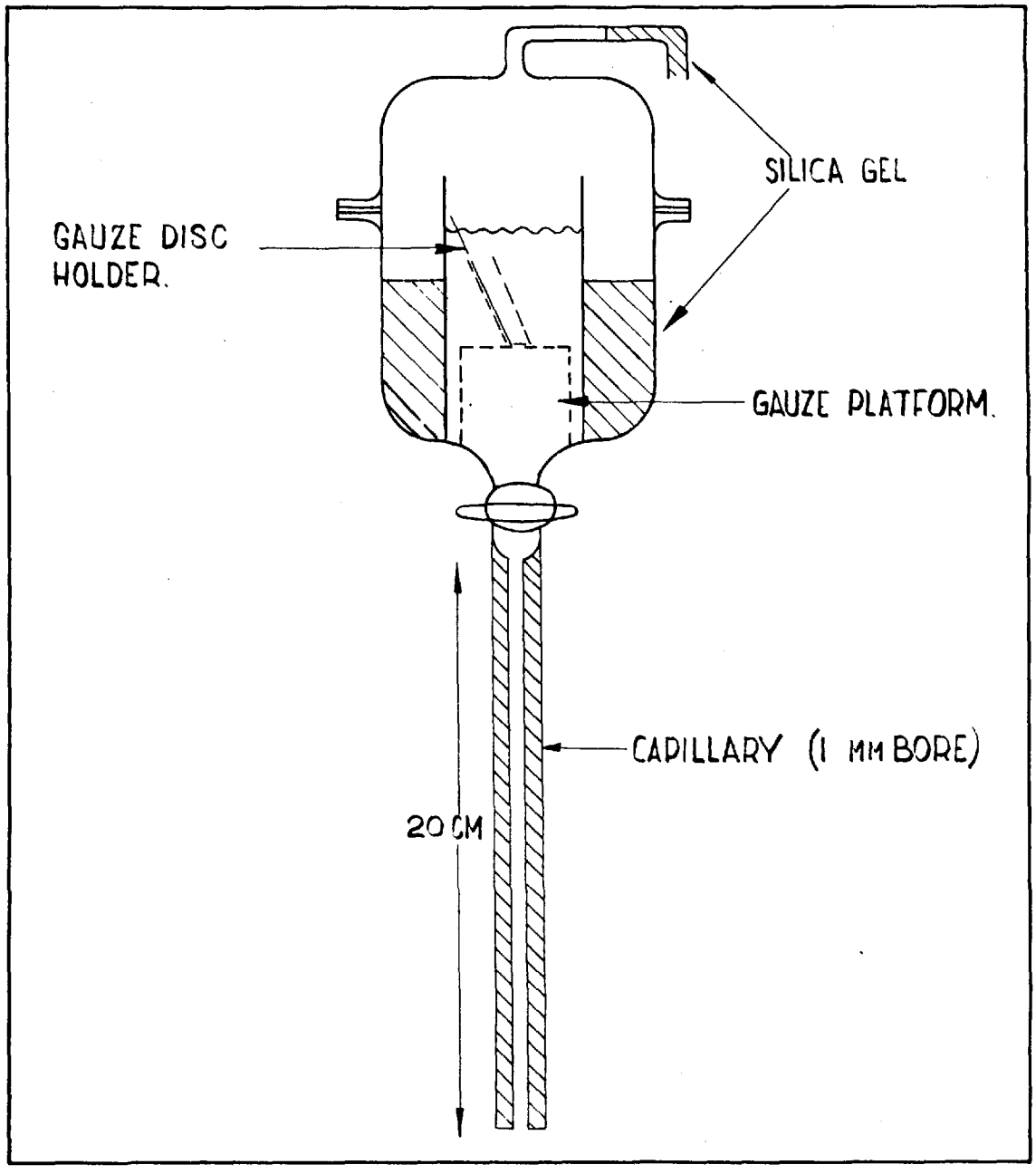

the size of the cover-slip and non-vertical drainage flow due to the circular character of the disc may occur. Thus the film formed on a circular cover-slip may contain ridges, leading to uneven deposition because of the variation in the geometry of the surface. Consequently, both the underlying glass surface and the coated glass surface were examined under the interference microscope, using a sodium lamp as the source of illumination. It was not possible to detect any differences in smoothness between the coated and uncoated discs. In Fig.(8.3.) is shown the interference fringes of a cut film, from which the thickness of the film was determined as 1500Å; hence it would not be possible with a film of this thickness for areas of uncoated glass to be present in the film and remain undetected in the interference microscope. It thus appears that the films are smooth to the limit of the interference measurements ($\simeq$300 Å). Electron micrographs of these "Formvar" surfaces (Fig.(8.4)) show that they are smooth to a high degree; the only "roughness" consists of low "mounds", not exceeding 50 Å in height and about 300 Å across, and these probably follow the contours of the underlying glass surface for the appearance of the coated and uncoated glass is similar. It is therefore unlikely that surface roughness could be the cause of such macroscopic variations in deposition such as those shown in Fig.(8.1).

It therefore appears that the non-uniformity of deposition is not due to the morphological characteristics of the films; it can therefore be due only to variations in the surface-chemical properties

FIG (8.3) INTERFERENCE FRINGES FOR A CUT "FORMVAR" FILM ON A GLASS COVER-SLIP. SODIUM LIGHT USED.

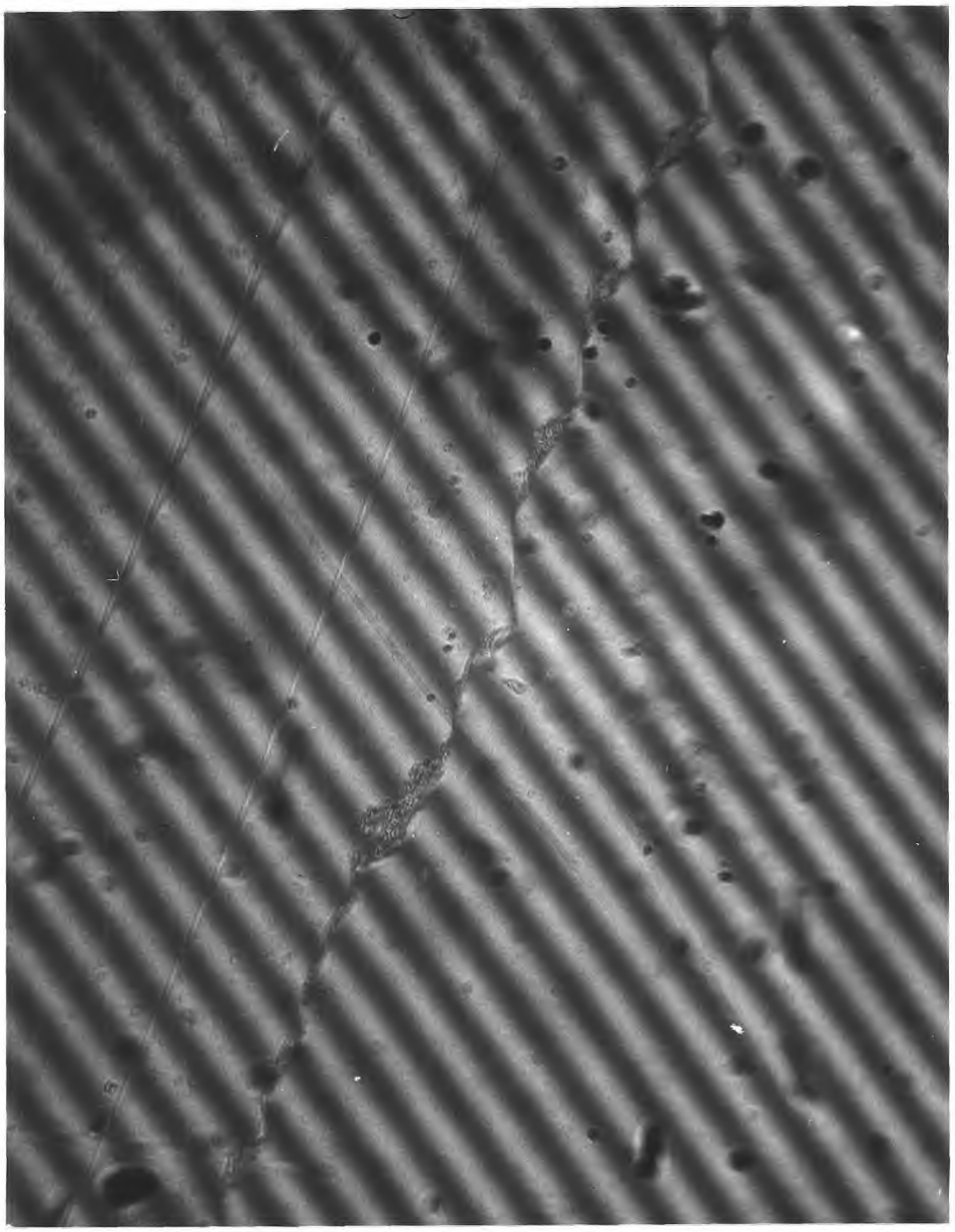

FIG (8.4a) ELECTRON-MICROGRAPH OF THE SURFACE OF A GLASS COVER-SLIP

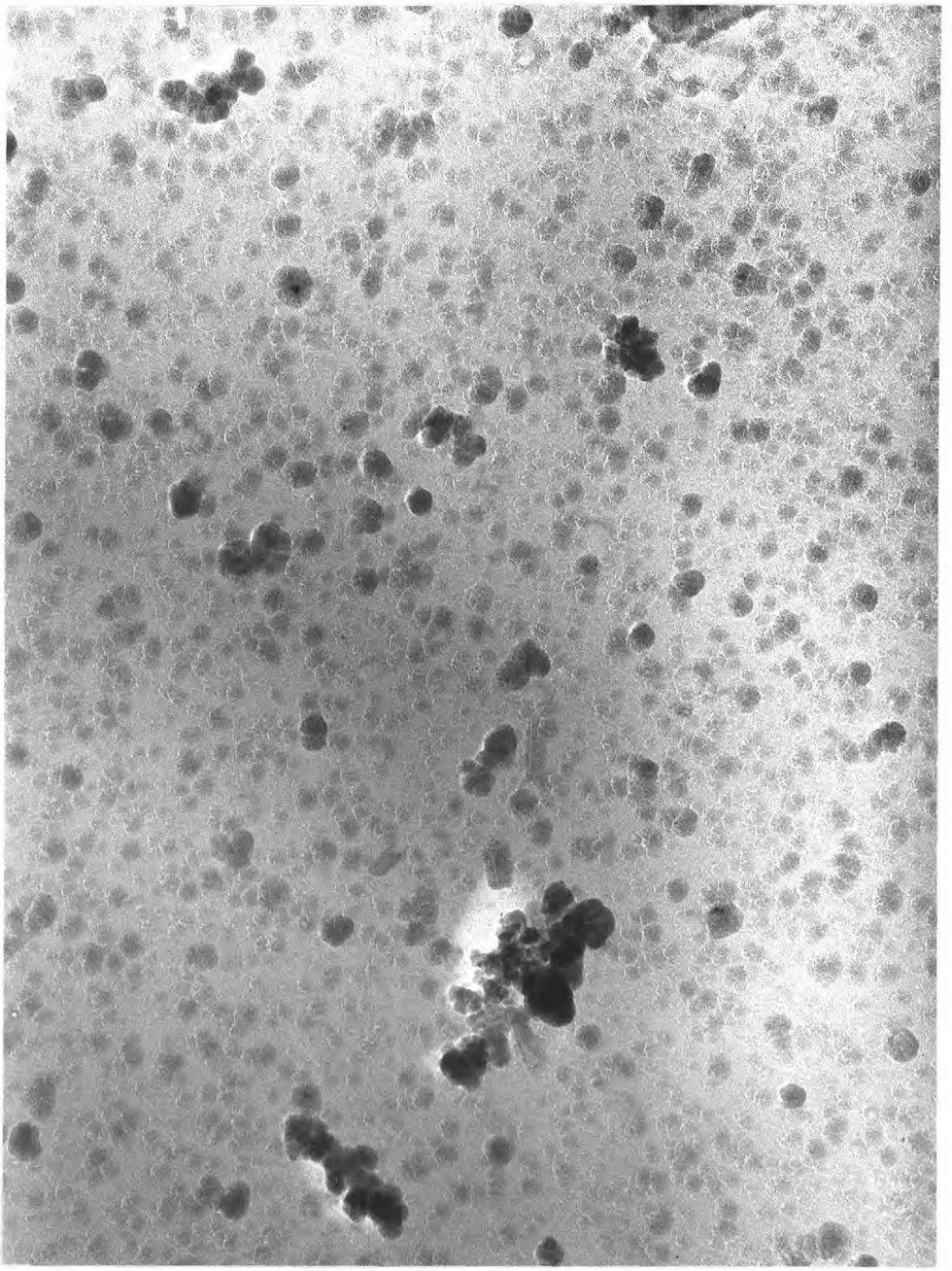

100,000 X

FIG (8.4b) ELECTRON-MICROGRAPH OF THE SURFACE OF A "FORMVAR" FILM ON A GLASS COVER-SLIP

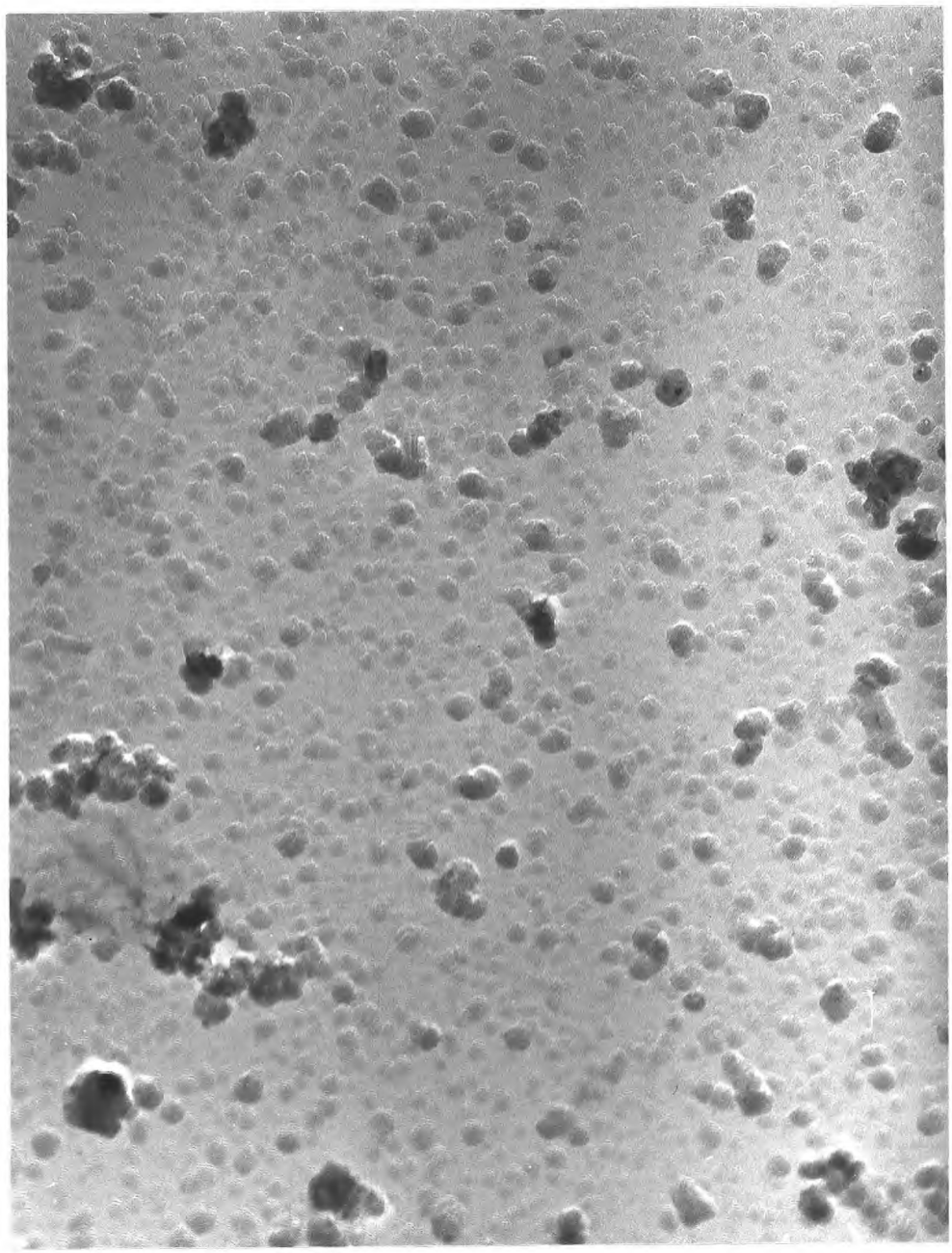

98,000 X

of these films or to hydrodynamic forces operative on deposited particles both during deposition and removal of the disc from the test solution.

If the surface-chemical nature of the plastic was the cause of heterogeneous deposition, then this would suggest that the plastic surface had varying zeta-potentials on its surface ranging from very high where no deposition occurred to very low where deposition readily occurred. The low deposition areas are, presumably, sites of charge brought about by ionizable groups on the surface, and the high deposition areas are possibly areas of hydrocarbon chain with few negative sites. When a drop of distilled water was placed on a freshly mounted "Formvar" surface, it was observed that the advancing contact angle was irregular in outline, which indicates a variation of local angle of contact. It is possible that this could have arisen from greasy contamination of the surface as a result of handling and exposure to air during mounting(9).

It was thought that it may be possible to adsorb an anionic surface-active agent on the low charge density sites whilst leaving the high charge density sites relatively unaffected. To test this hypothesis a deposition measurement was carried out in a solution of 10^{-6}M sodium hexadecyl sulphate and 10^{-4} sodium chloride. This resulted in a much lower deposition, but it appeared uniform. On increasing the electrolyte concentration to 10^{-2}M a relatively high and visually uniform deposition was observed. It, therefore, appeared

that the surface-active agent had indeed caused a "levelling" of the surface charge of "Formvar". Consequently, a series of deposition measurements were made in 10^{-6}M sodium hexadecyl sulphate and varying concentrations of sodium chloride. These results are shown in Fig.(8.5) where W is the stability ratio, which is given by the ratio of the theoretical maximum deposition (limited by diffusion only) to experimentally observed deposition.

8.2.1. Hydrodynamic Considerations

In Fig.(8.1a) it is seen that the deposition is "streaky". It seemed possible that these lines of deposition were caused by the movement of deposited particles by the passage of a meniscus (contact angle) over them. It was found that on removing the disc from water and 10^{-6}M sodium hexadecyl sulphate a contact angle was rapidly formed. It was, therefore, important to ascertain whether this movement of a meniscus led to any significant displacement of deposited particles. If removal of deposited particles was occurring, then the deposition measurements already carried out would be too low. It was, therefore, decided to arrange the experimental conditions so that an air/liquid meniscus did not pass over the disc surface and to determine whether the amount of deposition increased.

The method used was to add ethanol to the sol after completion of deposition so that a wetting film was obtained. Usually about 15% ethanol was used. The disc was given a final rinse in absolute

alcohol, otherwise the alcohol evaporated faster than the water and a contact angle gradually developed. As alcohol is known to cause coagulation of a polystyrene sol, it was essential that the test solution was so diluted before the addition of alcohol that the number of particles left, if deposited because of the alcohol, would be insignificant compared to the measured deposition. This procedure was difficult to arrange, for during dilution an air/liquid meniscus was not allowed to pass over the disc surface. Washing was made easier by isolating the disc surface from the rest of the sol by lowering it into contact with a 10 ml dish during the washing process. Dilution was continued until the sol concentration was less than 10^4 particles/ml.

It was found after this treatment that the deposition was about twice that without the alcohol treatment, Fig.(8.5). However, it was possible to remove all the deposited particles if, after washing, the disc was rotated for 15 minutes.

Leaving the particles to diffuse off after diluting, with no rotation, led to a reduction in the deposit by a factor of two after two days. It, therefore, appears that the particles were so weakly held that they could be removed by capillary forces and at least half of the particles were so weakly attached that they could diffuse away spontaneously.

One other test for the removal capacity of capillary forces was made. In this test, after rotation and dilution, the disc was rinsed only in 15% ethanol. It was then placed in a vertical position

FIG.(8.5) STABILITY RATIO AS A FUNCTION OF ELECTROLYTE CONCENTRATION FOR THE DEPOSITION OF POLYSTYRENE LATEX PARTICLES ON FORMVAR IN 10^{-6}M SODIUM HEXADECYL SULPHATE

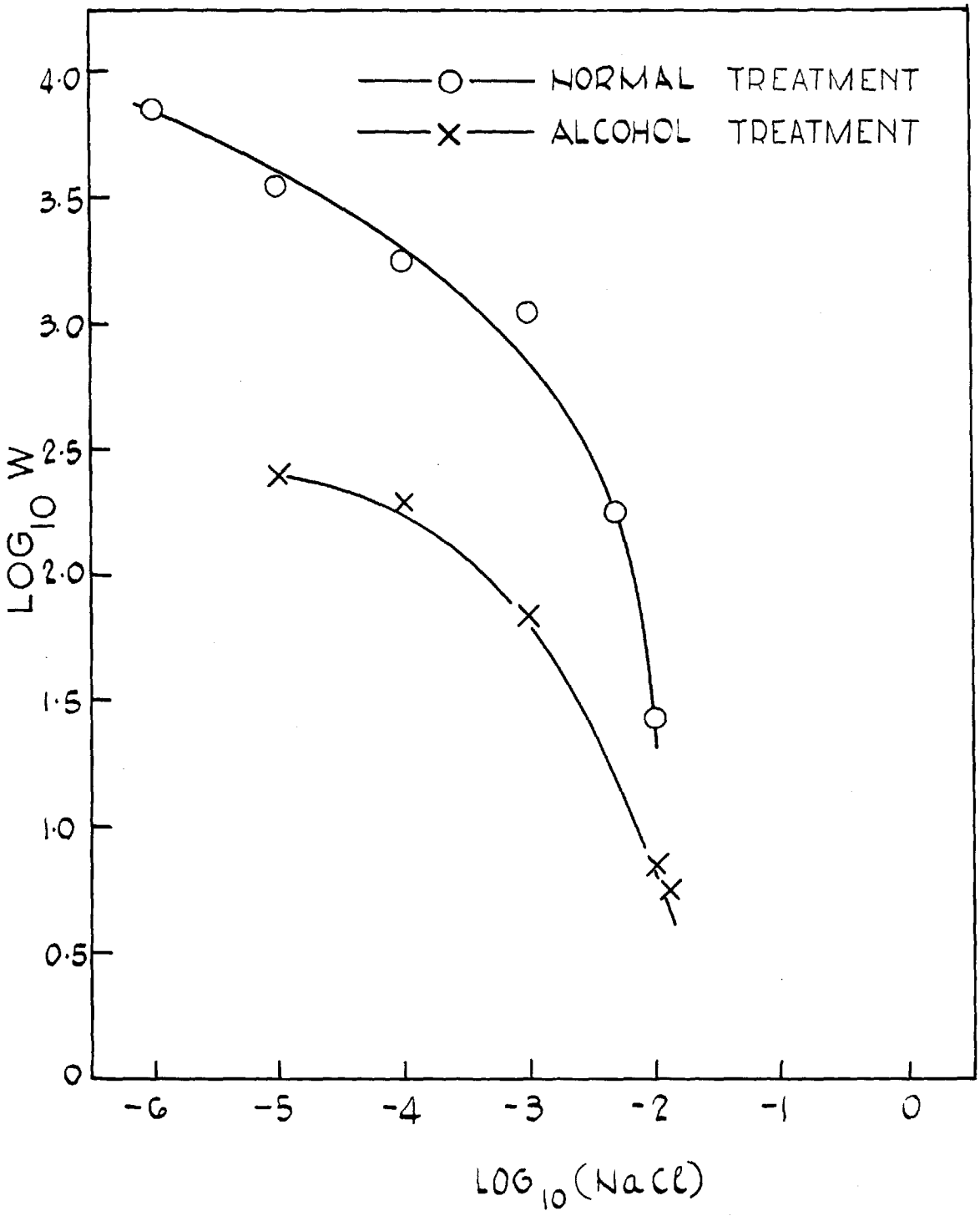

to dry. After a few minutes a meniscus formed and a drop of liquid collected at the bottom of the disc. The disc surface was then placed in a horizontal position for completion of drying. Microscopic examination revealed that most of the particles had collected into that final drop, showing that the meniscus had, indeed, caused the movement of the deposited particles.

It, therefore, appeared that the adhesion energy of the deposited particles was so weak that they could be readily removed by capillary forces. Because of this, the possibility of the movement of deposited particles due to the shearing forces present in the rotating disc was considered.

8.2.2. Hydrodynamic Forces Operating on Deposited Particles as a Result of Fluid Flow

The analysis of the hydrodynamic forces operating on bodies at plane surfaces due to laminar flow conditions is extremely complicated and has not been fully treated. Happel and Brenner[3] determined the drag forces on particles moving in a pipe under Poiseuille flow as a function of their position from the axis of the pipe. Later Maroudas[4] extrapolated the equations of Happel and Brenner for the case of a particle at rest on the wall of the tube. She obtained the following expression for the drag force (T_D)

$$T_D = 12\pi\eta(d^2/D)(1 - d/2D)U \qquad (1)$$

where d is the diameter of the particle, D the diameter of the pipe and U the fluid velocity, η is the viscosity of the fluid.

Jeffrey and Pearson[5] claimed to have shown the existence of a "lift force" on the particles normal to the wall of the pipe. However, their experiments were conducted on particles moving in a fluid, under Poiseuille flow, well away from the wall and consequently, they did not give any indication of the magnitude of this force near or at the surface of the pipe. Maroudas[4], from the considerations of a rotating cylinder in a fluid flow, derived an expression for the "Lift force" on a stationary particle at the wall of a pipe where the flow regime was Poiseuille. The expression obtained for the "lift force" (T_L) was

$$T_L = 16U^2\pi\rho_L (d/D)^2(1 - d/D)(1 - 2d/3D) \qquad (2)$$

where ρ_L is the density of the fluid.

By taking moments of the three forces acting on the particle (drag, lift and weight), assuming that all the forces act at the same point on the particle, about the centre of the particle, Maroudas[4] derived an expression for the minimum fluid velocity required to just start the particle moving. This minimum velocity, called the critical velocity, U_c, is given by

$$U_c = D\left\{\frac{-3\eta\left(1 - \frac{d}{2D}\right) \pm \sqrt{\left[3\eta\left(1 - \frac{d}{2D}\right)\right]^2 + \frac{2}{3}d^3 g \rho_L(\rho_S - \rho_L)\left(1 - \frac{d}{D}\right)\left(1 - \frac{2d}{3D}\right)}}{8d^2(1 - d/D)(1 - 2d/3D)\rho_L}\right\} \quad (3)$$

where ρ_S is the density of the particles and g is the acceleration due to gravity.

Equation (3) does not appear to offer any useful information on the fluid velocity required to remove deposited particles for it is derived on the basis that the only force keeping the particles on the surface is their weight (for the colloidal particles used in this investigation, 9.1×10^{-13} dyne, which is insignificant compared to the adhesional forces). Recently, Goldman, Cox and Brenner[6] and O'Neill[7] have analysed the problem of the shearing forces on a particle at rest on a plane surface in a fluid under Stokes's flow. In both analyses the main assumptions were that the fluid varies as a linear function of distance from the wall, the fluid is incompressible and the flow velocity is such that the inertial effects of the fluid can be neglected. They showed that there is no normal component of force to the surface, i.e. there are no 'lift forces'. The only force operating on the particle is in the direction of flow and is equal to the Stokes's shear force with a factor correcting for the effect of the wall. Their equation is

$$F = 6\pi\eta aUf \qquad (4)$$

where U is the fluid shear velocity at the centre of the particle and the factor f is 1.7009. They also showed that a couple acts on the sphere which would aid its rolling, and is given by

$$C = 8\pi\eta a^2 UG \qquad (5)$$

where G is a factor taking into account the effects of the wall and is numerically 0.944. Once the particle starts moving it continues to roll. The rolling motion contributes to the stream-lines around the particle (rotational flow) then producing a 'lift force' on the particle and eventually the particle lifts clear of the surface. Consequently, once a particle starts moving, it readily becomes detached (unless, of course, a potential barrier to detachment is present). Therefore, in the removal of the deposited particles by fluid flow the problem resolves itself into a question of what fluid velocity is required to start a deposited particle moving. Providing the fluid velocity about the particle is less than 10^{-1} cm s^{-1}, and the rate of change of fluid velocity with distance is linear, it would be justifiable to use equation (4) for the calculation of the shear force on the particle.

The fluid flow near the surface of a rotating disc was described fully by Cochran[8] in the following equations

$$\left.\begin{aligned} V_r &= r\omega F(\zeta) \\ V_\psi &= r\omega G(\zeta) \\ V_y &= (r\omega)^{1/2} H(\zeta) \\ p &= -\rho\nu\omega P(\zeta) \\ \zeta &= (\omega/\nu)^{1/2} y \end{aligned}\right\} \qquad (6)$$

where for small distances from the surface ($\zeta < 0.3$) the dimensionless distance functions, ($F(\zeta)$, $G(\zeta)$, $H(\zeta)$ and $P(\zeta)$) are given by

$$\left.\begin{aligned} F(\zeta) &= 0.51\zeta - 0.5\zeta^2 + 0.205\zeta^3 - 0.0316\zeta^4 \ldots. \\ G(\zeta) &= 1 - 0.616\zeta + 0.17\zeta^3 - 0.11\zeta^4 \ldots.. \\ H(\zeta) &= -(0.51\zeta^2 - 0.33\zeta^3 + 0.103\zeta^4 \ldots.) \\ P(\zeta) &= \text{const} - 1.94\zeta + 0.955\zeta^2 - 0.146\zeta^3 + 0.081\zeta^4 \ldots \end{aligned}\right\} \qquad (7)$$

From these flow equations the fluid flow relative to that at the disc surface can be calculated. A particle deposited on the disc experiences shear forces due to the relative fluid flow about the particle centre and the disc surface, and by substituting the value of the relative fluid velocity at the particle centre into equation (4) the shearing force on the particle may be calculated. It is also seen from equation (7) that the fluid velocity is linear with distance for $\zeta \ll 10^{-2}$, i.e. for less than 1μ from the surface, consequently the use of equation (4) for this system is justifiable. For simplicity fluid velocities relative to the disc surface were calculated for $\zeta = 10^{-3}$ (1630 Å) for a disc rotating at 360 r.p.m. and above the edge of a disc

2 cm diameter. The velocities are

$$\left.\begin{aligned} V_r &= 1.94 \times 10^{-2} \text{ cm } s^{-1} \\ V_\psi &= 1.41 \times 10^{-2} \text{ cm } s^{-1} \\ V_y &= 2.32 \times 10^{-6} \text{ cm } s^{-1} \end{aligned}\right\} \qquad (8)$$

and the pressure difference at this point

$$P - P_0 = 7.34 \times 10^{-4} \text{ dyn cm}^{-2} \qquad (9).$$

Therefore, the only significant fluid forces acting upon a deposited particle in the above designated position are those due to the radial and tangential fluid velocities. Assuming the pressure change acted over the total cross-sectional area of the particle then the "lift force" due to this pressure change would amount to only 5.5×10^{-13} dyne, which is less than the weight of the polystyrene particles relative to the fluid (9.1×10^{-13} dyne). As the adhesional forces are considerably larger than the weight of the particles, it is justifiable to assert that no significant "lift force", due to pressure differences in the rotating disc system, exists on deposited particles. On substituting V_r and V_ψ into equation (4) the shear forces acting on the particle due to shear flow are

$$\left.\begin{aligned} F_r &= 9.1 \times 10^{-8} \text{ dyn} \\ F_\psi &= 6.6 \times 10^{-8} \text{ dyn} \end{aligned}\right\} \qquad (10)$$

Resolving these forces yields a total shearing force parallel to the disc surface of 1.03×10^{-7} dyn. This can be assumed to be the maximum force on any deposited particle, for the fluid velocities and hence the shearing forces decrease as one moves towards the axis of rotation. The force of adhesion is usually greater than 10^{-7} dyn though it may be of the same order of magnitude for 'secondary minimum' deposits. Hence only if the deposition surfaces (plane and sphere) were mathematically pure and there was no deformation of either surface on deposition could the particles be removed by the hydrodynamic forces of the rotating disc system under the conditions used for deposition measurements. In practice, both surface roughness and deformation of surfaces during adhesion occur and consequently it is unlikely that these hydrodynamic forces could remove deposits in the 'primary minimum'. However, in the cases where removal was observed, it was found that deposition was always uniform except for a small region at the edge of the disc. Consequently, it seems that removal was occurring by diffusion and not by shearing forces.

It, therefore, seems that hydrodynamic shear forces in the experimental rotating disc system used does not cause removal of particles, though the particles can apparently diffuse away and be moved by capillary forces. Consequently, there is a good deal of uncertainty about what is happening to the deposited particles when the disc is removed from the sol. It is just possible that particles were actually being deposited by the process of taking the disc from the solution. If this were occurring it would have no significant

effect on the deposition onto the positively charged substrate (because of the low sol concentration), but as the particle concentration for the deposition onto "Formvar" was 100 times that for the deposition onto the positively charged film there may be a significant proportion of deposited particles which have deposited during the removal of the disc from the sol. It, therefore, became essential to examine deposition under conditions where these uncertainties did not arise. Consequently, a modification to the existing rotating disc apparatus was made, which is described in the next section.

8.3. A Modification to the Rotating Disc Apparatus

It was considered essential that deposits should be examined in the deposition medium without the need for removing the disc. For this to be done, the rotating disc system had to be inverted; because of the design of the apparatus (Fig.6.2) this was easily done. The microscope optical system described in Chapter (6) was used. The objective was sealed against water with silicone rubber and used as a water immersion objective. The apparatus is shown in Fig.(8.6), and the water seal for the reaction vessel in Fig.(8.7). The latter consisted of a "Teflon" (p.t.f.e.) block, made to fit a B/34 ground-glass socket, with a central hole drilled slightly larger than the diameter of the disc shaft. The disc shaft was made from polished stainless steel, the "Teflon" acted as a friction-free bearing, so that the speed of rotation of the disc was that of the motor. However, as the assembly was not a perfect water seal, a layer of mercury was

FIG (8.6) THE ROTATING DISC APPARATUS FOR MEASURING DEPOSITION IN SITU

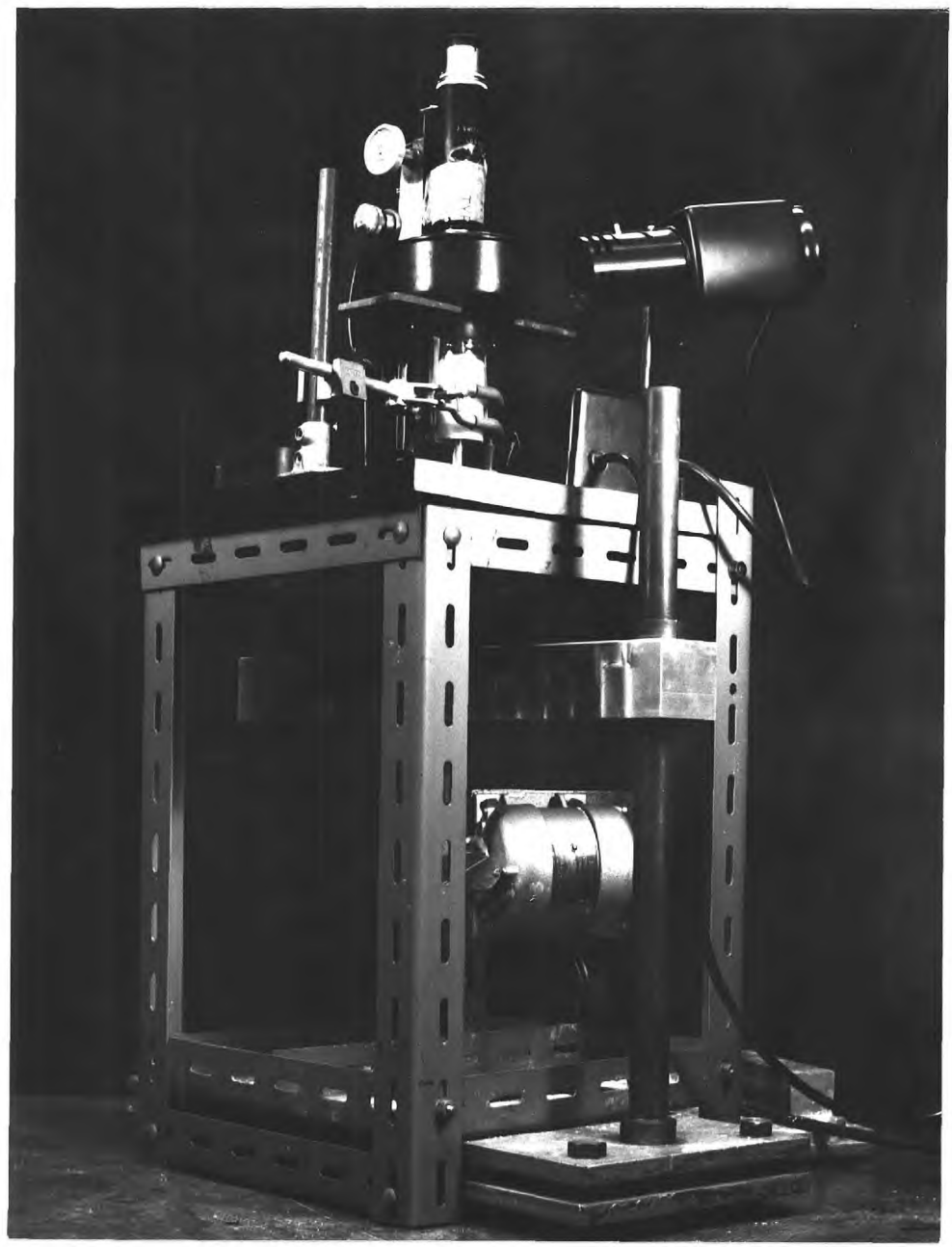

FIG.(8·7) DIAGRAM OF APPARATUS FOR MEASURING DEPOSITION IN SITU.

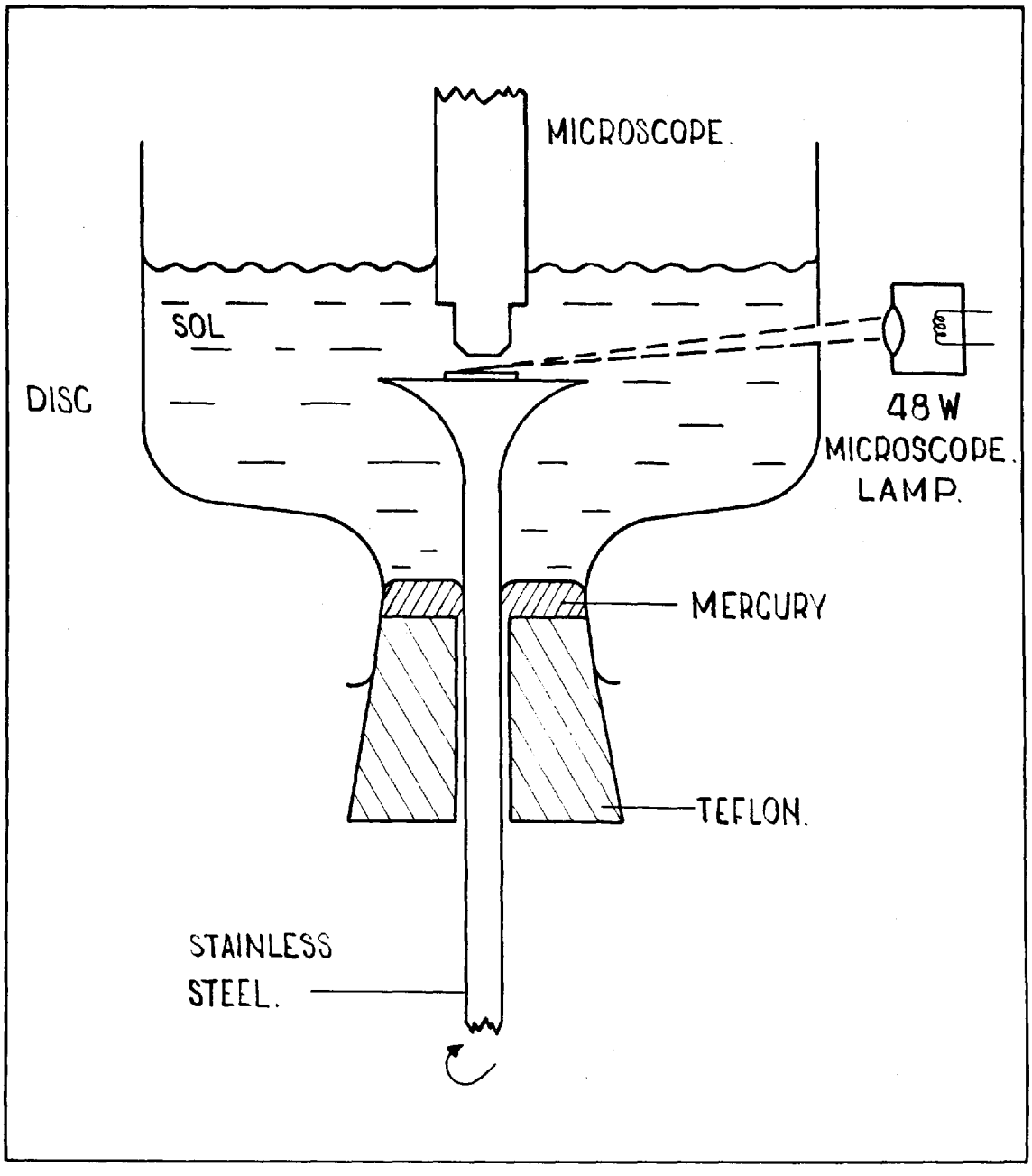

placed at the bottom of the dish to complete the seal.

The main difficulty with this apparatus was in arranging the illumination conditions so that deposited particles could be resolved. In setting up the illumination, a positively charged film (as used for the test of the Levich equation - Chaper 6) was used so that reliable particle counts both in the solution and in air could be made. Only when the particle counts were the same in the solution as in air was the illumination considered correct, for then it was certain that all deposited particles were being seen and counted. To achieve this condition the apparatus had to be used in a dark-room, and the outside of the dish painted black. Also all the metal parts of the microscope objective were blackened with matt paint. In this way stray illumination on the disc surface was eliminated and good resolution of particles was obtained. However, it was found that during the course of a series of measurements, the wax fixing the coated cover-glass to the disc tended to crystallize and thus reduced the contrast appreciably. This problem was overcome by mounting the cover-glass with an air pocket trapped underneath; this arrangement markedly increased the contrast and hence resolution of the deposited particles.

The rate of deposition was measured by rotating the disc for a given time (10 minute intervals) then stopping the motor, racking down the microscope objective and counting the deposited particles. This was repeated until a time period of from 60 to 90 minutes had been

covered.

8.4. Deposition Results

Using this modified rotating disc apparatus, the deposition measurements in 10^{-2}M NaCl and 10^{-6}M sodium hexadecyl sulphate solution were repeated. The deposition was found to be very much less than in the previous measurements (mean stability ratio of about 400). However, it was noticed that the depositions were not uniform, yielding areas where deposition did not occur and areas where the deposition was high (equivalent to W = 80). Consequently, any mean value of the stability ratio would have been meaningless. Therefore, a more concentrated solution of the surface-active agent was required to yield a uniform deposition. Unfortunately, owing to its solubility at room temperature, sodium hexadecyl sulphate could not be used. 10^{-4}M sodium dodecyl sulphate was used instead and this yielded reproducible and apparently uniform results. Deposition measurements were made at 0.3M and 0.1M sodium chloride concentration (Figs.8.8 - 8.9). However, in this case the deposition was not linear with time or proportional to sol concentration. At 5×10^{-2}M NaCl a peculiar form to the deposition curve occurred (Fig.8.11). In this case there appeared to be a reproducible time lag before deposition began and then deposition was linear with time. Careful examination of the deposition in the early stages revealed a slight non-uniformity of deposition. Consequently, the solution of electrolyte and surface-active agent were put into the apparatus for one hour before the sol was added. Subsequently, the

FIG. (8·8) THE RATE OF DEPOSITION OF POLYSTYRENE PARTICLES ON "FORMVAR" IN 10^{-4} M S.D.S & 0·3M NaCl.

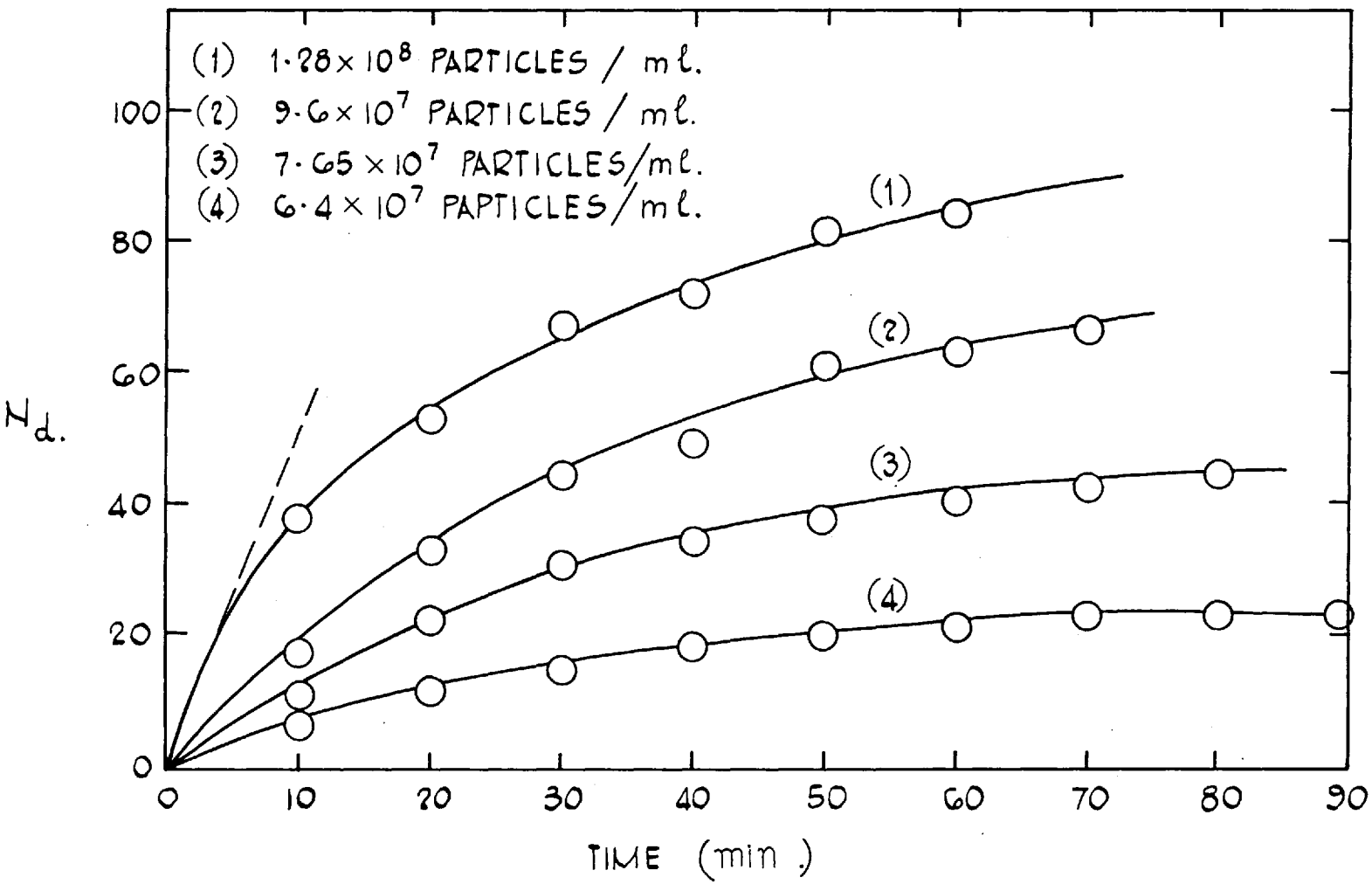

FIG. (8·9) THE RATE OF DEPOSITION OF POLYSTYRENE PARTICLES ON "FORMVAR" IN 10^{-4}M S.D.S. & 10^{-1} M NaCl.

(1.) 1.28×10^8 PARTICLES/ml.
(2.) 6.4×10^7 PARTICLES/ml.

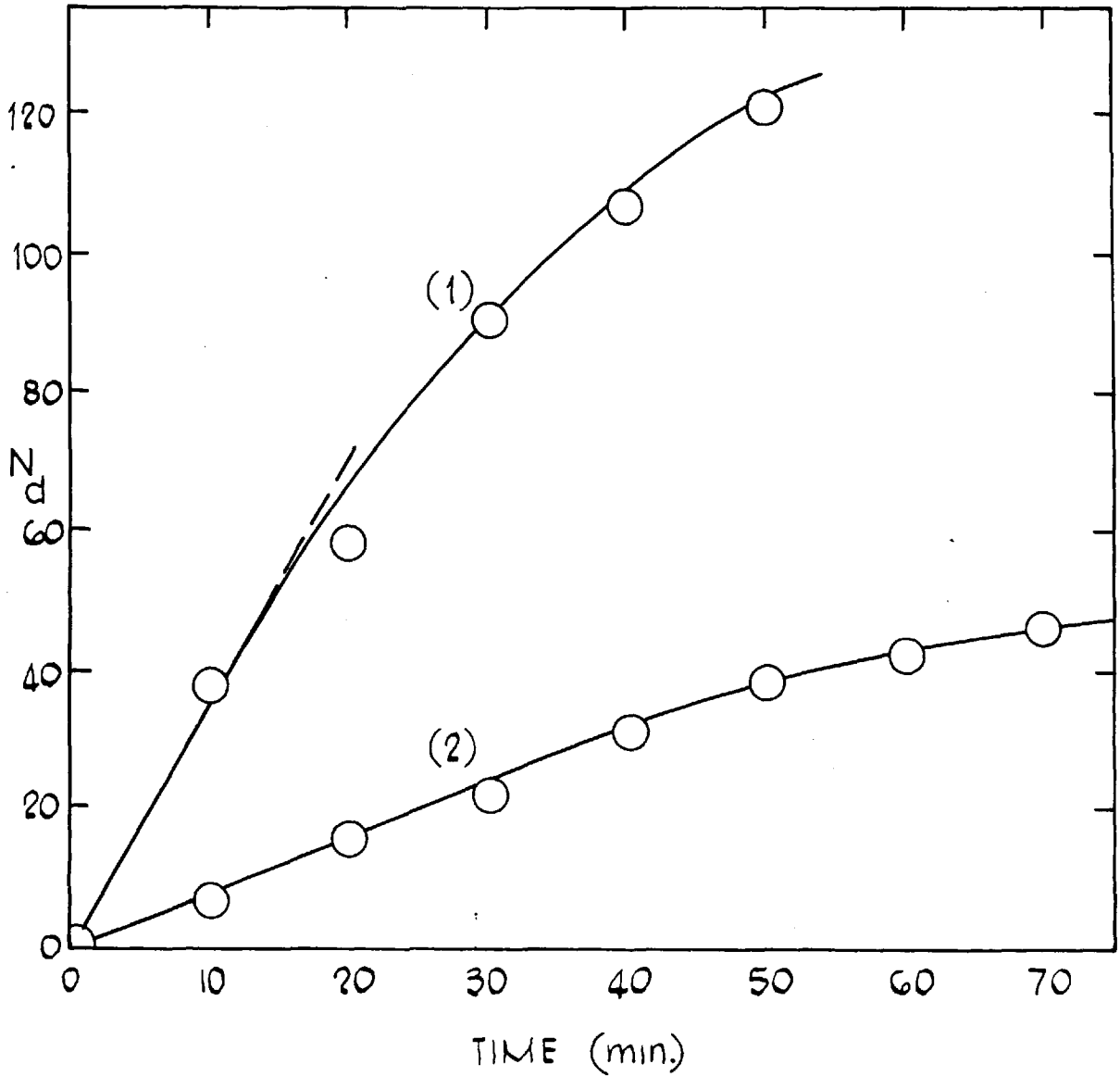

FIG. (8·10) THE RATE OF DEPOSITION OF POLYSTYRENE ON "FORMVAR".

(1.) 10^{-4} M S.D.S., 5×10^{-2} M NaCl.
(2.) 2×10^{-4} M S.D.S., 4×10^{-2} M NaCl
(3) 4×10^{-4} M S.D.S., 3×10^{-2} M NaCl

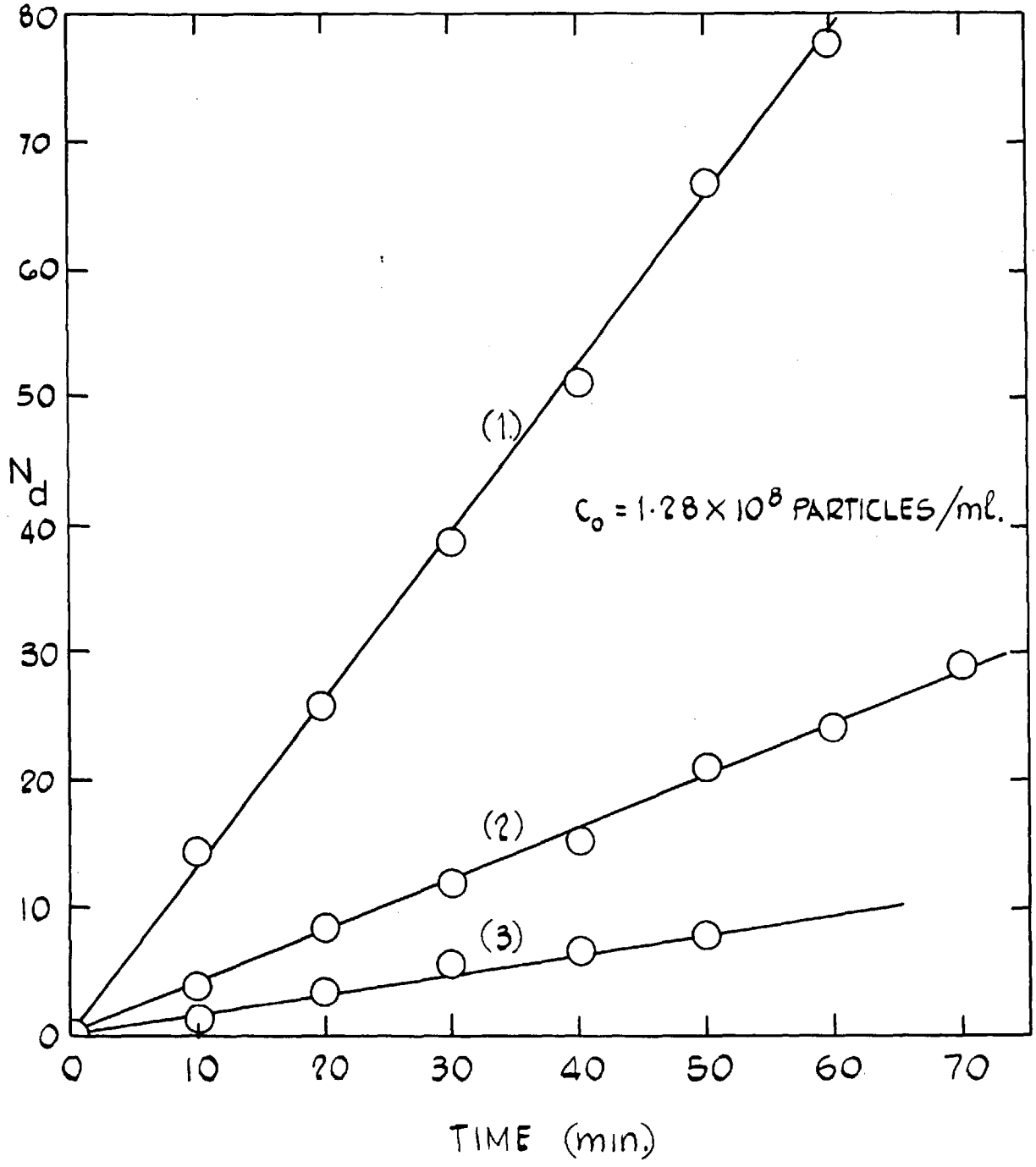

FIG. (8·11) THE RATE OF DEPOSITION OF POLYSTYRENE ON FORMVAR IN 10^{-4} M. S.D.S. AND 5×10^{-2} M. NaCl.

—○— NORMAL DEPOSITION

—●— 1h. CONDITIONING OF FORMVAR SURFACE BEFORE DEPOSITION.

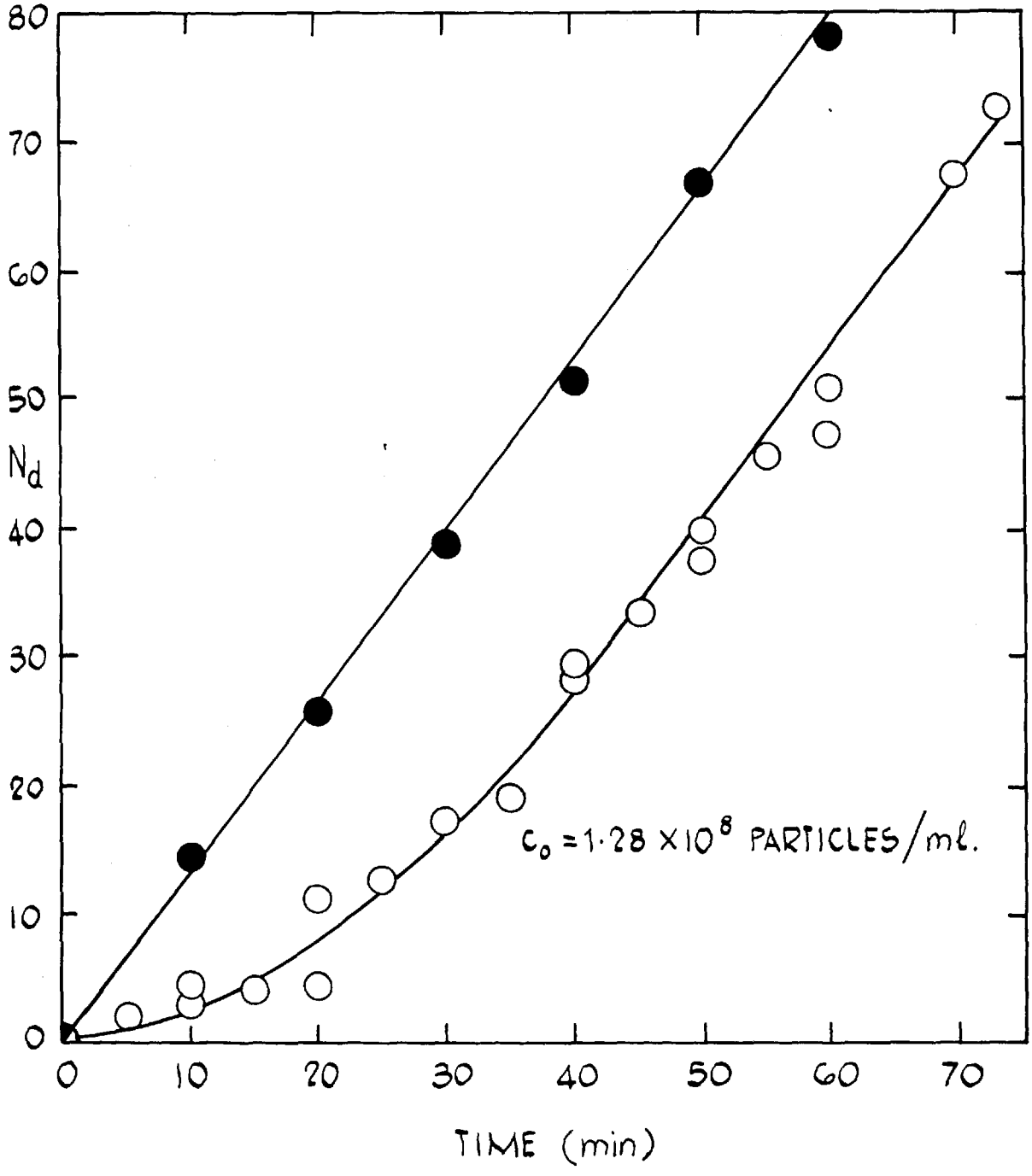

deposition was uniform and the rate of deposition was the same as on the linear part of the graph for the non-conditioned surface. It, therefore, appears that the initial "induction period" was due to the time of adsorption of the sodium dodecyl sulphate. For all subsequent deposition measurements one hour's conditioning of the disc was carried out before the latex sol was added. The results for 3, 4 and 5×10^{-2}M sodium chloride are shown in Fig.(8.10), from which it is seen that the rate of deposition was constant with time.

From the initial rates of deposition the stability ratio was calculated. This is given by the maximum possible deposition rate (obtained from the Levich equation) divided by the experimental deposition rate. These stability ratios for the five salt concentrations examined are shown in Fig.(8.12). At 10^{-2}M NaCl in 10^{-4}M sodium dodecyl sulphate solution no deposition was obtained over 80 minutes and, therefore, the system appears to be completely stable to deposition at this level of electrolyte.

It was necessary to examine the stability of the latex sol itself under the deposition conditions. It was found that for all salt concentrations up to 2M sodium chloride it was not possible to follow the coagulation of the latex sol by normal optical methods, for the optical density scarcely changed even when visible coagulation was observed, and even in 2M lanthanum nitrate solution, rapid coagulation did not occur. Where coagulation did occur, the flocs were very slow to settle (because of small density differences) which resulted in

FIG. (8·12) STABILITY RATIO AS A FUNCTION OF SODIUM CHLORIDE CONCENTRATION.

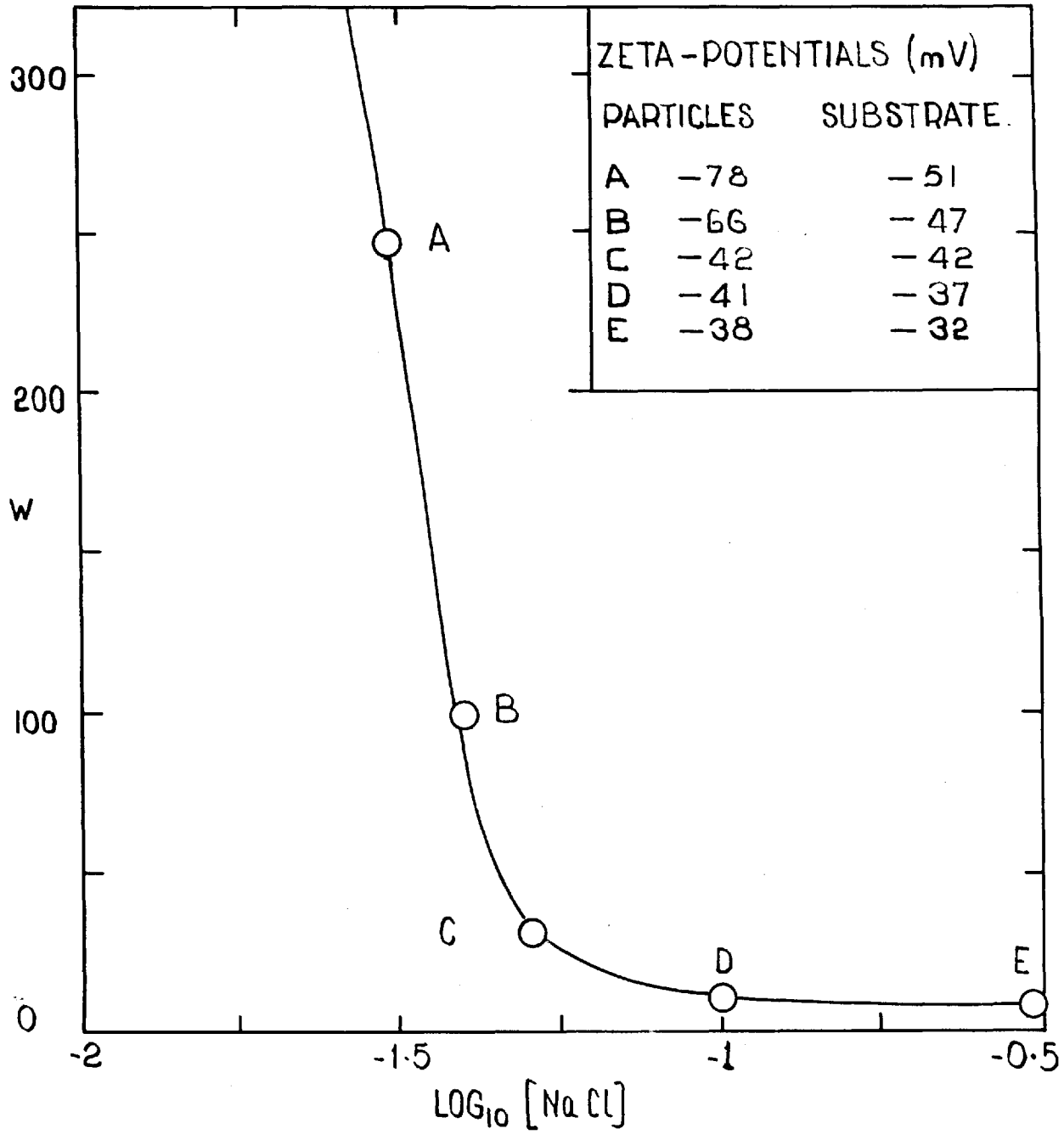

FIG (8.13) THE COAGULATION OF LATEX (2) WITH SODIUM CHLORIDE IN 10^{-4}M S.D.S.

(Particle concentration was 1.5×10^{9} particles /ml).

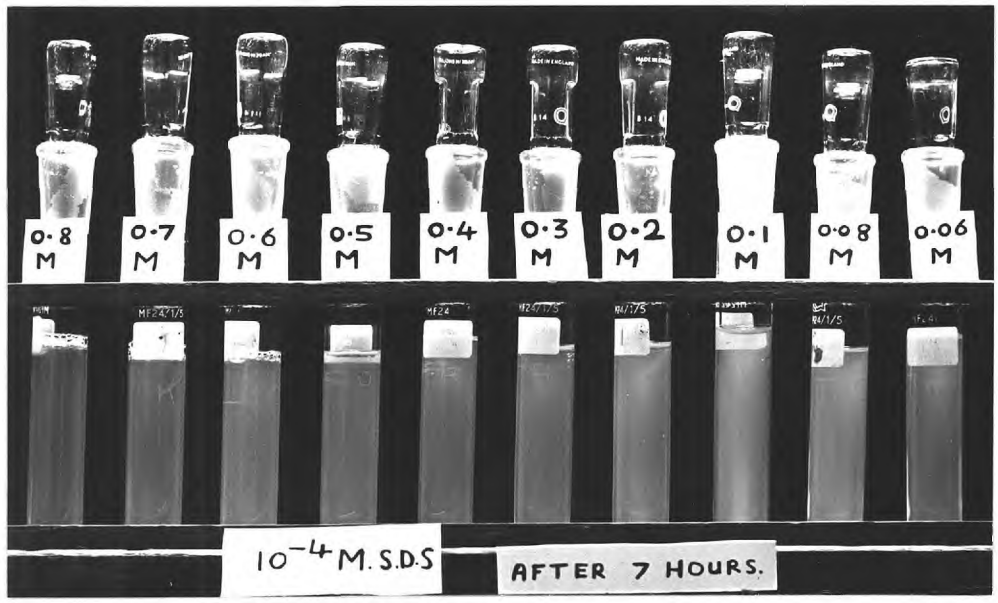

(a)

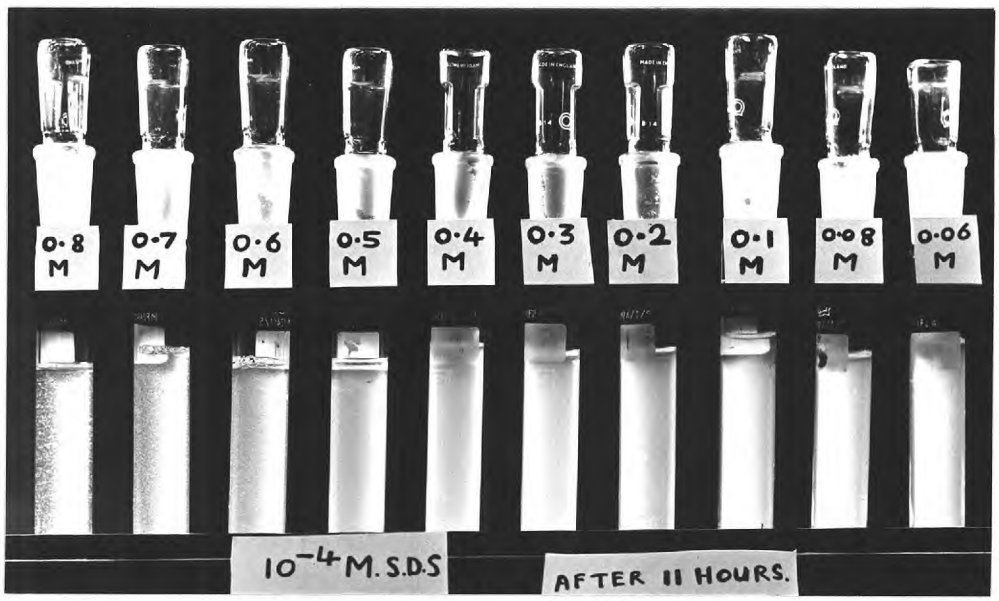

(b)

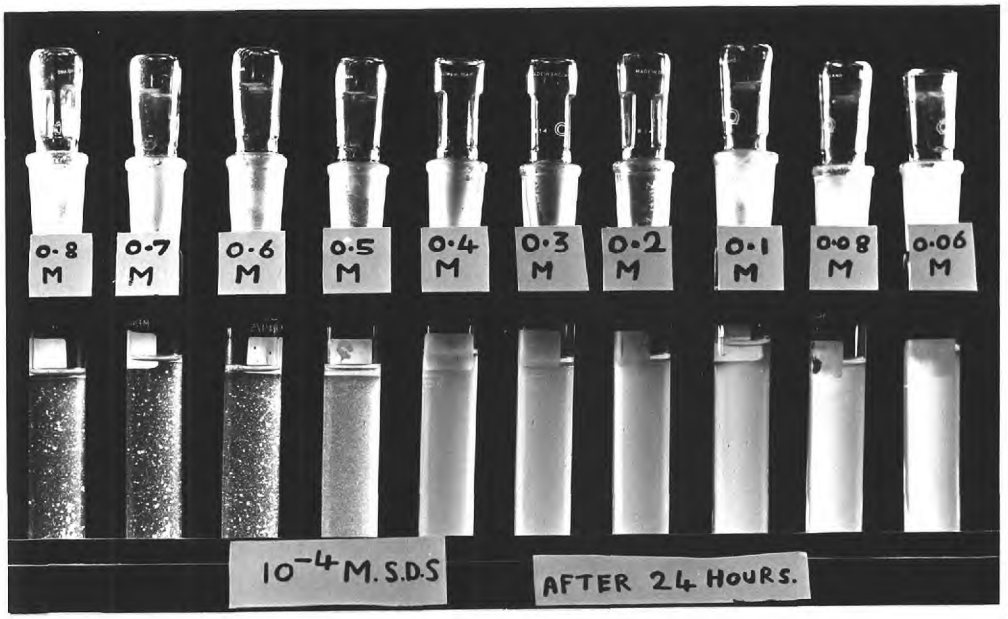
0·8 M
0·7 M
0·6 M
0·5 M
0·4 M
0·3 M
0·2 M
0·1 M
0·08 M
0·06 M
10⁻⁴ M. S.D.S
AFTER 24 HOURS.

(c)


0·8 M
0·7 M
0·6 M
0·5 M
0·4 M
0·3 M
0·2 M
0·1 M
0·08 M
0·06 M
10⁻⁴ M. S.D.S
AFTER 30 HOURS.

(d)

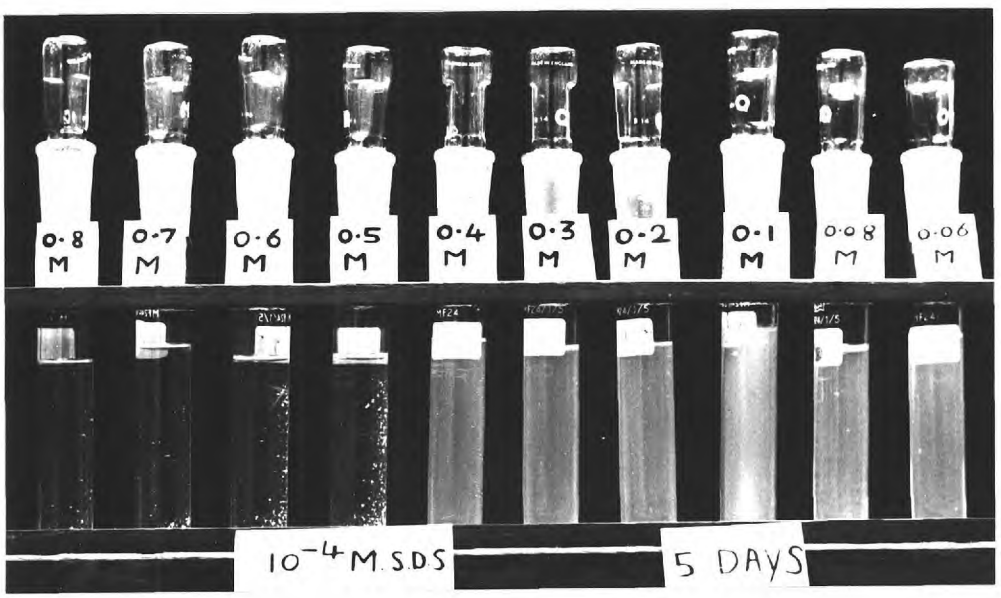

(e)

misleading coagulation data. Instead it was found that by comparing the appearance of the sols with added electrolyte after certain intervals of time (Fig.8.13), the conditions of sol stability could be easily gauged. With 10^{-4}M sodium dodecyl sulphate solution, after 20 h the sol was stable to sodium chloride concentrations of less than 0.6M and even after 48 h the sol was stable to electrolyte concentrations of less than 0.5M. Therefore, the sol is virtually completely stable to coagulation in the conditions used for all the deposition measurements.

8.5. References

(1) Kay, D.H. "Techniques for Electron Microscopy", Oxford, Blackwell Scientific Publications., pp. 71-72, (1965).

(2) Revell, R.S.M. and Agar, A.W. Brit. J. Appl. Phys. 6, 23, (1955).

(3) Happel, J. and Brenner, H. A.I. Ch. E. 3, 506, (1957).

(4) Maroudas, A. Ph. D. thesis, Univ. London, (1961).

(5) Jeffrey, R.C. and Pearson, J.R.A. J. Fluid Mech. 22, 721, (1965).

(6) Goldman, A.J., Cox, R.G. and Brenner, H. Chem. Engng.Sci. 22, 653, (1967).

(7) O'Neill, M.E. Chem. Engng. Sci. 23, 1293, (1968).

(8) Cochran, W. G. Proc. Camb. Phil. Soc. 30, 365, (1934).

(9) Trillat, J.J. and Motz, H. Trans. Faraday Soc. 31, 1127, (1935).

9.0 DISCUSSION

The main problem of this work is to relate the values of the stability ratio, Fig.(8.12), with theoretical potential energy curves, calculated on the basis of the D.L.V.O. theory, for the case of the interaction of a negatively charged sphere and a negatively charged plate.

The van der Waals attraction energy for the sphere-plate system, with neglect of "retardation", is covered by Hamaker's[1] original work on "sphere-sphere" interaction, one of the spheres being taken as having infinite radius. The appropriate expression is

$$V_{s-p} = -\frac{A}{6}\left[\frac{2a(H + a)}{H(H + 2a)} - \ln \frac{(H + 2a)}{H} \right] \qquad (1)$$

where $\underline{A}$ is the Hamaker constant, $\underline{a}$ the radius of the sphere and $\underline{H}$ the distance of separation of the surface of the sphere and the plate. This equation can be used for distances of approach $H \ll \lambda$, where λ is the characteristic wavelength of atom-dipole fluctuations in the dispersion energy theory, although it tends to overestimate V_{s-p} (see Section 4.3). For large distances, namely, for $H \geq 0.1\lambda$, the interaction energy is significantly lower than that given by equation (1), on account of retardation. Clayfield, Lumb and Miller[2] have derived the following approximate expression to allow for the retardation effect

$$V_{s-p} = -\frac{A}{\pi kT} \cdot \frac{4a^3}{H^2(H+2a)^2}\left[0.04083 - 0.006027\,\frac{\lambda}{\pi}\cdot\frac{2(H+a)}{H(H+2a)}\right.$$

$$\left. + 0.000117\,\frac{\lambda^2}{\pi^2}\cdot\frac{2(5H^2+10aH+6a^2)}{H^2(H+2a)^2}\right] \qquad (2)$$

Strictly, this is applicable only when $H > \lambda/\pi$. For the present calculations, λ has been taken as 10^{-5} cm; thus equation (2) is valid for $H > 80$ Å. Complete attraction energy curves were constructed by smooth interpolation between equations (1) and (2), Fig.(9.1).

The expression used for the calculation of the double-layer repulsion energy (sphere/plate) was that derived by Hogg, Healy and Fuerstenau[3] for materials of unlike surface potential, namely,

$$V_R = \frac{\varepsilon a(\psi_1^2+\psi_2^2)}{4}\left\{\frac{2\psi_1\psi_2}{\psi_1^2+\psi_2^2}\ln\left[\frac{1+\exp(-\kappa H)}{1-\exp(-\kappa H)}\right] + \ln(1-\exp(-2\kappa H))\right\} \qquad (3)$$

Total potential energy curves were calculated for the systems corresponding to points A - E in Fig.(8.12), with the usual assumption that ψ_1, ψ_2 of equation (3) can be approximated by the zeta-potentials. Before the theoretical potential energy curves can be calculated, an estimate of the total Hamaker constant for the interacting system must be made.

fig.(9·1) THE VAN DER WAALS ATTRACTION ENERGY (SPHERE-PLATE) WITH AND WITHOUT ALLOWANCE FOR RETARDATION. $A = 10^{-13}$ ergs. $a = 1540$ A

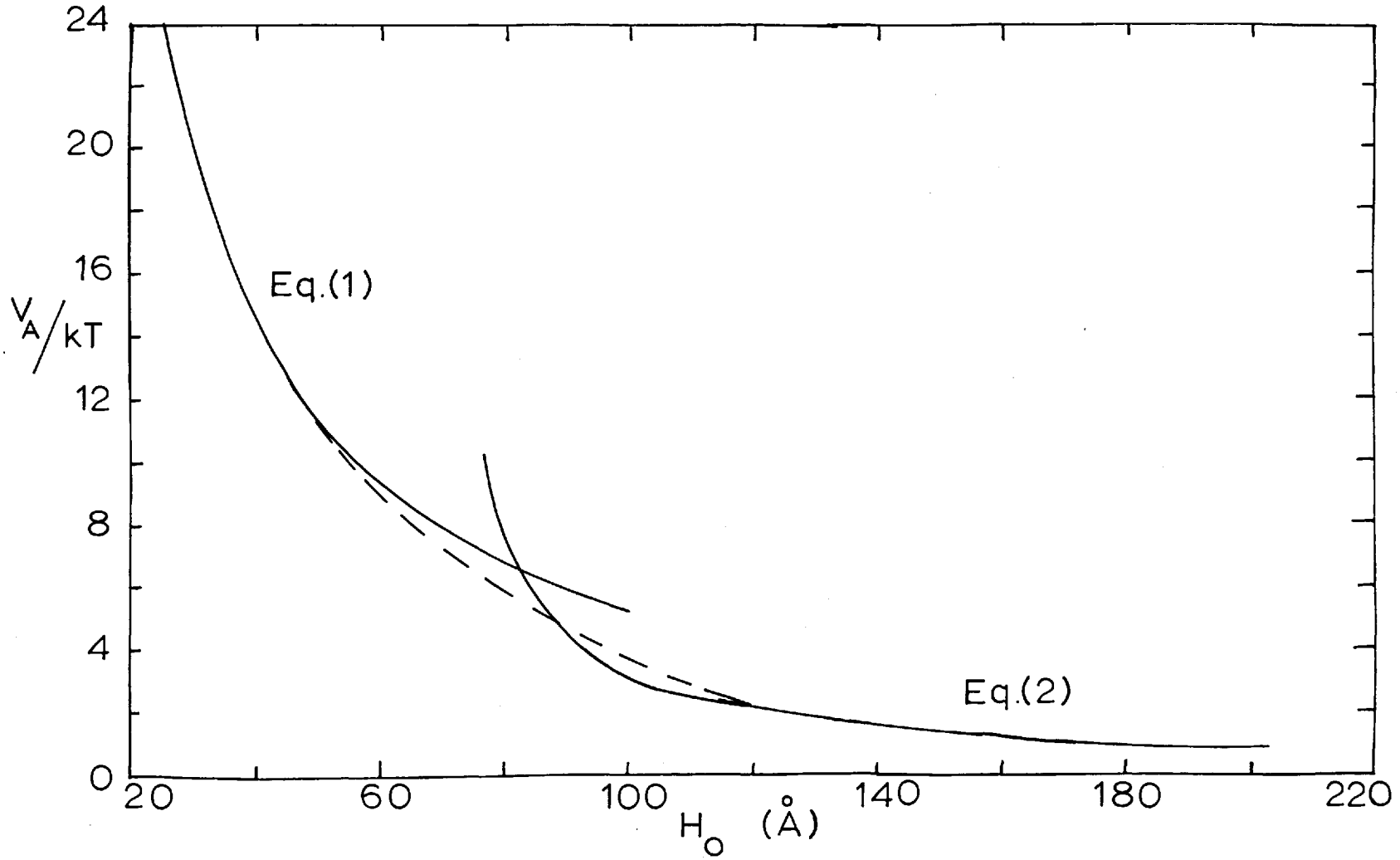

9.1. The Hamaker Constant

In the system under investigation, the two interacting surfaces (polystyrene and "Formvar") probably have different Hamaker constants. The total Hamaker constant for the interaction of two dissimilar materials in water ($A_{12/3}$) is given by

$$A_{12/3} = A_{12} + A_{33} - A_{13} - A_{23} \qquad (4)$$

where A_{11}, A_{22} and A_{33} are the Hamaker constants of material (1), material (2) and water in vacuo respectively. This total interaction energy cannot be calculated exactly because only the term A_{33} in equation (4) is known. However, by making the assumption that the geometrical mean law holds, i.e. that

$$A_{ij} = \sqrt{A_{ii} \cdot A_{jj}} \qquad (5)$$

where A_{ij} is the Hamaker constant for the interaction of particles of material i and material j in a vacuum. Also from the consideration[13] that

$$\left.\begin{aligned} A_{11/3} &= \left(\sqrt{A_{11}} - \sqrt{A_{33}}\right)^2 \\ A_{22/3} &= \left(\sqrt{A_{22}} - \sqrt{A_{33}}\right)^2 \end{aligned}\right\} \qquad (6)$$

where $A_{11/3}$ and $A_{22/3}$ are the Hamaker constants for material (1) and

material (2) in water respectively, the following approximate expression for the total Hamaker constant for two dissimilar materials in water ($A_{12/3}$) is obtained from equation (4),

$$A_{12/3} = \sqrt{A_{11/3} \cdot A_{22/3}} \qquad (7)$$

where A_{11} and $A_{22} > A_{33}$. Consequently, from values of the Hamaker constant of Polystyrene and "Formvar" in water, it is possible to estimate the magnitude of the total Hamaker constant for the interaction of the two materials.

In Table (1) is collected a variety of experimentally determined values for the Hamaker constants of organic materials in water, and in Table (2) theoretical values of these materials.

It is seen from these values that there is considerable uncertainty about the absolute value of the Hamaker constant in water. However, all the organic materials investigated have Hamaker constants of between 10^{-14} and 5×10^{-13} ergs. Consequently, it is probable that polyvinylformaldehyde has a similar Hamaker constant to polystyrene. However, even assuming that polystyrene has a Hamaker constant as low as 10^{-14} ergs and "Formvar" one as high as 10^{-12} ergs will, on application of equation (7), yield a total Hamaker constant for their interaction in water of 10^{-13} ergs. It, therefore, seems unlikely that the total Hamaker constant for the interaction of polystyrene with "Formvar" in water lies outside the range

TABLE 1

Experimental Hamaker Constants for the Interaction of a Variety of Organic Materials in Water

Material	Method	$A_{11/3}$ (ergs)	Ref.
Polystyrene Latex	Coagulation ($BaNO_3$)	$0.103 - 1.10 \times 10^{-13}$	(6)
	" ($NaClO_4$)	$0.4 - 0.7 \times 10^{-13}$	(7)
Styrene/ butadiene Latex	Coagulation ($NaNO_3$)	$0.3 - 0.38 \times 10^{-13}$	(9)
	" ($MgCl_2$)	$0.2 - 1.1 \times 10^{-13}$	(9)
	" ($La(NO_3)_2$)	$0.4 - 2.6 \times 10^{-13}$	(9)
A variety of latexes	Coagulation (NaCl)	$0.9 - 1.5 \times 10^{-12}$	(10)
	" ($CaCl_2$)	$0.8 - 1.4 \times 10^{-12}$	(10)
Paraffin wax	Coagulation (KCl)	1.78×10^{-13}	(11)
	" ($KCl + BaCl_2$)	1.36×10^{-13}	(11)
	" ($KCl + Pb(NO_3)_2$)	1.78×10^{-13}	(11)
	" ($KCl + UO_2(NO_3)_2$	1.49×10^{-13}	(11)
Arachidic acid	Coagulation (various ions)	$0.015 - 0.18 \times 10^{-13}$	(12)

TABLE 2

Theoretical Hamaker Constants for the Interaction of a Variety of Organic Materials in Water

Material	$A_{11/3}$ (ergs)	Ref.
Polystyrene	5×10^{-13}, 9×10^{-13}	(14)
	$2.75 - 4.78 \times 10^{-13}$	(6)
	$0.34 - 2.6 \times 10^{-13}$	(7)
	0.5×10^{-13}	(8)
Polyethylene	0.2×10^{-13}	(8)
Paraffin wax	1.60×10^{-13}	(11)
	0.2×10^{-13}	(8)
Stearic acid	$0.79 - 3.68 \times 10^{-14}$	(12)

$A_{12/3} = 0.1 - 1.0 \times 10^{-13}$ ergs. Consequently, theoretical potential energy curves were calculated for this range of Hamaker constant (Appendix 5 and 6). The total potential energy curves for the coagulation of polystyrene particles dispersed in water are shown in Fig.(9.2 and 9.3), and for the deposition of polystyrene on to a plane "Formvar" film in Fig. (9.4-6).

Before these theoretical curves can be compared to the experimentally observed deposition, it is necessary to obtain a relationship between the potential energy barrier and the stability ratio. This is derived in the next section.

9.2. The Relation between the Stability Ratio and the Potential Energy Barrier to Deposition.

In the rotating disc system the mass flux arriving at the disc surface is controlled solely by linear diffusion, the effective diffusion path length being controlled by the speed of rotation of the disc. Therefore, the problem that has to be resolved is the effect of a potential gradient upon the rate of linear diffusion.

The theory of linear diffusion in a potential field was formulated by Kramers[4] who arrived at the following expression for the stationary diffusion flux, j, between two planes, A and B, along a potential, V, which is a function of the distance H, only :-

FIG(9·2) TOTAL POTENTIAL ENERGY CURVES FOR THE INTERACTION OF TWO SPHERICAL POLYSTYRENE PARTICLES IN 0·1 M NaCl AND 10^{-4}M S.D.S.

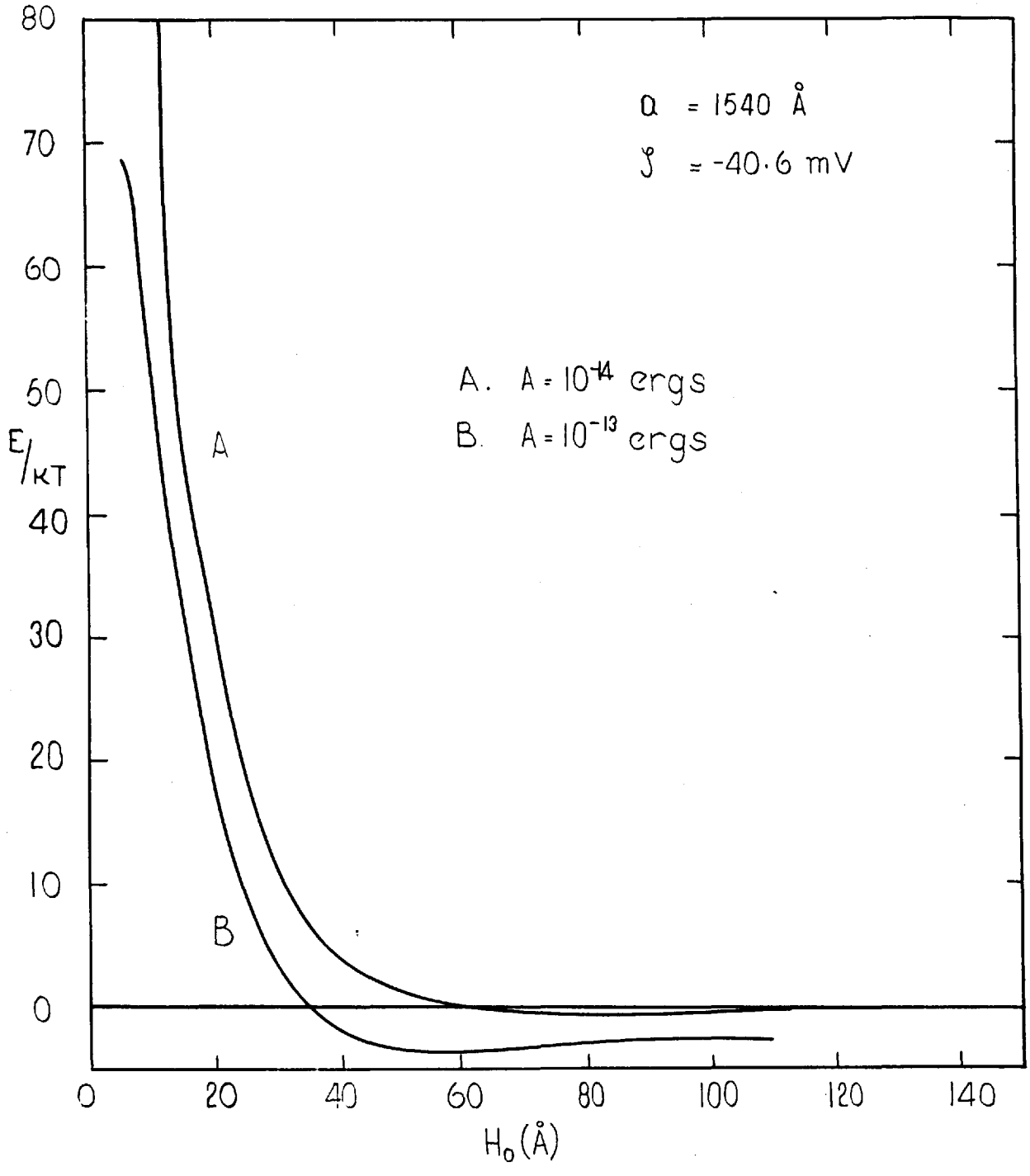

FIG(9.3) TOTAL POTENTIAL ENERGY CURVES FOR THE INTERACTION OF TWO SPHERICAL PARTICLES IN 0·3 M NaCl AND 10^{-4} M S.D.S.

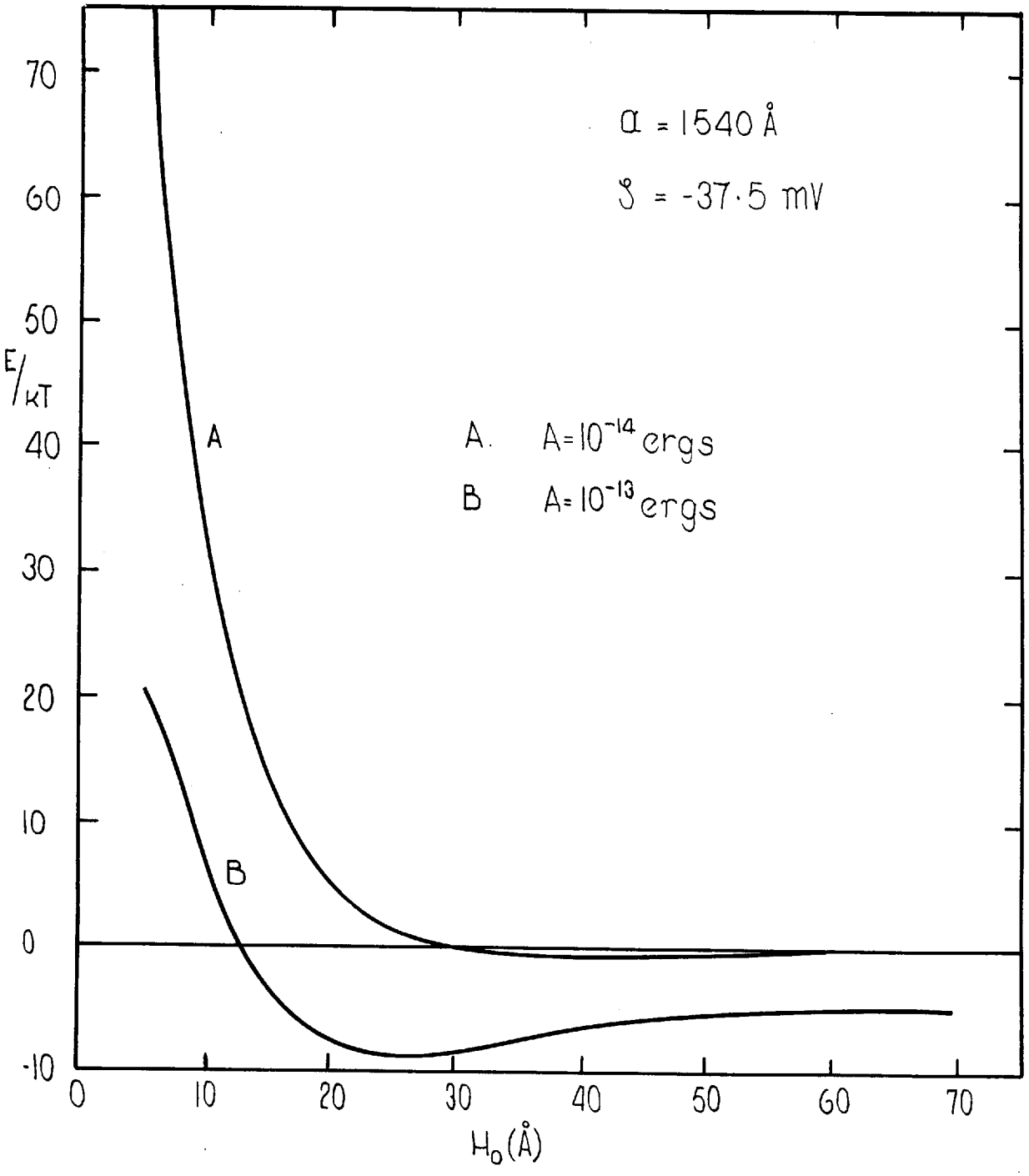

FIG(9.4) TOTAL POTENTIAL ENERGY CURVES FOR THE INTERACTION BETWEEN A SPHERE AND A PLATE IN 0·3 M NaCl AND 10^{-4} M S.D.S.

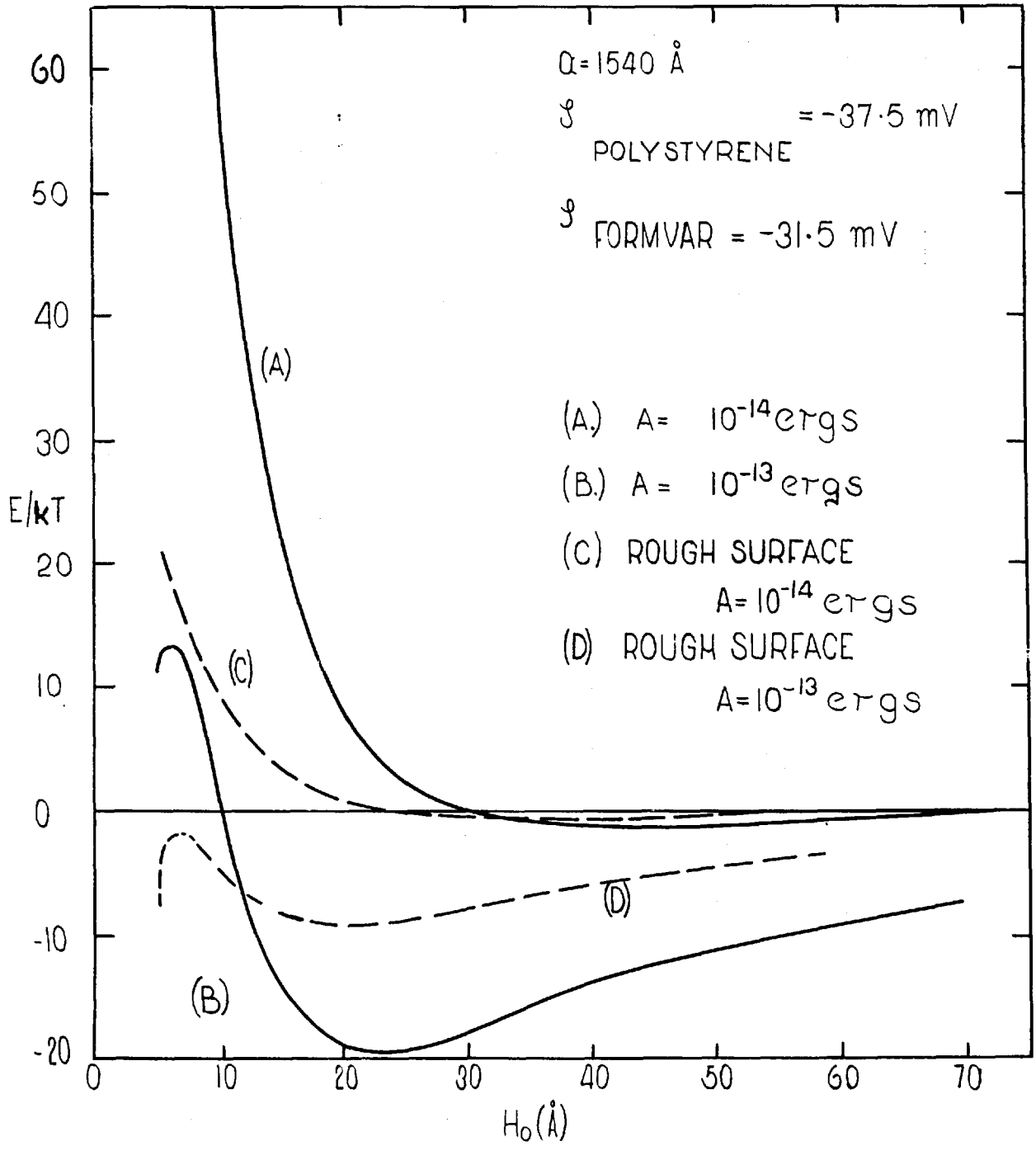

FIG(9·5) TOTAL POTENTIAL ENERGY CURVES FOR THE INTERACTION BETWEEN A SPHERE AND A PLATE IN 0·1 M NaCl AND 10^{-4} M S.D.S.

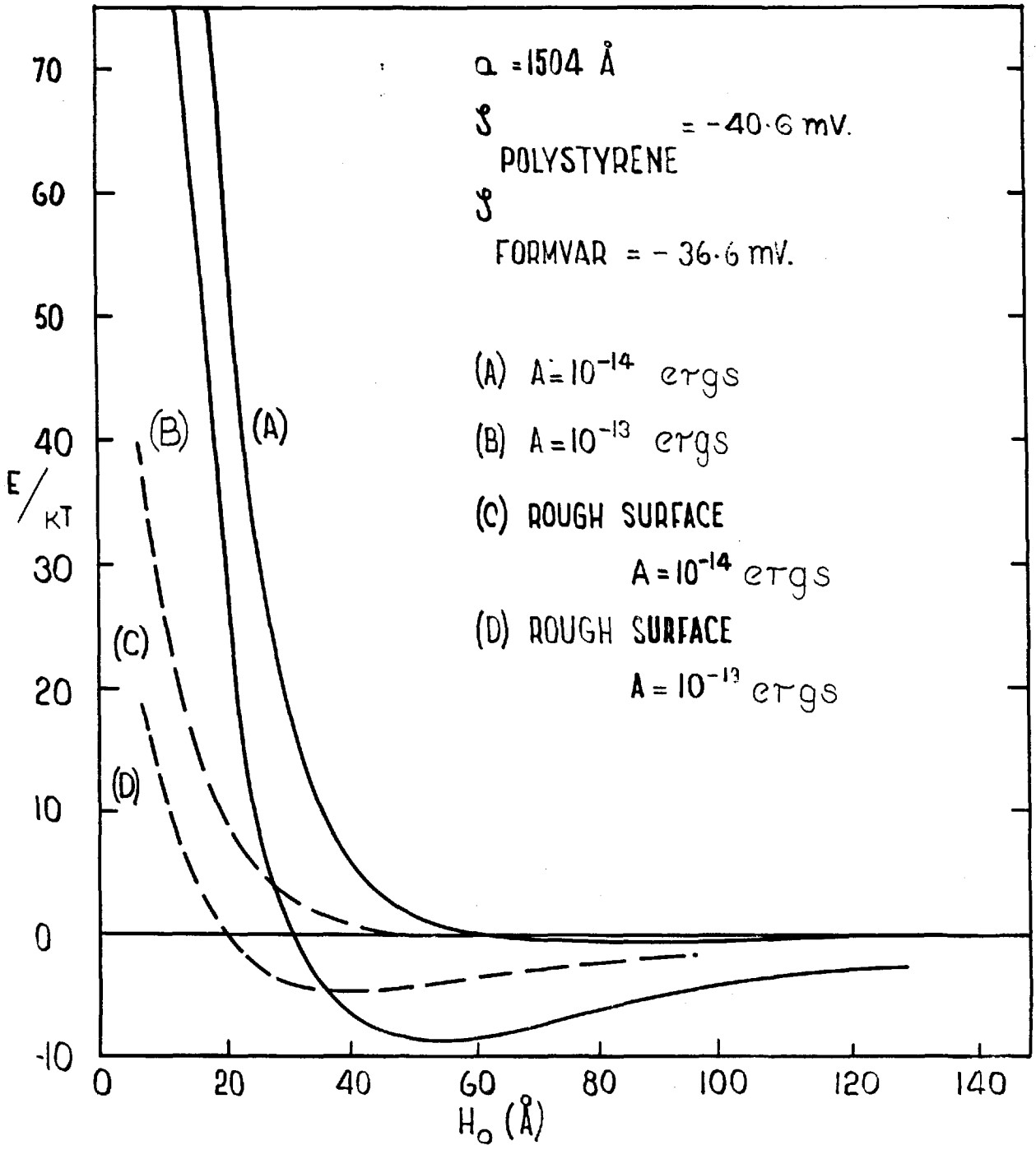

FIG.(9·6) TOTAL POTENTIAL ENERGY CURVES FOR THE INTERACTION BETWEEN A SPHERE AND A PLATE IN 0·05M NaCl AND 10^{-4}M S.D.S.

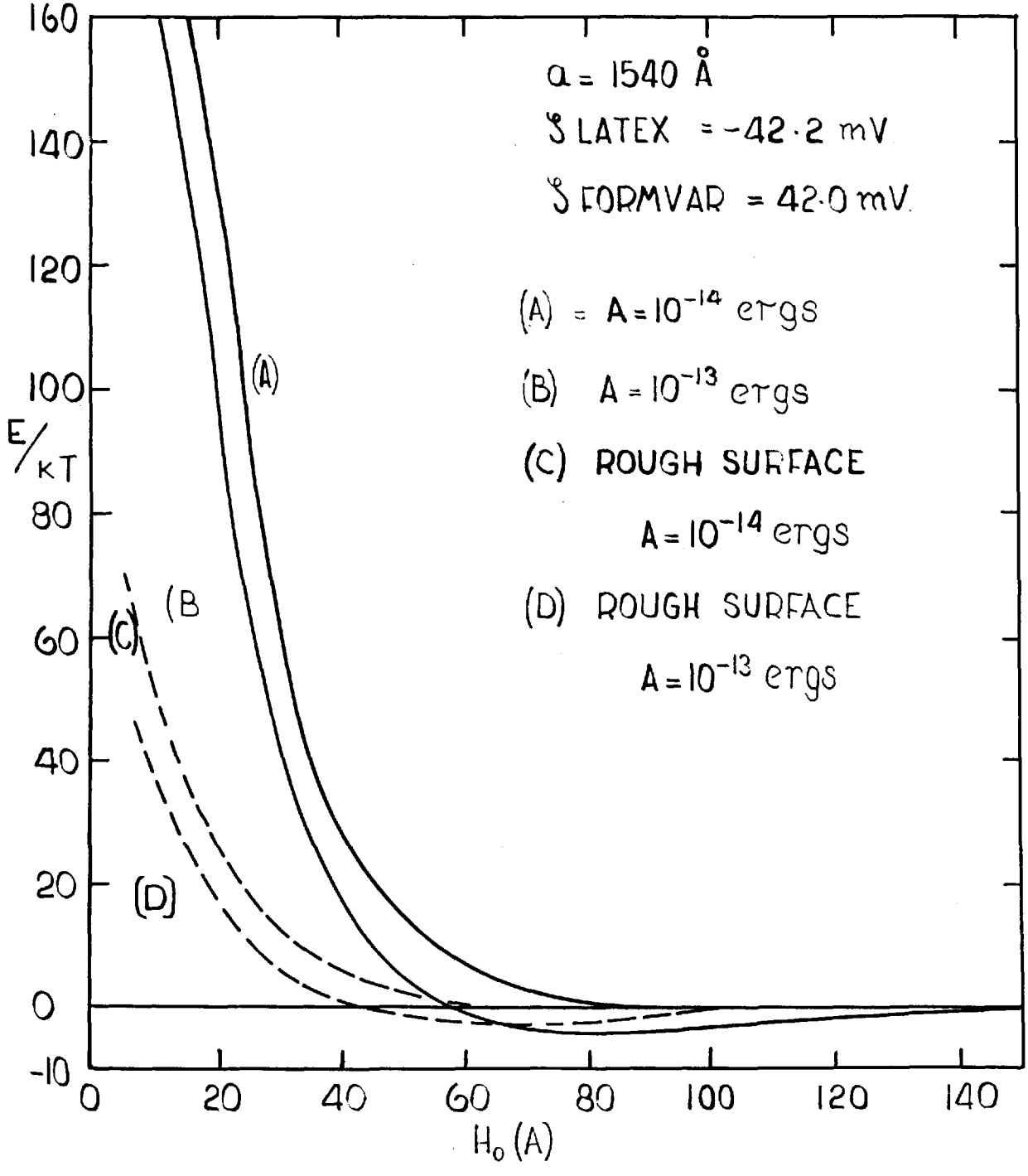

$$j = \frac{D\left[C \exp (V/kT) \right]_B^A}{\int_A^B \exp (V/kT) dH} \qquad (7)$$

where C is the local concentration of particles.

In the present problem, the total diffusion path can be divided into three parts, Fig.(9.7), namely, (1) the section where the diffusion is controlled solely by Fick's law (i.e. where there is no significant potential field), (2) the section subject to the potential energy barrier (from plane Y to plane B), and, (3) the section from the potential energy maximum (V_m) to the wall. Every particle arriving at plane B will rapidly be deposited, so that the stationary concentration of particles at plane B can be taken as zero.

Section (1) (δ_1 in thickness) comprises practically all of the Nernst diffusion Layer (thickness δ), which in the rotating disc experiments was of the order of 10^{-4} cm. Calculated potential energy curves (Figs. 9.4-6) show that Section (2) is generally less than 100 Å (δ_2) and Section (3) is of the order of 5 Å (δ_3). Since $\delta_1 >> (\delta_2 + \delta_3)$, $\delta_1 \approx \delta$. Equation (7) can now be simplified by noting that at the outermost plane (A) $C = C_o$ (the concentration of particles in the bulk solution), while at plane B, $C = 0$ and $V = V_m$.

FIG. (9·7) SCHEMATIC REPRESENTATION OF THE DIFFUSION PATH OF PARTICLES APPROACHING A PLANAR SURFACE IN THE PRESENCE OF AN ENERGY BARRIER.

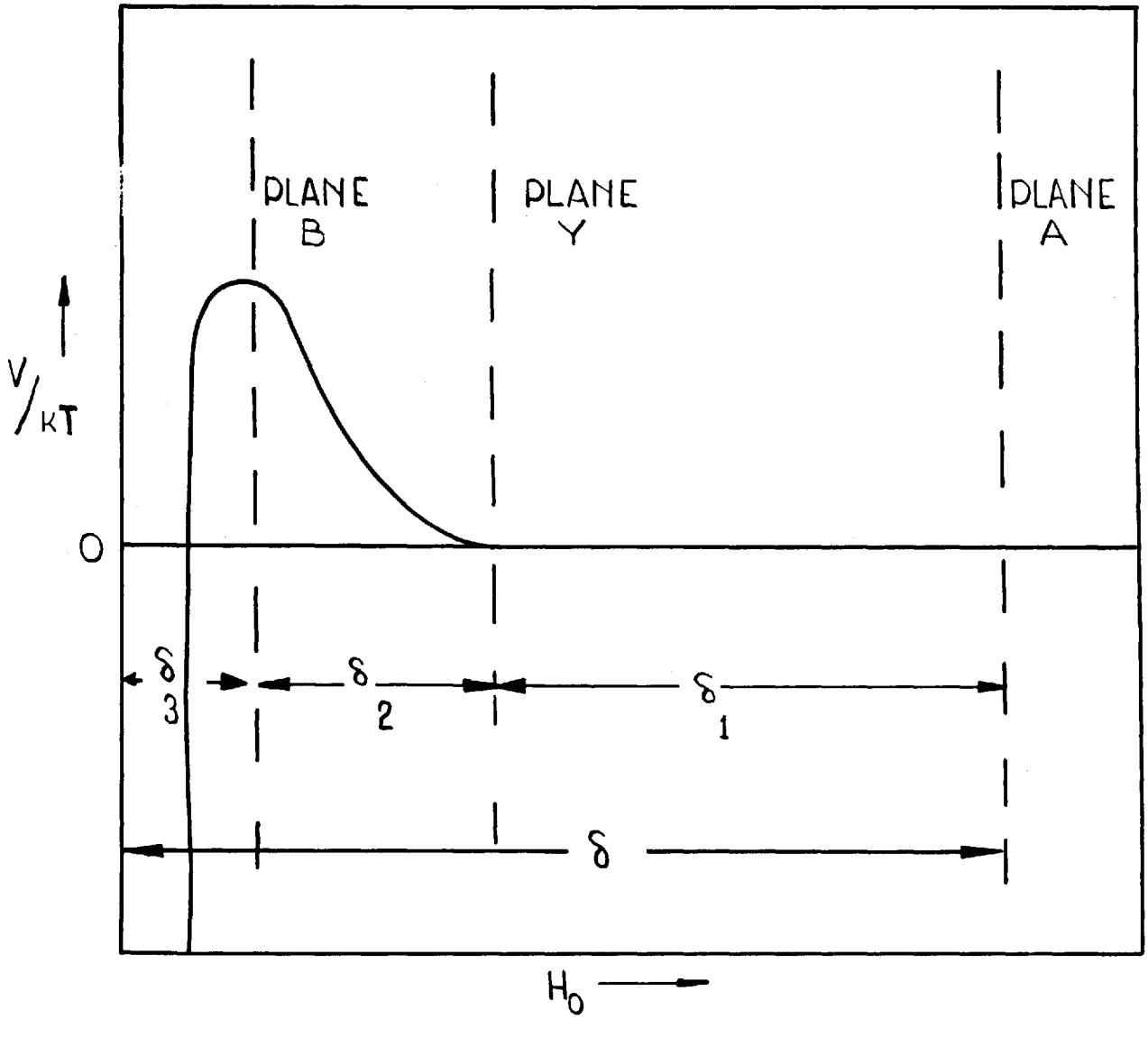

Hence

$$j = \frac{DC_o}{\int_A^B \exp(V/kT)dH} \qquad (8)$$

The maximum flux possible (in the absence of a repulsive potential barrier) is given by

$$j_m = \frac{DC_o}{\delta} \qquad (9)$$

Hence, the stability ratio is given by

$$W = \frac{1}{\delta}\int_A^B \exp(V/kT)dH \qquad (10).$$

This equation is the linear analogue of the well-known Fuchs expression for the stability of sols (radial diffusion)[5].

If potential energy curves are assumed, W can be evaluated by graphical integration of equation (10). Alternatively a useful approximation can be obtained by treating the potential energy curve as effectively flat over section (1) together with a rise in potential over section (2).

Dividing the integral into these two parts,

$$W = \frac{1}{\delta}\int_{A}^{Y} \exp\,(V/kT)dH + \frac{1}{\delta}\int_{Y}^{B} \exp\,(V/kT)dH \qquad (11)$$

the first term approximates closely to unity (as V = 0, and $\delta_1 \gtrsim \delta$); hence

$$W = 1 + \frac{1}{\delta}\int_{Y}^{B} \exp\,(V/kT)dH \qquad (12).$$

In general, the second term should be evaluated over the effective range of the potential energy curve; but for the case of a high barrier and negligible secondary minimum (e.g. Fig.(9.6 lines A and C) an approximate value can be obtained by treating the barrier as a linear rise from V = 0 to V = V_m over a distance δ_2, giving the approximate working equation

$$W \quad 1 + \frac{\delta_2}{\delta}\left[\frac{\exp\,(V_m/kT)}{(V_m/kT)}\right] \qquad (13)$$

where $V_m > 0$. As δ_2/δ varies from 2×10^{-3} to 8×10^{-3} in practice (Figs. 9.4-6), W remains fairly small for V_m/kT values of less than 10, (see Table 3).

9.3. Comparison of Theory and Experiment

When W values were calculated from the theoretical potential energy curves, (Fig.9.4-6), it was found that the theoretical values were orders of magnitude higher than the experimental values (Fig.8.12)

TABLE 3

The Influence of the Potential Energy Barrier on the Stability Ratio for Deposition

V_m/kT	$W(\delta_2/\delta = 2 \times 10^{-3}$ (Fig.9.4)
0.1	1.0
5.0	1.1
10.0	3.2
12.0	2.8×10
15.0	4.1×10^2
17.0	2.8×10^3
20.0	4.8×10^4

for the range of Hamaker constants used.

The particles counted were definitely not retained in a 'secondary minimum', as they could not be removed when the sol was replaced by a solution of much lower ionic strength and the disc rotated for two days. Furthermore, the deposition rate was less than j_{max}; in other words, the particles had surmounted a potential energy barrier, not fallen into a potential well.

It was, therefore, necessary to consider alternative explanations to account for the deposition observed.

Theoretically, the sol should coagulate before deposition occurs, for in sphere-plate interactions both the repulsion and a attraction energies are twice those for the sphere-sphere interactions, and hence the potential energy barrier to deposition should be about twice that for coagulation of the sol. In practice, it was found that deposition was approaching the maximum rate whilst the sol remained stable. Consequently, it appears that the potential energy barrier for the sphere-plate interaction was actually less than that for the sphere-sphere interaction. There are two possible ways in which this could arise.

(1) The Hamaker constant of the "Formvar"/water system ($A_{FF/W}$) might be so much greater than that for the polystyrene/water system ($A_{PP/W}$), that the total Hamaker constant for the interaction of polystyrene with "Formvar" in water ($A_{PF/W}$) could be greater than

that for polystyrene with polystyrene in water. However, to account for the experimental deposition in the light of coagulation data in this way would necessitate that $A_{PF/W}$ was very much greater than twice $A_{PP/W}$. Even if $A_{PF/W}$ was only three times that of $A_{PP/W}$ it would need $A_{FF/W}$ to be nine times that of $A_{PP/W}$ (from equation (7)). From the values of Hamaker constants reported for organic materials in water (Tables 1 and 2) it is unlikely that these two polymers could have such widely different Hamaker constants. Therefore, the discrepancy between deposition data and coagulation data lies in a different explanation.

(2) It is known from the electron micrographs of the "Formvar" surface (Fig. 8.4b) that the surface was not perfectly plane, but consisted of small mounds of roughly spherical shape, about 50 Å high and 300 Å in radius. Consequently, the interaction energy of polystyrene spheres with a "Formvar" surface should not have been calculated on a sphere-plate model, but a large sphere interacting with a small sphere. In that case the repulsion term for deposition would be less than that for coagulation (instead of twice). However, the interaction of a sphere with a rough plane surface is not simple to calculate, for in some cases the underlying plane surface beneath the spherical projections makes a contribution to the total potential energy of interaction. In appendix (7.0) an approximate expression for the interaction energy of a spherical particle and a spherical projection on a plane surface has been derived. It is seen in

Appendix (5 and 6) and in Figs.(9.4-6) that the rough surface has the effect of reducing the total interaction energy to less than one quarter of that for a smooth surface. It, therefore, seems that surface roughness could qualitatively explain why deposition occurs while the sol is completely stable. (Similarly, Nordin[15] has indicated from theoretical calculations that the interaction of two corrugated flat plates would be less than that between two smooth plates).

The potential energy curves for the deposition on to a rough surface (Figs. 9.4-6), shown as broken lines, yield a theoretical value of W much lower than for the smooth surface; but in most cases, it is still very much larger than the experimental value.

Furthermore, although experiment and theory could be fitted for the highest salt concentration by choosing a value of the Hamaker constant of 8×10^{-14} ergs, this value was inadequate for the results of the other electrolyte concentrations. Therefore, the surface roughness effects, important though they are, are not alone sufficient to explain all the measured depositions.

Other refinements to the D.L.V.O. theory might also be considered. Firstly, the use of equation (12) in place of the approximation (equation 13) would somewhat reduce W, but graphical integration of equation (12) showed that for all the theoretical curves at the experimental electrolyte concentrations, the reduction

is less than a factor of two. Secondly, the assumption of "constant charge" instead of "constant potential" would, if anything, slightly increase the repulsion at close distances of approach ($\chi_H < 0.5$)[16]. Thirdly, it is well-known that the dielectric constant in the inner part of the diffuse electrical double-layer is likely to be less than 80 and this would also tend to reduce the repulsion. Sparnaay[17] has examined this problem together with the effect of the ionic sizes and concludes that the corrections are negligibly small for concentrations of the order of 10^{-3} M, but rise to a contribution of from 10-20% at 10^{-2}M. His treatment is incapable of analysing concentrations as high as those used in this investigation, though the magnitude of the effect is probably greater than 20%. Fourthly, strictly, the "discreteness-of-charge" effect ought to be taken into account for the present system as the average separation between charges has been estimated to be about 40 Å - i.e. comparable with the critical distance between the particles and the plate. This also would be expected to result in a small decrease in repulsion energy[18]. However, it is unlikely that these refinements of the double-layer theory could explain effects orders of magnitude different from those calculated on classical double-layer theory. Furthermore, it would not be justifiable to attempt to fit theory and experiment because the results in Fig. (8.12) take no account of vitally important evidence revealed by the curves in Figs. (8.8 and 8.9), which suggest that the true explanation of why the deposition was always greater than the theoretical is probably of quite a different

nature.

In contrast to the deposition of negative particles on to a positive surface (Chapter 6), the deposition of negative particles on to a negative surface was, firstly, not linear with time, and secondly, not proportional to sol concentration. The results will, therefore, be referred to as "anomalous deposition". Its origin has not been fully investigated, but some tentative deductions can be made from the results of Chapter 8.

The non-linearity of deposition with respect to time was not noticeable at low ionic concentrations (Fig.8.10), but became detectable above N_d = 40 with 0.1 M NaCl, (Fig.8.9), and was very marked from N_d = 10 upwards with 0.3 M NaCl (Fig. 8.8). As these depositions represent only a very small fractional coverage of the surface (N_d = 100 is equivalent to a fractional coverage of $\approx 10^{-3}$), they cannot be ascribed to incipient saturation in the Langmuir sense, unless it is postulated at the same time that the number of sites effectively available for deposition is very small compared with the geometrical capacity of the plane surface. (Even if the particles can be considered to deposit only on to the spherical projections on the surface, the available sites for deposition would still effectively be equivalent to the geometrical area of the plane surface, because the deposition sites would then be about 400 Å apart whilst the diameter of the particles is 3000Å). Furthermore, the available number of sites must be supposed to decrease as the

concentration of electrolyte increases (since curvature sets in at lower values of N_d).

Combined with the anomaly of deposition contrary to the potential energy curves for the surface as a whole, it is suggested that some heterogeneity of electrostatic potential must exist. "Anomalous deposition" could occur on to areas with less negative potential than the average value. The effect of added electrolyte would be to reduce the effective spread of such areas and possibly also reduce their inequality of potential by further adsorption of anionic surface-active agent (through the common ion effect).

In support of this heterogeneity hypothesis is the observation of gross microscopic unevenness of deposition on to plain "Formvar" films (Fig. 8.1). Although the use of sodium dodecyl sulphate served to eliminate obvious heterogeneity, there was no means of ensuring that it produced uniformity of potential on a submicroscopic scale. Weakly charged areas would not need to be large to provide a "hole" in the general potential energy barrier. For example, Figs. (9.4-6), shows that the range of action of surface forces is less than 100 Å, whereas the radius of the latex particles was 1540 Å. It can easily be shown, therefore, that even with contact between sphere and plate the effective area exerting a force on the sphere would be confined to a spot about 200 Å radius for a smooth plate and about 100 Å for a rough plate as designated in Appendix (7.0).

An alternative explanation of the above evidence might be sought in an incipient coagulation of the sol, increasing with time and with salt concentration. Since the mass transfer is proportional to the radius of the particles to the power $-2/3$ and the number of particles in the sol, then if all the particles were coagulated into doublets the deposition rate would be reduced by a factor of three assuming the barrier to deposition of doublets was the same as that for single particles. However, as the potential energy barrier to the deposition of double-particles with its axis parallel to the plate would be double that for the sphere-plate, it might be expected that a marked reduction in deposition rate with time would result if coagulation of the sol was occurring. Against this hypothesis, however, is the fact that the optical turbidity of the sols did not change detectably over a long period unless much higher salt and sol concentrations were used than those employed in the deposition measurements (see Fig.8.13). In addition, a direct test was carried out for the system with the medium of highest electrolyte concentration (0.3 M); particle counts made on samples of the sol before and after one hour in the rotating disc apparatus showed a reduction of count of less than 10%, which is totally inadequate to explain a fall in deposition rate by a factor of three within 30 minutes (Fig.8.8). (Incidentally, similar tests with and without rotation of the disc showed no difference, eliminating the possibility of orthokinetic coagulation.) The dependence of "anomalous deposition" on sol concentration also tells against this

theory (see below). Heterogeneity, therefore, remains the most plausible explanation of the non-linearity of deposition with time.

The effect of varying the sol concentration was particularly surprising. Whereas for the deposition of negatively charged particles on to a positively charged plate deposition rates were accurately proportional to sol concentrations (Fig.6.4), for negative particles on to a negative surface, the kinetic order appeared to be about 2, both with 0.1 M NaCl (Fig.8.9) and 0.3 M NaCl (Fig.8.8). This suggests that deposition occurred via coupled pairs of particles, which would pre-suppose that a small proportion of the polystyrene particles are held together in a "secondary minimum". These double-particles would then be held near the plate surface in a much deeper "secondary minimum" because the energy of interaction between double-particles and the plate (axis parallel to the plate) would be four times that for the sphere-sphere interactions. From the available potential energy curves, it would not be expected that the doublet-plate "secondary minimum" would be greater than 5kT and consequently, the "secondary minimum" for the sphere-sphere interaction would be about a kT deep.

A tentative theory to account for all the facts could be based on the establishment of a small population of doublets in the "secondary minima" with respect to one another and to the plate. Such double-particles would traverse the rotating disc in spiral lines at a distance of about 50 Å from the surface and on encountering "favourable"

sites would have a chance of passing over a locally low potential energy barrier into the primary minimum. A "favourable" site might be a projection which also carried a weak electrostatic potential. The evidence available from the present work is not sufficient to justify more detailed speculation as to the origin of "anomalous deposition".

9.4. References

(1) Hamaker, H.C. Physica 4, 1058, (1937).

(2) Clayfield, E.J., Lumb, E.C. and Miller, W.L. Proc. 5th Intern. Congress on Surface Active Agents. (Barcelona), (1968), in the press.

(3) Hogg, R., Healy, T.W. and Fuerstenau, D.W., Trans.Faraday Soc. 62, 1638, (1966).

(4a) Kramers, H.A. Physica, 7, 284, (1940).

(4b) Chandrasekhar, S. Rev. Mod. Phys. 15, 41, (1943).

(5) Derjaguin, B.V. Trans. Faraday Soc. 36, 203, (1940).

(6) Ottewill, R.H. and Shaw, J.N. Disc. Faraday Soc. 42, 154, (1966).

(7) Watillon, A. and Joseph-Petit, A.-M., Disc. Faraday Soc. 42, 143, (1966).

(8) Fowkes, F.M. Ind. Eng. Chem. 56, 40, (1964).

(9) Force, C.G. and Matijevic, E. Koll. Z. 224, 51, (1968).

(10) Neiman, R.E., Lyashenko, O.A. and Kirdeeva, A.P. Coll. J. URSS. 28, 92, (1966).

(11) Srivastava, S.N. and Haydon, D.A. Trans.Faraday Soc. 60, 971, (1964).

(12) Ottewill, R.H. and Wilkins, D.J. Trans.Faraday Soc. 58, 608, (1962).

(13) Overbeek, J. Th. G., in "Colloid Science" Vol.1. ed. Kruyt, H.R. Elsevier, Amsterdam, p.268, (1952).

(14) Schenkel, J.H. and Kitchener, J.A. Trans. Faraday Soc. 56, 161, (1960).

(15a) Nordin, J.S., Ph.D. thesis, Univ. of Minnesota (1965).

(15b) Nordin, J.S., Tsuchiya, H.M. and Fredrikson, A.G. Biotechnology and Bioengineering, 9, 545, (1967).

(16) Frens, G., thesis, University of Utrecht, the Netherlands, (1968).

(17) Sparnaay, M.J. Rec. Trav. Chim. 77, 872, (1958).

(18a) Levine, S., Bell, G.M. and Calvert, D. Can. J. Chem. 40, 518, (1962).

(18b) Levine, S. and Bell, G.M. J. Phys. Chem. 67, 1408, (1963).

(18c) Levine, S., Mingins, J. and Bell, G.M. J. Phys. Chem. 67, 2095, (1963).

(18d) Levine, S. and Bell, G.M. Disc. Faraday Soc. 42, 69, (1966).

10.0 GENERAL CONCLUSIONS

It has been shown that for the case of maximum deposition rate (negative particles depositing on to a positive plate) the mass transfer of particles to the surface of the rotating disc is accurately described by the Levich diffusion equation[1]. As the agreement depends on the correctness of the diffusion coefficient of 0.3μ diameter particles which was calculated from the Stokes-Einstein equation, the results also constitute a confirmation of the validity of this equation.

In the case of negatively charged particles depositing on to a negatively charged plane surface, it was found that non-uniform deposition occurred. A surface-active agent was required to reduce the magnitude of this non-uniformity of deposition to undetectable limits. Nevertheless, when an apparently uniform deposit was obtained by this method, it was found that the deposition was orders of magnitude higher than that predicted on the basis of the Derjaguin-Landau-Verwey-Overbeek theory of colloid stability, although the regions of non-deposition were explicable by the theory. A correction to the total potential energy of interaction for a rough surface resulted in lower energy barriers than predicted for smooth surfaces, but still not sufficiently low to explain the observed deposition. It has also been emphasized that the deposition measured was not into the 'secondary minimum', as shown by the slow

rate and the impossibility of removing the deposits by long rotation of the disc in a dispersion medium of lower ionic strength. In view of the fact that with no surface-active agent the deposition was visibly non-uniform on a microscopic scale, it was postulated that the non-uniformity was due to the variations in surface potential. With the surface-active agent present, the deposition, which appeared uniform on a microscopic scale, could not be proved to be uniform on a sub-microscopic scale. Therefore, the deposition results were interpreted on the basis of both surface roughness and local variations in surface potential. This conclusion was dictated also by the anomalous kinetics.

It is, therefore, evident that this seemingly almost ideal model system for studying forces of interacting surfaces fell short of ideality on the grounds of surface roughness and heterogeneity of surface potential. It has been shown theoretically that a small degree of surface roughness reduces the total potential energy barrier for the deposition of a sphere on to the plate markedly. It is probable that practically <u>all</u> solid surfaces (except possibly cleavage surfaces of high quality mica etc., over small areas) will have some degree of surface roughness and consequently, the deposition rate will <u>always</u> be <u>faster</u> than that predicted on the basis of the D.L.V.O. theory of colloid stability for perfectly smooth bodies. Therefore, for a better test of this theory a surface smooth to molecular dimensions is required. Such a surface could be obtained by using a liquid surface (e.g. mercury).

It is expected that a 'clean' mercury surface would be smooth to the degree required (i.e. projections of less than $^{1}/\chi$), and would exhibit no variations in surface potential.

Conversely, it appears from this work that deposition studies could be a way of studying heterogeneities on the sub-microscopic scale. In 1942 Thiessen[2] showed the existence of a variation in surface potential between the edges and faces of kaolin platelets using a deposition technique. It is now envisaged that even smaller variations than those found by Thiessen could be examined by carefully controlled deposition experiments. Therefore, this work has indicated a new technique that could be used for studying small heterogeneities of surface properties of materials such as glass, plastics, metals and polished minerals.

10.1. References

(1) Levich, V.G. "Physico-chemical Hydrodynamics", Prentice-Hall, (N.Y.) pp. 60-72, (1962).

(2) Thiessen, P.A. Z. Electrochem. 48, 675, (1942).

APPENDIX 1

The Experimental Results for the Deposition of Polystyrene Latex Particles on a Poly-2-vinyl Pyridine/Styrene Copolymer Surface

A.1.1. Deposition at Constant time (t = 30 min)

	360 r.p.m.		240 r.p.m.		120 r.p.m.	
Sol.Conc. Particles/ml x 10^7	N_d	$j/\omega^{1/2}C_o(\times10^6)$	N_d	$j/\omega^{1/2}C_o(\times10^6)$	N_d	$j/\omega^{1/2}C_o(\times10^6)$
6.6	-	-	-	-	320	7.60
5.5	454	7.53	378	7.68	265	7.71
4.4	376	7.71	289	7.28	206	7.51
3.3	286	7.75	238	7.97	146	6.89
2.2	191	8.13	146	7.32	102	7.29
1.1	92	7.60	72	7.13	51	7.27

A.1.2. Deposition at Constant Sol Concentration

	360 r.p.m. (C_o = 4.4x10^7 p/ml)		240 r.p.m. (C_o = 4.2x10^7 p/ml)		120 r.p.m. (C_o = 5.5x10^7p/ml)	
Time(min)	N_d	$j/\omega^{1/2}C_o(\times10^6)$	N_d	$j/\omega^{1/2}C_o(\times10^6)$	N_d	$j/\omega^{1/2}C_o(\times10^6)$
30	376	7.71	285	7.54	265	7.71
25	310	7.66	245	7.04	222	7.58
20	258	7.93	195	7.55	184	7.83
15	193	7.92	151	8.00	131	7.48
10	123	7.65	97	7.78	92	7.74

A.1.3. Deposition at Different Depths of Immersion of Disc Surface

Depth of Disc surface from Bottom of Dish (cm)	240 r.p.m. (C_o = 1.1x10^7 p/ml, t = 30 min.) N_d	$j/\omega^{1/2}C_o$ (x 10^6)
0.4	72.9	7.22
1.4	71.4	7.09
2.5	72.0	7.13
3.5	72.4	7.17
4.0	72.0	7.13
4.5 ≡ to top of solution		

Theoretical Deposition rate constant ($0.62\ D^{2/3}\nu^{-1/6}$) = 7.66 x 10^{-6}.

The mean Experimental rate constant ($j/\omega^{1/2}C_o$) = 7.59 ± 0.3 x 10^{-6}.

APPENDIX 2

A.2.1. The Electrophoretic Mobility of Polystyrene Latex Particles as a Function of NaCl Concentration with 10^{-6}M Sodium Hexadecyl Sulphate

Ionic Strength	U(μ/Volt/sec)	ζ (mV) Helmholtz Eq.
10^{-6}	- 2.14	- 30.0
10^{-5}	- 3.47	- 48.5
5×10^{-5}	- 3.74	- 52.0
10^{-4}	- 4.13	- 57.8
2×10^{-4}	- 4.53	- 63.4
4×10^{-4}	- 4.36	- 61.0
10^{-3}	- 4.40	- 61.6
5×10^{-3}	- 4.04	- 56.6
10^{-2}	- 3.20	- 44.8
5×10^{-2}	- 1.57	- 22.2
10^{-1}	- 0.86	- 12.0

A.2.2. The Electrophoretic Mobility of Polystyrene Latex Particles as a Function of NaCl Concentration

A.2.2.1. In 4 x 10^{-4}M Sodium Dodecyl Sulphate

NaCl conc.(M)	U(μ/volt/sec)	ζ(mV) Helmholtz Eq.
10^{-2}	- 5.15	- 72.0
2 x 10^{-2}	- 5.20	- 72.9
3 x 10^{-2}	- 5.17	- 72.4
4 x 10^{-2}	- 4.06	- 56.9
5 x 10^{-2}	- 3.36	- 47.0

A.2.2.2. In 2 x 10^{-4}M Sodium Dodecyl Sulphate

NaCl conc.(M)	U(μ/Volt/sec)	ζ (mV) Helmholtz Eq.
3 x 10^{-2}	- 5.23	- 73.2
4 x 10^{-2}	- 4.31	- 60.4
5 x 10^{-2}	- 2.85	- 39.9
10^{-1}	- 2.72	- 38.0

A.2.2.3. In 10^{-4}M Sodium Dodecyl Sulphate

NaCl conc.(M)	U/μ/volt/sec)	ζ (mV) Helmholtz Eq.
3 x 10^{-2}	- 5.16	- 72.2
4 x 10^{-2}	- 4.30	- 60.3
5 x 10^{-2}	- 2.92	- 40.9
10^{-1}	- 2.77	- 38.7

A.2.3. The Electro-osmotic Mobility of Water at a Formvar surface as a Function of NaCl Concentration

A.2.3.1. In 4 x 10^{-4}M Sodium Dodecyl Sulphate

NaCl conc.(M)	U(μ/volt/sec)	ζ(mV) of Formvar
10^{-2}	5.84	- 81.6
2 x 10^{-2}	4.79	- 67.2
3 x 10^{-2}	3.69	- 51.6
4 x 10^{-2}	3.16	- 44.2
5 x 10^{-2}	3.02	- 42.3

A.2.3.2. In 2 x 10^{-4}M Sodium Dodecyl Sulphate

NaCl Conc.(M)	U(μ/volt/sec)	ζ(mV) of Formvar
3 x 10^{-2}	3.64	- 50.9
4 x 10^{-2}	3.36	- 47.1
5 x 10^{-2}	3.09	- 43.3
10^{-1}	2.65	- 37.0

A.2.3.3. In 10^{-4}M Sodium Dodecyl Sulphate

NaCl conc.(M)	U(μ/volt/sec)	ζ(mV) of Formvar
3 x 10^{-2}	3.67	- 51.3
4 x 10^{-2}	3.37	- 47.2
5 x 10^{-2}	3.01	- 42.2
10^{-1}	2.62	- 36.6

APPENDIX 3.0

THE DEPOSITION OF POLYSTYRENE LATEX SPHERES ON TO 'FORMVAR'

A.3.1. 0.3M NaCl and 10^{-4}M S.D.S.

	N_d			
t (min)	1.28×10^8 p/ml	9.6×10^7 p/ml	7.65×10^7 p/ml	6.4×10^7 p/ml
10	38.2	17.7	10.6	6.0
20	53.2	32.4	22.4	10.5
30	67.5	44.4	30.4	14.2
40	71.9	49.2	34.1	17.5
50	79.1	60.2	36.8	19.2
60	81.6	63.0	40.6	21.1
70	84.0	66.5	42.2	22.8
80			44.6	22.6
90				22.6

A.3.2. 0.1M NaCl and 10^{-4}M S.D.S.

	N_d	
t (min)	1.28×10^8 p/ml	6.4×10^7 p/ml
10	38.2	7.1
20	58.4	15.8
30	90.5	22.6
40	106.9	31.6
50	120.9	38.7
60		42.4
70		45.8
80		52.5

A.3.3. 5×10^{-2}M NaCl and 10^{-4}M S.D.S.

1.28×10^{8} particles/ml

	N_d			
t (min)	Run (1)	Run (2)	Run (3)	1 h conditioning of surface before addition of sol.
5		2.2		
10	2.9		4.4	14.4
15		3.9		
20	4.2		11.3	25.7
25		12.5		
30	17.1		17.1	38.6
35		18.9		
40	28.1		29.4	51.6
45		33.2		
50	37.5		39.8	67.0
55		45.6		
60	51.0		47.1	78.0
70	67.6			
73			60.4	
80	72.5			

A.3.4. 1.28×10^{8} particles/ml

	N_d	
	2×10^{-4}M S.D.S.	4×10^{-4}M S.D.S.
t	4×10^{-2}M NaCl	3×10^{-2}M NaCl
10	3.7	1.2
20	8.3	3.3
30	11.8	5.6
40	15.3	6.6
50	20.8	7.6
60	24.3	
70	28.9	
80	32.7	

A.3.5. Stability Ratios for Deposition for Co = 1.28×10^8 particles/ml

[NaCl] (M)	Initial rate of Deposition/min	W
0.3	5.0	8
0.1	3.6	11
0.05	1.3	30
0.04	0.4	99
0.03	0.016	247
0.01	NO DEPOSIT	∞

APPENDIX 4.0

Total Potential Energy for the Interaction of Latex Spheres of radius 1540 Å

A.4.1. 0.3 M NaCl [$\kappa = 1.8 \times 10^7$] and 10^{-4} M S.D.S. $\zeta = -37.5$mV

	V/kT		
H_o(Å)	A = 10^{-13} ergs	A = 5×10^{-14}ergs	A = 10^{-14} ergs
5.01	20.52	51.17	75.69
5.56	18.44	46.74	69.42
6.67	16.66	39.86	59.02
7.79	13.78	33.33	49.01
8.90	10.10	27.10	40.70
10.01	6.75	21.75	33.61
11.12	3.66	17.01	27.69
12.24	1.17	13.17	22.81
13.35	- 1.02	9.93	18.69
14.46	- 2.94	7.06	15.10
15.57	- 4.46	4.84	12.32
16.69	- 5.56	3.04	9.96
19.47	- 7.59	- 0.26	5.62
22.25	- 8.48	- 2.09	2.99
25.03	- 8.69	- 3.03	1.49
27.81	- 8.40	- 3.36	0.64
33.37	- 7.53	- 3.40	-0.12
38.93	- 6.27	- 2.90	-0.18
44.49	- 5.59	- 2.71	-0.39
50.06	- 4.97	- 2.43	-0.43
55.62	- 4.41	- 2.37	-0.41

A.4.2. 0.1 M NaCl and 10^{-4}M S.D.S.

ζ = -40.6 mV. $[\kappa = 1.04 \times 10^{7}]$

	V./kT		
H_o(Å)	A = 10^{-13} ergs	A = 5×10^{-14}ergs	A = 10^{-14} ergs
5.78	68.71	95.81	117.53
6.74	67.47	90.42	108.78
7.71	64.51	84.36	100.24
8.67	60.91	78.41	92.41
9.63	56.82	72.42	84.90
11.56	48.32	61.12	71.36
13.49	40.34	51.19	59.87
15.41	32.90	42.30	49.82
17.34	26.31	34.61	41.24
19.27	20.76	28.18	34.11
21.20	16.19	22.88	28.22
23.12	12.21	18.34	23.24
25.05	8.76	14.41	18.92
26.98	6.28	11.46	15.60
28.90	4.07	8.89	12.75
33.72	0.06	4.19	7.49
38.54	-1.35	1.82	4.36
43.35	-2.88	1.00	2.48
48.17	-3.34	-0.71	1.39
57.80	-3.43	-1.31	0.40
67.44	-2.96	-1.19	0.24
77.07	-2.79	-1.28	0.08
86.71	-2.54	-1.23	-0.18
96.34	-2.27	-1.12	-0.20

APPENDIX 5.0

Total Potential Energy for the Interaction of a Latex Sphere of Radius 1540 Å with a Plane Surface (Formvar)

A.5.1. 0.3 M NaCl and 10^{-4}M S. D. S.

$\zeta_{Latex} = -37.5$ mV, $\zeta_{Formvar} = -31.5$ mV

	V/kT		
H_o (Å)	A = 10^{-13} ergs	A = 5×10^{-14} ergs	A = 10^{-14} ergs
5.01	11.30	73.6	123.4
5.56	13.02	69.0	113.8
6.67	13.09	59.1	95.9
7.79	9.09	49.6	78.3
8.90	4.35	39.0	66.6
10.01	- 0.46	30.3	54.9
11.12	- 4.58	23.0	45.1
12.24	- 8.96	16.0	36.0
13.35	-11.07	11.9	30.2
14.46	-14.04	7.26	24.3
15.57	-16.45	4.12	19.8
16.69	-16.65	1.41	15.9
19.47	-18.94	-3.59	8.77
22.25	-19.52	-6.10	4.64
25.03	-19.30	-7.44	2.05
27.81	-18.52	-7.91	0.57
33.37	-16.39	-7.70	-0.75
38.93	-14.39	-7.02	-1.11
44.49	-12.55	-6.21	-1.13
50.06	-10.99	-5.47	-1.06
55.62	- 9.94	-4.96	-0.98

A.5.2. 0.1 M NaCl and 10^{-4}M S.D.S.

ζ_{Latex} = -40.6 mV, $\zeta_{Formvar}$ = 36.6 mV

	V/kT		
H_o(Å)	A = 10^{-13} ergs	A = 5×10^{-14} ergs	A = 10^{-14} ergs
5.78	112.5	166.2	209.2
6.74	111.9	157.5	193.9
7.71	106.0	146.5	178.5
8.67	100.3	135.8	164.3
9.63	93.7	125.7	151.2
11.56	79.3	105.9	127.1
13.49	65.7	88.4	106.6
15.41	53.0	72.8	88.6
17.34	42.1	59.5	73.4
19.27	32.6	48.2	60.6
21.20	22.8	37.4	48.7
23.12	17.9	31.0	41.3
25.05	12.2	24.1	33.6
26.98	7.91	18.9	27.6
28.90	4.27	14.4	22.5
33.72	- 2.31	6.29	13.2
38.54	- 5.68	1.77	7.73
43.35	- 7.50	- 0.97	4.25
48.17	- 8.30	- 1.46	2.21
57.80	- 8.25	- 3.50	0.30
67.44	- 7.34	- 3.44	- 0.32
77.07	- 6.12	- 2.98	- 0.46
86.71	- 4.89	- 2.40	- 0.43
96.34	- 3.88	- 1.93	- 0.37

A.5.3. 0.05M NaCl and 10^{-4}M S.D.S.

ζ_{Latex} = -42.2 mV. $\zeta_{Formvar}$ = -42.0 mV

	V/kT		
H_o(Å)	A = 10^{-13} ergs	A = 5×10^{-14} ergs	A = 10^{-14} ergs
5.45	196.9	253.9	299.5
6.82	197.6	242.6	278.6
8.18	190.1	227.8	257.9
9.55	180.4	212.6	238.3
10.91	168.5	196.7	219.3
12.27	156.8	181.7	201.7
13.64	145.1	165.6	185.5
16.36	122.6	141.1	155.9
19.09	102.5	118.2	130.8
21.82	84.2	97.9	108.8
24.54	68.4	80.5	90.2
27.27	55.1	65.9	74.6
30.00	42.6	53.0	60.2
32.72	35.1	43.9	51.0
35.45	27.0	35.2	41.7
38.18	20.8	28.4	34.4
40.91	15.7	22.6	28.2
47.72	6.13	12.0	16.8
54.54	0.92	6.00	10.1
61.36	- 2.22	2.25	5.81
68.18	- 3.62	0.22	3.30
81.81	- 4.10	- 1.30	0.94
95.45	- 3.45	- 1.45	0.15
109.08	- 2.82	- 1.21	- 0.08
122.72	- 2.03	- 0.98	- 0.14
136.35	- 1.66	- 0.82	- 0.14

A.5.4. 0.04M NaCl and 2 x 10^{-4}M S.D.S.

ζ_{Latex} = - 66.2 mV $\zeta_{Formvar}$ = 47.2 mV.

	V/kT		
H_o(Å)	A = 5x10^{-13}ergs	A = 10^{-13} ergs	A = 10^{-14} ergs
6.10	17.8	423.4	514.7
7.62	83.8	407.4	480.2
9.15	116.1	385.3	445.9
10.67	129.8	361.2	413.0
12.20	135.9	335.9	380.9
13.72	132.4	310.8	350.9
15.24	127.0	287.3	323.4
18.29	111.3	242.9	272.5
21.34	92.2	204.0	229.1
24.39	71.7	169.2	191.2
27.44	53.3	139.3	158.6
30.49	39.5	114.7	131.6
33.54	21.4	90.7	106.3
36.59	12.0	76.2	90.4
39.63	3.07	61.0	73.9
42.68	- 3.82	49.3	61.3
45.73	-10.2	39.2	50.4
53.35	-20.6	20.9	30.3
60.98	-25.6	10.4	18.5
68.60	-26.1	4.14	10.9
76.22	-24.9	0.70	6.47
91.46	-19.4	- 1.78	2.19
106.71	-14.0	- 1.99	0.69
121.95	-10.4	- 1.80	0.14
137.20	- 8.17	- 1.53	- 0.03
152.44	- 7.00	- 1.36	- 0.09

A.5.5. 0.03M NaCl and 4×10^{-4}M S.D.S.

$\zeta_{Latex} = -78.2$ mV, $\zeta_{Formvar} = -50.9$ mV.

	V/kT		
H_o(Å)	A = 5×10^{-13} ergs	A = 10^{-13} ergs	A = 10^{-14} ergs
5.28	106.7	579.5	685.9
7.04	218.0	566.8	645.3
8.80	260.9	540.9	603.9
10.56	276.4	509.6	562.1
12.32	278.6	477.0	521.6
14.09	267.1	442.3	481.7
15.85	256.9	410.1	444.6
17.61	242.7	381.4	410.2
21.13	207.9	320.8	346.6
24.65	173.4	269.8	291.5
28.17	140.8	224.6	243.5
31.69	112.4	185.8	202.4
35.21	86.4	152.2	167.0
38.73	63.1	122.4	135.7
42.25	49.9	103.6	115.7
45.77	34.3	83.7	94.8
49.30	22.7	68.2	78.5
52.82	13.2	55.2	64.6
61.62	- 4.24	31.0	38.9
70.42	-11.9	17.4	24.0
79.23	-15.1	8.89	14.3
88.03	-15.0	4.25	8.58
105.63	-12.2	0.24	3.03
123.24	- 9.27	- 0.87	1.02
140.85	- 7.50	- 1.14	0.29
158.45	- 6.78	- 1.22	0.03
176.06	- 6.34	- 1.22	- 0.07

APPENDIX 6.0

The Total Potential Energy for the Interaction between a Sphere and a Rough Plate

Roughness assumed to consist of spherical projections 44 Å high and 333 Å across (Fig.8.4b), from which the radius of the spherical segment is readily calculated to be 336 Å.

A.6.1. IN 0.3M NaCl and 10^{-4}M S.D.S.

$\zeta_{Latex} = -37.5$ mV, $\zeta_{Formvar} = -31.5$ mV.

A.6.1.1. Attraction Energy ($A = 10^{-13}$ ergs)

H_o(Å)	$-V_A/kT$ (Segment $H = H_o$)	$-V_A/kT$ (Sp-pl $H = H_o + 44$ Å)	$-V_A/kT$
5.01	20.4	11.4	31.8
5.56	13.6	11.3	24.9
6.67	9.50	10.9	20.4
7.79	7.40	10.7	18.1
8.90	6.08	10.5	16.6
10.01	5.30	10.3	15.6
11.12	4.87	10.1	14.9
12.24	4.45	9.87	14.3
13.35	4.10	9.58	13.7
14.46	3.78	9.38	13.2
15.57	3.43	9.19	12.6
16.69	3.12	9.06	12.2
19.47	2.55	8.50	11.1
22.25	2.11	8.00	10.1
25.03	1.79	7.54	9.33
27.81	1.47	7.08	8.55
33.37	0.99	6.24	7.23
38.93	0.70	5.45	6.15
44.49	0.51	4.77	5.28
50.06	0.41	4.18	4.59
55.62	0.34	3.59	3.93

A.6.1.2. Repulsion Energy

H_o(Å)	V_R/kT (Segment a = 336 Å)	V_R/kT (sp-pl H = H_o + 44 Å)	V_R/kT
5.01	24.33	0.06	24.39
5.56	22.39	0.05	22.44
6.67	18.82	0.04	18.86
7.79	15.80	0.035	15.84
8.90	13.17	0.03	13.20
10.01	10.93	0.02	10.95
11.12	9.07	0.02	9.09
12.24	7.33	0.01	7.34
13.35	6.24	0.01	6.25
14.46	5.12	0.005	5.13
15.57	4.24	0.004	4.24
16.69	3.49	0.001	3.49
19.47	2.12	-	2.12
22.25	1.31	-	1.31
25.03	0.79	-	0.79
27.81	0.48	-	0.48
33.37	0.18	-	0.18
38.93	0.065	-	0.065
44.49	0.024	-	0.024
50.06	0.009	-	0.009
55.62	0.003	-	0.003

A.6.1.3. Total Potential Energy

	V/kT		
H_o	$A = 10^{-13}$ ergs	$A = 5 \times 10^{-14}$ ergs	$A = 10^{-14}$ ergs
5.01	- 7.39	8.49	21.2
5.56	- 2.40	10.0	20.0
6.67	- 1.55	8.66	16.8
7.79	- 2.26	6.79	14.0
8.90	- 3.38	4.90	11.5
10.01	- 4.63	3.15	9.39
11.12	- 5.84	1.64	7.60
12.24	- 6.98	0.19	6.91
13.35	- 7.44	-0.61	4.87
14.46	- 8.03	-1.47	3.81
15.57	- 8.38	-2.06	2.98
16.69	- 8.69	-2.61	2.27
19.47	- 8.93	-3.43	1.01
22.25	- 8.80	-3.74	0.30
25.03	- 8.54	-3.86	-0.14
27.81	- 8.07	-3.82	-0.38
33.37	- 7.05	-3.42	-0.54
38.93	- 6.08	-3.01	-0.55
44.49	- 5.21	-2.62	-0.50
50.06	- 4.58	-2.29	-0.45
55.62	- 3.93	-1.96	-0.39

A.6.2. IN 0.1M NaCl and 10^{-4}M S.D.S.

$\zeta_{Latex} = -40.6$ mV, $\zeta_{Formvar} = -36.6$ mV.

A.6.2.1. Attraction Energy ($A = 10^{-13}$ ergs)

H_o(Å)	$-V_A/kT$ (Segment $H = H_o$)	$-V_A/kT$ (sp-pl $H = H_o + 44$ Å)	$-V_A/kT$
5.78	12.40	11.20	23.60
6.74	9.26	10.98	20.24
7.71	7.48	10.73	18.21
8.67	6.30	10.56	16.86
9.63	5.51	10.36	15.87
11.56	4.70	9.98	14.68
13.49	4.19	9.55	13.74
15.41	3.53	9.19	12.72
17.34	3.06	8.90	11.96
19.27	2.64	8.52	11.16
21.20	2.27	8.20	10.47
23.12	1.99	7.88	9.87
25.05	1.74	7.52	9.26
26.98	1.54	7.21	8.75
28.90	1.36	6.90	8.26
33.72	0.96	6.20	7.16
38.54	0.71	5.50	6.21
43.35	0.54	4.90	5.44
48.17	0.44	4.36	4.80
57.80	0.32	3.38	3.70
67.44	0.22	2.68	2.90
77.07	0.18	2.20	2.38
86.71	0.13	1.81	1.94
96.34	0.10	1.60	1.70

A.6.2.2. Repulsion Energy

H_o(Å)	V_R/kT (Segment a = 336 Å)	V_R/kT (sp-pl H = H_o + 44 Å)	V_R/kT
5.78	39.39	2.80	42.19
6.74	36.36	2.54	38.90
7.71	33.40	2.30	35.70
8.67	30.69	2.10	32.79
9.63	28.23	1.90	30.13
11.56	23.72	1.56	25.28
13.49	19.90	1.29	21.19
15.41	16.58	1.04	17.62
17.34	13.76	0.84	14.60
19.27	11.42	0.68	12.10
21.20	9.23	0.51	9.74
23.12	7.86	0.40	8.26
25.05	6.44	0.36	6.80
26.98	5.34	0.30	5.64
28.90	4.40	0.22	4.62
33.72	2.67	0.11	2.78
38.54	1.65	0.08	1.73
43.35	1.00	0.01	1.01
48.17	0.61	-	0.61
57.80	0.22	-	0.22
67.44	0.082	-	0.082
77.07	0.030	-	0.030
86.71	0.011	-	0.011
96.34	0.004	-	0.004

A.6.2.3. Total Potential Energy

	V/kT		
H_o (Å)	A = 10^{-13} ergs	A = 5×10^{-14} ergs	A = 10^{-14} ergs
5.78	18.6	30.4	39.8
6.74	18.7	28.8	36.9
7.71	17.5	26.6	33.9
8.67	15.9	24.3	31.1
9.63	14.3	22.7	28.5
11.56	10.6	17.9	23.8
13.49	7.45	14.3	19.8
15.41	4.90	11.3	16.4
17.34	2.64	8.60	13.4
19.27	0.94	6.50	11.0
21.20	-0.73	4.49	8.69
23.12	-1.61	3.31	7.27
25.05	-2.46	2.15	5.87
26.98	-3.11	1.24	4.76
28.90	-3.64	0.47	3.79
33.72	-4.38	-0.82	2.06
38.54	-4.48	-1.37	1.11
43.35	-4.43	-1.69	0.47
48.17	-4.19	-1.79	0.13
57.80	-3.48	-1.63	-0.15
67.44	-2.82	-1.37	-0.21
77.07	-2.35	-1.16	-0.21
86.71	-1.93	-0.96	-0.18
96.34	-1.70	-0.85	-0.17

A.6.3. IN 0.05M NaCl and 10^{-4}M S.D.S.

ζ_{Latex} = -42.2 mV, $\zeta_{Formvar}$ = -42.0 mV.

A.6.3.1. Attraction Energy (A = 10^{-13} ergs)

H_o (Å)	$-V_A/kT$ (Segment $H = H_o$)	$-V_A/kT$ (Sp-pl $H = H_o + 44$ Å)	$-V_A/kT$
5.45	14.10	11.26	25.36
6.82	9.10	10.98	20.08
8.18	6.82	10.66	17.48
9.55	5.59	10.37	15.96
10.91	4.95	10.06	15.01
12.27	4.43	9.80	14.23
13.64	4.00	9.53	13.53
16.36	3.21	9.04	12.25
19.09	2.61	8.58	11.19
21.82	2.19	8.04	10.23
24.54	1.84	7.61	9.45
27.27	1.50	7.19	8.69
30.00	1.26	6.72	7.98
32.72	1.03	6.31	7.34
35.45	0.86	5.92	6.78
38.18	0.73	5.58	6.31
40.91	0.63	5.20	5.83
47.72	0.45	4.40	4.85
54.54	0.36	3.69	4.05
61.36	0.29	3.08	3.37
68.18	0.23	2.61	2.84
81.81	0.16	1.99	2.15
95.45	0.10	1.60	1.70

A.6.3.2. Repulsion Energy

H_o(Å)	V_R/kT (Segment a = 336 Å)	V_R/kT (sp-pl H = H_o + 44 Å)	V_R/kT
5.45	55.69	16.10	71.79
6.82	51.51	14.57	66.08
8.18	47.54	13.20	60.74
9.55	43.84	11.95	55.79
10.91	40.29	10.78	51.07
12.27	37.01	9.70	46.71
13.64	34.03	8.79	42.82
16.36	28.58	7.18	35.76
19.09	23.98	5.85	29.83
21.82	19.98	4.80	24.78
24.54	16.58	4.00	20.58
27.27	13.75	3.37	17.12
30.00	11.12	2.78	13.90
32.72	9.46	2.28	11.74
35.45	7.76	1.83	9.59
38.18	6.43	1.47	7.90
40.91	5.30	1.23	6.53
47.72	3.21	0.75	3.96
54.54	1.99	0.43	2.42
61.36	1.20	0.27	1.47
68.18	0.73	0.17	0.90
81.81	0.27	0.06	0.33
95.45	0.099	0.01	0.11

A.6.3.3. Total Potential Energy

	V/kT		
H_o (Å)	$A = 10^{-13}$ ergs	$A = 5 \times 10^{-14}$ ergs	$A = 10^{-14}$ ergs
5.45	46.4	59.1	69.3
6.82	46.0	56.0	64.1
8.18	43.3	52.0	59.0
9.55	39.8	47.8	54.2
10.91	36.1	43.6	49.6
12.27	32.5	39.6	45.3
13.64	29.3	35.1	41.5
16.36	23.5	29.6	34.5
19.09	18.6	24.2	28.7
21.82	14.6	19.7	23.8
24.54	11.1	15.8	19.6
27.27	8.43	12.8	16.3
30.00	5.92	9.90	13.1
32.72	4.40	8.09	11.0
35.45	2.81	6.19	8.91
38.18	1.59	4.75	7.27
40.91	0.70	3.63	5.95
47.72	-0.89	1.51	3.47
54.54	-1.63	0.41	2.01
61.36	-1.90	-0.23	1.13
68.18	-1.94	-0.50	0.62
81.81	-1.82	-0.77	0.11
95.45	-1.59	-0.74	-0.06

APPENDIX 7.0

An Approximate Method for the Calculation of the Total Potential Energy of Interaction between a Sphere and a Rough Plane Surface

If the assumption is made that the surface roughness of the plane surface is composed of spherical projections (which is approximately true for the "Formvar" surface (Fig.8.4)), then the total potential energy of interaction between a sphere and such a rough surface can be calculated analytically. With this model the repulsive part of the total potential energy of interaction can be calculated by considering the energies of interaction between two spheres (one of which is the sphere comprising the spherical projection on the plane surface), and adding to this the energy contribution of the plane surface beyond the spherical projection. The expression for the potential energy of interaction of dissimilar double-layers[1] is

$$V_R = \frac{\varepsilon a_1 a_2 (\psi_1^2 + \psi_2^2)}{4(a_1 + a_2)} \left[\frac{2\psi_1\psi_2}{\psi_1^2 + \psi_2^2} \ln\left(\frac{1 + \exp(-\kappa H)}{1 - \exp(-\kappa H)}\right) + \ln\left(1 - \exp(-\kappa H)\right) \right] \qquad (1)$$

From this it can be seen that if the radius of the spherical projections are less than that of the particle, then the repulsion

energy will be less than that for two equal sized spheres and much less than half that for the particle and a smooth plane surface. This expression is valid only if κa_1 and $\kappa a_2 >> 1$, and $H << a_1$ and a_2. Under these conditions the contribution of the underlying plane surface is negligible in comparison to that of the spherical projection (for example at 0.3M NaCl, see Appendix 6.1.2.). However, if these conditions are not fulfilled, then the contribution of the underlying plane will be significant. When this occurs, the repulsion energy calculated is too large because the repulsion energy is a surface effect and contributions from within the body of the surface have been included, i.e. that part of the plane surface within the spherical projection and that part of the sphere comprising the spherical projection within the underlying plane surface. This situation occurs only when the double-layers are not thin, which in this work is for ionic strengths less than or equal to 5×10^{-2}. At an ionic strength of 5×10^{-2} the contribution of the underlying plane surface is about 25% (see appendix 6.3.2.).

To the repulsion energy must be added the attraction energy between a sphere and a spherical projection on a plane surface. This is a much more complicated case than the repulsion energy and is considered in the next section.

A.7.1. <u>The Attraction Energy between a sphere and a Spherical Projection on a Plane Surface</u>

In Fig.A.7.1. is shown the geometry of the system of a sphere

FIG (A·7·1) GEOMETRICAL REPRESENTATION OF A SPHERE APPROACHING A SPHERICAL PROJECTION ON A PLANE SURFACE.

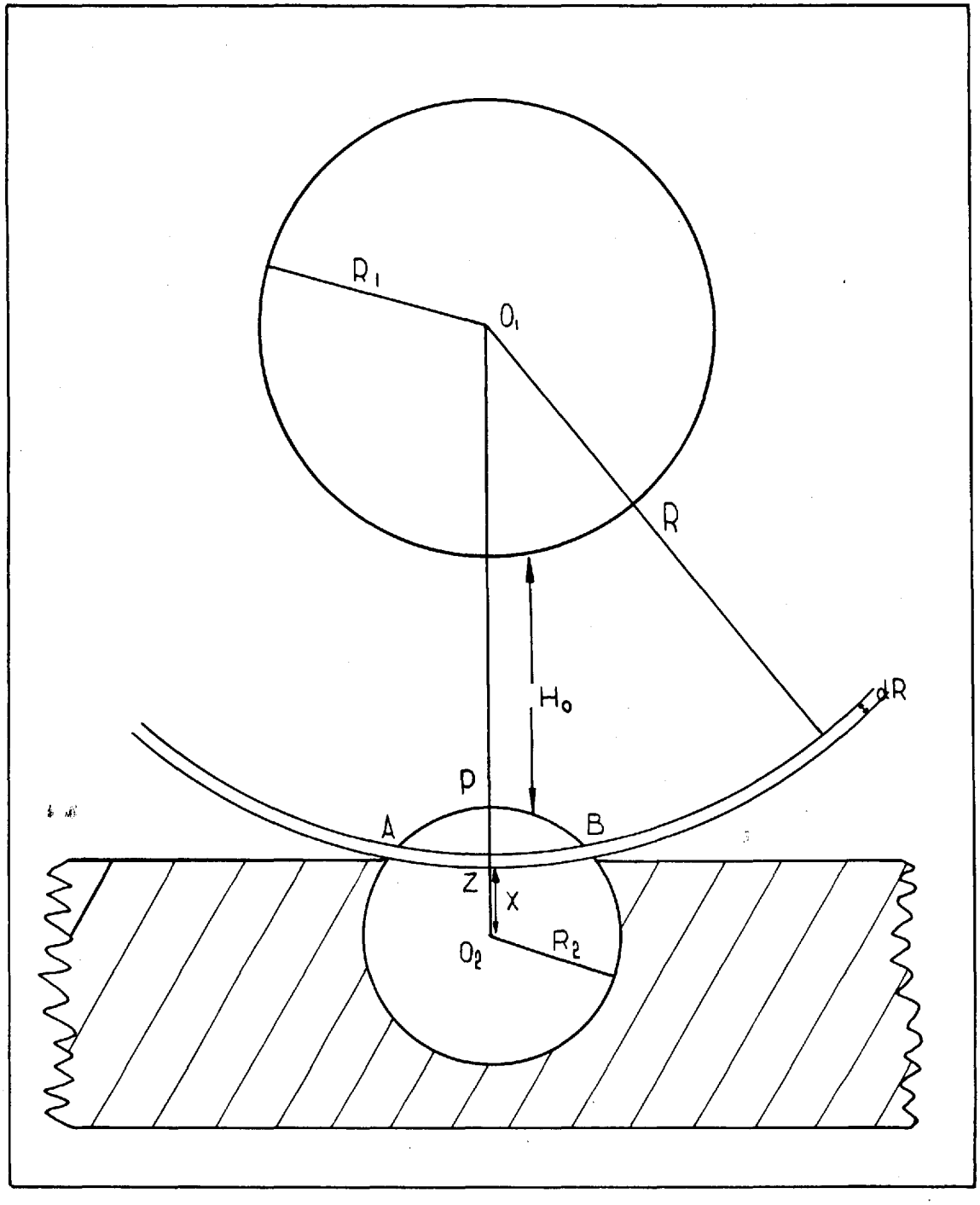

approaching a spherical projection on a plane surface. The energy of attraction between the sphere, centre O_1, and the spherical segment (PAB) of the sphere, centre O_2, is given by

$$V_{s\text{-}seg} = -\int_{V_1} dV_1 \int_{V_2} dV_2 \cdot \frac{q^2 \lambda}{r^6} \qquad (2)$$

where V_1 is the total volume of the sphere (centre O_1) and V_2 is the total volume of the segment (PAB) of the sphere (centre O_2). q is the number of atoms per cm^3 of material in the bodies and $\underline{\lambda}$ is the wavelength characteristic of the atom dipole fluctuations, and $\underline{r}$ is the distance between the atoms. Equation (2) can be solved analytically following the method of Hamaker[2].

By his method the energy of attraction of the two spheres is obtained by considering, firstly, an atom at position $\underline{z}$. Then the attraction energy between this atom and the sphere, centre O_1, is given by

$$V_p = -\int_{R-R_1}^{R+R_1} \frac{q\lambda}{r^6} \cdot \frac{\pi r}{R} \left[R_1^2 - (R - r)^2 \right] dr \qquad (3)$$

and, secondly, the attraction between sphere, centre O_1, and sphere, centre O_2, (assuming that the two spheres are composed of the same material) is given by

$$V_{ss} = -\int_{C-R_2}^{C+R_2} V_p \cdot \frac{q\pi R}{C} \left[R_2^2 - (C - R)^2 \right] dR \qquad (4)$$

where $C = O_1O_2$. However, for the case where the sphere, centre O_2, is embedded partially in a plane surface, only the interaction of the sphere, centre O_1, with the spherical cap, PAB, is required. This is readily obtained by a suitable change in the limits of the integral in equation (4). Therefore, the energy of interaction between the sphere, centre O_1, and the spherical cap (PAB) is given by

$$V_{s\text{-}seg} = -\int_{C-R_2}^{C-x} V_p \cdot \frac{q\pi R}{C} \left[R_2^2 - (C - R)^2 \right] dR \qquad (5)$$

where the height of the spherical projection above the plane surface is given by $(R_2 - x)$. The complete expression for this interaction energy is then given by

$$V_{s\text{-}seg} = q^2\pi^2\lambda \int_{C-R_2}^{C-x} \int_{R-R_1}^{R+R_1} \frac{1}{r^2} \left[R_1^2 - (R-r)^2 \right] \frac{R}{C} \left[R_2^2 - (C-R)^2 \right] dR.dr \qquad (6)$$

which on evaluation yields

$$V_{S\text{-}seg} = -\frac{A}{12}\left\{\frac{R_1}{C}\left[\frac{(C^2 - R_2^2 + 2CR_1 + R_1^2)}{(C - x + R_1)^2} - \frac{(C^2 - R_2^2 + 2CR_1 + R_1^2)}{(C - R_2 + R_1)^2}\right.\right.$$

$$\left. + \frac{(C^2 - R_2^2 + R_1^2 - 2CR_1)}{(C - x - R_1)^2} - \frac{(C^2 - R_2^2 + R_1^2 - 2CR_1)}{(C - R_2 - R_1)^2}\right]$$

$$+ \frac{1}{C}\left[\frac{(C^2 - R_2^2 - 3R_1^2 - 2R_1C)}{(C - x + R_1)} - \frac{(C^2 - R_2^2 - 3R_1^2 - 2R_1C)}{(C - R_2 + R_1)}\right.$$

$$\left. + \frac{(R_2^2 - C^2 + 3R_1^2 - 2CR_1)}{(C - x - R_1)} - \frac{(R_2^2 - C^2 + 3R_1^2 - 2CR_1)}{(C - R_2 - R_1)}\right]$$

$$\left. + 2\ln\left(\frac{C - x + R_1}{C - x - R_1}\right)\left(\frac{C - R_2 - R_1}{C - R_2 + R_1}\right)\right\} \qquad (7)$$

From the examination of Fig.(A.7.1) it can be seen that the energy of attraction calculated from equation (7) is too large at close distances of approach. This is because in the derivation of equation (7) the arc AZB was used and assumed to approximate closely to the plane AB. For large separation distances this assumption is probably correct. Therefore, when the components to the energy calculated from equation (7) are added to those of the underlying plate the total energy is too large, at close distances of approach, as the effect of the segment AZB is included twice. Nevertheless,

the error should not be large and this treatment gives a good indication of the magnitude of such surface roughness effects.

A.7.2.References

(1) Hogg, R., Healy, T.W. and Fuerstenau, D.W. Trans. Faraday Soc. 62, 1638, (1966).

(2) Hamaker, H.C. Physica 4, 1058, (1937).